Trace Elemental Analysis of Some Simple Ayurvedic Formulations Using PIXE and XRF

Thesis submitted to University of Calicut

in partial fulfilment of the requirements

for the award of the degree of

Doctor of Philosophy

in

Physics

By

SALMA IBRAHIM R V

Reg. No : PHYPHD 19

under the guidance of

Dr. M. M. Musthafa

Professor

DEPARTMENT OF PHYSICS

UNIVERSITY OF CALICUT

15^{th} November 2021

DECLARATION

I hereby declare that the work presented in this thesis entitled **"Trace Elemental Analysis of Some Simple Ayurvedic Formulations Using PIXE and XRF"** is based on the original work done by me under the supervision of Dr. M. M. Musthafa, Department of Physics, University of Calicut, and has not been included in any other thesis submitted previously for the award of any degree.

University of Calicut

Date: 16.11.2021

Salma Ibrahim R V

Department of Physics
UNIVERSITY OF CALICUT

Dr. M.M. Musthafa
Professor & Former Head
Department of Physics,
E-mail: mmm@uoc.ac.in, mm_musthafa@rediffmail.com

Calicut University P.O
Kerala, India-673 635
Tel: +91 4942497415
mobiloe: +91 9745509190

15th November, 2021

CERTIFICATE

*This is to certify that that the corrections/ suggestions, recommended by the adjudicators, have been incorporated in the thesis submitted by Ms. Salma Ibrahim R.V. to the University of Calicut entitled "**Trace elemental analysis of some simple ayruvedic formulations using PIXE and XRF**". It is also certified that the contents in the thesis and the soft copy are one and the same*

Prof. (Dr). M.M. Musthafa
Research Supervisor

CERTIFICATE

Certified that the work presented in this thesis entitled **"Trace Elemental Analysis of Some Simple Ayurvedic Formulations Using PIXE and XRF"** is a bonafide work done by Mrs. Salma Ibrahim R V under my guidance for the award of the degree of Doctor of Philosophy in the Department of Physics, University of Calicut and that this work has not been included in any other thesis submitted previously for the award of any degree.

University of Calicut

Date: 17.11.2021

Dr. M. M. Musthafa

(Research Supervisor)

DEPARTMENT OF PHYSICS * UNIVERSITY OF CALICUT - 673 635 *

Dr. M.M. MUSTHAFA
Professor
Department of Physics
University of Calicut
Kerala-673 635, India

List of Publications

1. Salma Ibrahim, M. M. Musthafa, M. Mohamed Aslam, K. M. Abdurahman, M. Sudarshan, M. Elumalai, J. S. Brahmaji Rao, G. V. S. Ashok Kumar, K. Sundararajan, Trace elemntal fingerprinting of Ayurvedic formulation Nishakatakadi using XRF and NAA, Journal of Radioanalytical and Nuclear Chemistry DOI:10.1007/s10967-021-07659-2.

2. R V Salma Ibrahim, M. M. Musthafa, K. M. Abdurahman, M. Aslam, Trace elemental fingerprinting of Ayurvedic medicine-Triphala Churna using XRF and ICPMS, Journal of Radioanalytical and Nuclear Chemistry DOI:10.1007/s10967-019-06909-8

3. Salma Ibrahim R. V., Musthafa M. M., Midhun C. V., Swapna Lily Cyriac, Sajeev S., Measurement and analysis of photonuclear reactions on thick target samples of biological importance, Indian Journal of Pure and Applied Physics, 58(2020): 404-408

4. Salma Ibrahim, M. Aslam, M. M. Musthafa, Trace elemental fingerprinting of selected herbs used in Ayurveda using XRF and ICPMS, Journal of Pharmacognosy and Phyto-chemistry (2019) 8(3) 2278-4136

List of International / National conference presentations:

1. Trace elemental fingerprinting of Amalakyadi churna using XRF and PIXE, International Conference on Theoretical and Experimental Physics (ICTEP-2020) , Farook College, Calicut, Kerala, 2020

2. Gamma Activation for trace elemental analysis of herbal medicine Phyllanthes emblica, National Conference on Nuclear Structure and Nuclear Reactions, AMU, Aligarh, March 2020

3. Measurement and analysis of photonuclear reactions on thick target samples of biological importance, International Conference on New Frontiers in Nuclear Physics (ICNFNP19), Department of Physics, BHU, 2019

4. X-ray fluorescence fingerprinting of trace elements in Ayurvedic medicine Triphala Churna, 14th Biennial DAE-BRNS Symposium on Nuclear and Radiochemistry (NUCAR-2019), BARC, Mumbai, 2019

5. Trace elemental analysis of Ixora coccinea using ED-XRF, ICGST MES Kveeyem College, Valanchery, Malappuram, 2018

6. ED-XRF analysis of some herbs used to cure respiratory diseases in Ayurvedic treatment, International Conference on Application of Radiotracers and Energetic Beams in Sciences (ARCEBS-19), SINP, Kolkata,2019

7. Trace elemental analysis of some medicinal herbs used in Kerala using EDXRF, 21 st DAE-BRNS National Symposium on Radiation Physics, RRCAT, Indore, 2018

8. Trace elemental anaysis of some medicinal plants commonly used in traditional Indian medicines, National Seminar on Radiation-Medical, Industrial, and Research Applications, Sir Syed College, Kerala, 2016

List of Seminars/ Workshops/ Schools attended:

1. National Workshop on Environmental Radioactivity Measurements (ERM-2019) January 2019, IGCAR, Kalpakkam

2. Digital typography using Latex, November 2019, Government Arts and Science college, Meenchada, Calicut

3. National seminar on theoretical physics. March 2017, University of Calicut, Kerala.

4. National workshop on fourier transform and digital signal processing. Jan 2017, S.A.R.B.T.M GOVT. College, Koyilandi, Kerala.

5. National workshop on foundations of statistical and quantum mechanics. Jan 2017, S A.R.B.T.M GOVT. College, Koyilandi, Kerala.

6. Course on accelerators and detectors, IUAC Accelerator School, March 2016

7. National seminar on ibnul-haytham and his world of science. November 2015, University of Calicut, Kerala.

8. National conference on enchanting developments in advanced materials. July 2015, University of Calicut, Kerala.

9. 28th Kerala Science congress, University of Calicut during 28-31 2016

Dedicated to My Better Half and Li'l Master

Acknowledgements

On my way to realizing a dream, I remember so many faces with gratitude, who rendered their help in various ways. I wish to express my gratitude to every one of them. I am indebted to my guide Dr. M. M. Musthafa who has been supportive throughout my work, whose scholarly advice helped me to complete the work successfully. His optimistic approach taught me to seek opportunities in all the hardships. I am thankful to our Head of the Department, Dr. AM Vinodkumar for all the benevolent support that was rendered for my research. I am indebted to Dr. Antony Joseph, Dr. P. P. Pradyumnan, Dr. Muhammed Shahin Thayyil and Dr. Libu K Alexander who extended their laboratory facilities and Dr.C. D Ravikumar for his moral support throughout my research period.

I take this opportunity to express my heartfelt gratitude to Dr. M Abdul Khader, CNST, University of Kerala, who was the beacon of inspiration for me to pursue my research. It is a great pleasure to express my sincere gratitude to A. K. Sinha and Dr. M Sudarsan, UGC-DAE-CSR Kolkata Center for providing experimental facilities at the Kolkata center. I express my heartfelt gratitude to Dr. R Kumar, Head of RCL, IGCAR, for the help rendered to perform activation studies at his center. I acknowledge my sincere gratitude to Dr. R. Sundararajan, Dr. G.V.S. Ashok Kumar and Mr. Brahmaji Rao, MC and MFCG, IGCAR, who were always ready to help me irrespective of their busy schedule. I am grateful to Dr. S. Sajeev and Dr. Swapna Lily Cyriac, KIMS, Trivandrum for their timely help and support

With pleasure, I would like to thank Dr. M. Aslam, Associate Professor, Govt. Arts and Science College, Kozhikode, for the interesting discussions and advice which helped me to overcome the difficulties and to clarify doubts. I thank Dr. Shibu Vardhan, Department of Zoology, Dr. K. Muraleedharan and Mr. Satheesan K., Department of Chemistry, Dr. A. K. Pradeep, Department of Botany, Dr. Thara Menon, Department of Biotechnology for their help in carrying out different steps of my research work. I am thankful to Director, CSIF, and all the technicians there for their help and co-operation.

I thank all my colleagues in the department of physics especially, Hajara, Abdurahman, Shaima, Shan, Midhun, Shana, Gokul and Bhagyasree for their constructive criticism and scaffolding. I cherish the moments with them in the department as well as at seminars and experiments. I also take this opportunity to thank my friends in the sister departments for their help and support. I am grateful to UGC for providing me financial support through the UGC BSR fellowship. I express my appreciation to all non-teaching staff of the Department of Physics for their help and co-operation during the tenure of my work.

I am blessed with a highly supportive family who shaped me into what I am now. The trust of my Uppa and the prayers of my Umma are invaluable for me and words are not enough to express my gratitude for them. I am greatly indebted to my husband, in-laws, brother and sister who struggled along with me during my research period but still stood by my side to realize my dream. My heartfelt gratitude to my son who was understanding beyond expectations on all the days I was out of station for experiments. Above all, I am grateful to God Almighty for all his blessings, and for granting me so many well-wishers and making me capable of completing this research work successfully.

Salma Ibrahim R V

Contents

List of Figures

List of Tables

Chapter 1

Introduction

1.1 Introduction

Innovations and advances in physics are the fundamental keys in the development of various tools and techniques in various branches of science and technology. Medical science is one of the important branches of science whose development and progress depend heavily on the advancement in physics. The discovery of X-rays by Wilhelm Roentgen has marked a revolution in diagnostic imaging and material characterization, whereas the discovery of the phenomena of radioactivity by Henry Becquerel introduced novel methods for energy production and radiation therapy. The invention of the cyclotron by E. O. Lawrence in 1929 boosted the developments in high energy physics using energetic ion beams. A remarkable discovery of the neutron by James Chadwick, later the development of activation analysis by Hevesy, expanded the horizons of physics and its applications further. The development of high-energy acceleration techniques produced energetic beams of ions, particles such as neutrons and positrons which were utilized as analytical probes contributed immensely in industry and academic research [1]. The discovery of semiconductor detectors with high sensitivity and a better resolution was a major breakthrough that revolutionized the field of qualitative and quantitative analysis of materials. Later, the development of modern techniques for data analysis improved the ability to analyze trace and

ultra-trace levels which have applications in environmental contamination surveying, geological prospecting, biomedical investigations, etc.

Elemental analysis involves the qualitative and quantitative determination of elements in any sample matrix. Depending on the concentration, they are classified as major, minor, and trace elements of which the typical concentration 1 to 100 ppm are considered as trace elements. The techniques for analysis of trace elements have been developed rapidly in response to the increase in the need for the accurate measurements of significantly less quantity of elements in diverse types of sample matrices. Even though the concentration is of sub-ppm levels, their detection is highly decisive in many applications. There are many specific areas of research and industry where the presence of certain elements at extremely low concentrations has a significant impact. Trace elements have been at the focus of attention for decades with considerable emphasis on their role in biology, biomedical sciences, environmental sciences, geology, archaeology, and material sciences [2], [3], [4], [5]. In the human body, many elements functions as essential elements, whereas some others are toxic, carcinogenic and mutagenic [6]. Several techniques have been developed over the past decades for the qualitative and quantitative estimation of elements especially at minute quantities with high sensitivity and accuracy.

An analytical technique for the determination of constituent elements in a sample requires that the sample possesses a characteristic measurable property, which acts as a fingerprint of the element. The specific property should be unique to a particular element to distinguish it from others and to quantify each element. Chemical methods make use of the chemical properties of the elements. Such methods involve elaborate chemical treatments with various reagents. If the characteristic property is a photon emitted from a sample, then the energy of the photon will identify the element and the number of photons per second counted from the sample gives the quantitative aspects. Atomic spectroscopy relies on characteristic absorption or emission spectra of elements. Nuclear techniques involve the detection and measurement of characteristic radiations or particles

emitted from the nuclei of constituent elements. The common principle behind the ion beam techniques is the interaction of energetic beams with the elements in the sample. The projectile loses its energy continuously as it travels through the medium due to collisions with the nucleus and with electrons. Secondly, the product of these interactions is emitted from the sample, with probabilities determined by the respective interaction cross-section, and are finally measured and collected as spectra carrying information on the chemical composition of the sample and elemental depth distributions. Despite the advancements in atomic and nuclear analytical techniques, no method can be considered suitable to tackle all sample types and to determine all the elements. So, the selection of appropriate techniques for a particular analytical problem is a challenging task. It is important to understand and recognize the capabilities and limitations, and to gauge the suitability and complementarity for a particular analytic task.

There are different methods for the identification and quantification of elements at trace levels. This can be generally classified as potentiometry, voltammetry, atomic spectrometry, X-ray methods, and nuclear methods. Atomic Absorption Spectrometry (AAS), Inductively Coupled Plasma Mass spectroscopy (ICPMS), and High-Performance Liquid Chromatography (HPLC), are generally considered as destructive techniques that need chemical dissolution of the samples before analysis. X-ray Fluorescence (XRF), Neutron Activation Analysis (NAA), Photon Activation Analysis (PAA), Rutherford Backscattering Spectrometry (RBS), Elastic Recoil Detection Analysis (ERDA), Particle induced Xray Emission (PIXE), Particle Induced Gamma emission (PIGE), and Nuclear Reaction Analysis (NRA) are some of the non-destructive techniques. X-ray spectroscopy and nuclear methods offer very low detection limits and the least matrix effects. Many of the techniques can be set up simultaneously with the same infrastructure and many of the methods are used complementarily to get reliable data.

Trace element analysis has been considered as a hot topic of research in various disciplines. Many reports are available on the importance of trace

elemental analysis in environmental samples. The importance of trace elements in biological systems is reviewed by Elisa et al [7]. A recent study conducted by Jingzhao Lu reported the impact of trace elemental pollution in soil and water resources due to mineral mines [8]. Analysis of different sample types like herbal samples was conducted by using different modalities of XRF [9], [10].

PIXE has been used for determination of major and trace elements in diverse matrix types namely archaeological samples like ancient coins [9], geochemical samples like minerals and ores [10], water [13], and soil samples [11]. Elemental analysis of biological samples like blood [12], [16], kidney [13] and hair samples [18] and herbal samples with medicinal properties [19], [20] have been reported by different authors using the PIXE technique. The multi-elemental nature, diverse range, and high sensitivity make it a suitable candidate for the elemental determination of thick samples with complex matrix composition.

Neutron activation has been routinely used for determination of trace elements with high sensitivity. NAA is used as one of the methods in certification of standard reference samples [21], [22], [34]. Application of NAA for the trace elemental characterization of herbal samples have been reported by many authors [24], [25], [26]. ICPMS method have been widely used as a sensitive technique in different sample types such as forensic, geological samples [27], [28], biological samples [29], [30], [31], etc.

A review paper on standardization methods of Ayurvedic medicines reports the importance of HP-LC, HP-TLC, and GC-MS techniques for quantitative analysis of traditional herbal products [32]. Reports on the application of AAS [33], HPLC [34], NAA [35], and ICPMS [36] for trace elemental analysis of Ayurvedic herbal products is also available. However, limited reports are available on non-destructive techniques of herbal formulations using atomic or nuclear techniques [37], [38].

1.2 Scope of Trace Elemental Analysis

Ethno-pharmacology has been identified as an important area of research as the number of stakeholders is increasing around the globe. The use of ethnic systems of medicines is not limited to the treatment of diseases but extends to tonics, energy boosters rejuvenators, dietary supplements, etc. Herbal formulations have gained widespread acceptability as therapeutic agents for diabetes, arthritis, liver diseases, cough remedies, memory enhancers etc. Ghosh et al. provide encouraging evidence for the application of herbal medicines as psychopharmacological drugs in the treatment of depression, anxiety and insomnia [39], [40].

There are coded systems of herbal formulations as well as numerous uncoded versions popular in many countries over the decades. Ayurveda, Siddha, Unani, and Homoeopathy are the most familiar coded formulations prevailing in India. India is a leader in the manufacturing and export of Ayurvedic medicines, and the market of raw and finished herbal products is growing day by day. Medicinal plants contain many active organic molecules, tannins, resins, and essential and non-essential elements. Besides the organic compounds, it is very well established that many trace elements play a vital role in the normal metabolism of the human body. It is reported that trace elements play a vital role in the formation of active constituents and thus imparts medicinal as well as toxic properties. Each medicinal plant is characterized by a number of trace elements which is responsible for the production of active constituents that determines its medicinal property.

Each plant exhibits its own metal uptake and accumulation behaviour, which is the basis for herb characterization by elemental pattern, that can be applied for adulteration detection [41]. Even though herbal medicines are considered natural and safe, they are not free from adverse side-effects. The excess of trace elements in the human body adversely affects normal metabolism [7]. Accidental mixing of toxic environmental pollutants while collection, preparation,

and storage is also a serious concern. No comprehensive data of trace elements in Ayurvedic formulations are available yet. The absence of a strict regulatory standard for quality assurance gives way to adulterations. The presence of adulterants has been reported largely in herbal formulations available in the market [1]. It is reported that many herbal products available in the market contain toxic elements beyond permissible limits.

In the conventional allopathic system of medicine, the chemical compounds present in each medicine are under strict monitoring, and the effects of excess intake, side effects, and the presence of toxic elemental contents are all scientifically established and are well declared on the distributor's manual. But such a standardized system of quality assurance is absent in the case of alternative treatment of medicines which include Homoeopathy, Unani, Siddha, and Ayurveda. All these therapies involve the utilization of specific parts of plants, in crude or refined form, collected from different geographical areas growing under different environmental conditions. In order to ensure safety, efficacy, and quality, there is a growing demand for accurate determination of constituents in each Ayurvedic preparation. In order to use a medicine for a considerably long duration, the composition must be free from toxic contents, especially an intolerable amount of trace elements. In order to ensure this, proper licensing procedures incorporating quality and safety is necessary. However, most studies on medicinal plants pertain to constituents such as essential oils, vitamins, glycosides, and other organic components, while little has been reported about the elemental composition of different plants and their corresponding Ayurvedic preparation.

The Ayurvedic Pharmacopoeia of India has set standards for quality assurance of Ayurvedic formulations based on chemical and physical properties like alcoholic content analysis, ash test, estimation of certain phenolic compounds, chromatographic fingerprints, etc. There is a wide variation in the values of such parameters for crude drugs of plant origin with respect to their chemical contents. Therefore, such variations have to be taken into account while

setting maximum and minimum values of parameters, while setting standards of compound formulations. The above parameters do not assure complete quality standards concerning the correct constituents of the drug. All the above methods are based on chemical principles. The analysis is expensive, time-consuming, and are difficult to reproduce. Analytical techniques using characteristic X-rays enables one to quantify many elements with much less effort, with high sensitivity, sufficient accuracy, and repeatability. Identifying the characteristic x-rays or gamma rays from an element can give qualitative and quantitative information of the sample in any complex matrix. These non-destructive methods based on nuclear analytical techniques offer a novel quality assurance criterion based on trace elemental analysis.

In essence, the screening of the elemental composition of the medicinal plants is an essential part of‘ quality control of herbal formulations, which establishes its purity safety, and efficacy. The possibility of adulteration comes when there is an increasing demand and a shortage of raw materials. The variation in the chemical composition starts right from the collection of the samples and continues during processing and storage. The change in elemental contents of medicines due to the intentional addition of cheap, much available herb instead of a costly one, is of great concern. The quality, efficacy, and safety of herbal medicines can only be ensured by undergoing a systematic study on elemental profiles. Utilizing the elemental information from different techniques, an elemental fingerprint of the herbal formulation can be generated. Keeping this in view, a systematic analysis of trace elemental profile of selected Ayurvedic formulations, viz. Triphaladi Churna, Nishakatakadi decoction, Amalakyadi Churna, and Balachaturbhadrika Churna has been carried out.

Utilizing the elemental information from different techniques, it is proposed to generate a fingerprint of herbal formulations based on trace elemental profile. The thesis is divided into five chapters. Chapter 1 gives a general introduction of the trace elemental techniques in quality analysis of Ayurvedic formulations. Chapter 2 gives a brief description of various techniques employed for

elemental analysis. Chapter 3 gives the details of the materials and methodologies adopted for trace elemental analysis of formulations reported in this thesis. Observations of the measurements are also tabulated in this chapter. A detailed analysis of the results is carried out in Chapter 4. A comprehensive analysis of trace elemental profiles of various formulations and the role of constituent herbs is described in Chapter 5. Conclusive remarks are also presented in this chapter with prospects of future work to be carried out in this respect. This study is expected to provide a reliable data for fingerprinting each Ayurvedic formulation with the help of PIXE, XRF, and other nuclear and chemical techniques.

Bibliography

[1] Ewa Bulska, Anna Ruszczynska (2017) Physical Sciences Reviews, 25, 1-14

[2] Falah S. Al-Fartusie, Saja N. Mohssan (2017), Indian Journal of Advances in Chemical Science 5(3), 127-136

[3] Roberto Terzano, Melissa A. Denecke, Gerald Falkenberg, Bradley Miller, David Paterson, Koen Janssens (2019), Pure and Applied Chemistry, 91 1030 DOI: https://doi.org/10.1515/

[4] Shanika Nanayakkaraab, SenevirathnaKouji, H.Harada, RohanaChandrajith, ToshiakiHitomi, Tilak, Abeyseker, EriMuso, TakaoWatanabe, AkioKoizumi (2019), Journal of Trace Elements in Medicine and Biology 54, 206-213

[5] Bruno Reynard, Vincent Balter (2014), Palaeogeography, Palaeoclimatology, Palaeoecology, 416, 4-16

[6] Sathyaprasad C, Burjonrappa, MalkiMiller (2012), Journal of Pediatric Surgery, 47, 760-771 https://doi.org/10.1016/j.jpedsurg.2012.01.015

[7] Elisa Andresen, Edgar Peiter, Hendrik Kupper(2018), Journal of Experimental Botany, 69, 909–954

[8] TJingzhao Lu, Hongwei Lu, Kaiwen Lei, Weipeng Wang, Yanlong Guan (2019), Environmental Science and Pollution Research 26, 24630–24644

[9] Rogerta Dalipi, LauraBorgese, KouichiTsuji, ElzaBontempi, Laura E. Depero (2018), Journal of Food Composition and Analysis, 67, 128-134

[10] Sakina Yagi, Alia E. Abd Rahman, Gihan O.M. ELhassan, Abdelhafeez M.A. Mohammed (2013), Journal of Applied and Industrial Sciences, 1 (1): 49-53

[11] B. Tripathy, Tapash R. Rautray, A.C. Rautray, V. Vijayan (2010), Applied Radiation and Isotopes 68, 454–458

[12] A.K. Mohanty a, S.K. Das, V. Vijayan, D. Sengupta, S.K. Saha (2003), Nuclear Instruments and Methods in Physics Research B 211, 145–154

[13] Oyuntsetseg Bolormaa, Jamsranjav Baasansuren, Katsunori Kawasaki,

[14] Oyuntsetseg Bolormaa, Jamsranjav Baasansuren, Katsunori Kawasaki, Makiko Watanabe, Toshiyuki Hattroi (2007), Nuclear Instruments and Methods in Physics Research B 262, 385–390

[15] P. Sarita, G. J. Naga Raju, M. Ravi Kumar, A. S. Pradeep, S. Bhuloka Reddy (2013), J Radioanal Nucl Chem, 297:431–436, DOI 10.1007/s10967-012-2398-2

[16] P. Sarita, G. J. Naga Raju, A. S. Pradeep, Tapash R. Rautray, B. SeetharamiReddy, S. Bhuloka Reddy, V. Vijayan (2012), J Radioanal Nucl Chem, 294:355–361, DOI 10.1007/s10967-011-1505-0

[17] S. Bhuloka Reddy, M. John Charles, G.J. Naga Raju, V. Vijayan, B. Seetharami Reddy, M. Ravi Kumar, B. Sundareswar

[18] A.S. Pradeep, G.J. Naga Raju, S. Abdul Sattar, P. Sarita, A. Durga Prasada Rao, Dinesh Kumar Ray, B. Seetharami Reddy, S. Bhuloka Reddy (2003), Nuclear Instruments and Methods in Physics Research B 207, 345–355

[19] G.J. Naga Raju, P. Sarita, G.A.V. Ramana Murty, M. Ravi Kumar, B. Seetharami Reddy, M. John Charles, S. Lakshminarayana, T. Seshi Reddy, S. Bhuloka Reddy, V. Vijayan (2006), Applied Radiation and Isotopes 64, 893–900

[20] S. Abdul Sattar, B. Seetharami Reddy, V. Koteswara Rao, A. S. Pradeep, G. J. Naga Raju, K. Ramanarayana, P. V. Madhusudana Rao, S. Bhuloka Reddy (2012), J Radioanal Nucl Chem, 294:337–341

[21] Apple Leaves, Standard Reference Material 1515, National Institute of Standards and Technology, https://www-s.nist.gov/srmors/certificates/1515.pdf

[22] Peach Leaves, Standard Reference Material 1547, National Institute of Standards and Technology, https://www-s.nist.gov/srmors/certificates/1547.pdf

[23] https://nucleus.iaea.org/rpst/Documents/rs_iaea-v-8.pdf(2006) 161–166

[24] Rajurkar N. S, Damame M. M (1998), Appl. Radiat. Isot. 49 No 7, 773-776

[25] Paul C., Kumar A., Garg A. N. (2006), J. Pharm. and Biomed.Analysis 41, 825-832.

[26] Oladipo M. O. A., Njinga R. L., Baba A., Muhammad H. L. (2012), App.Rad. Isotop., 70, 917-921.

[27] Andrea Ulrich, Christoph Moor, Heinz Vonmont, Hans-Rudolf Jordi, Martin Lory (2004), Analytical and Bioanalytical Chemistry, 378, 1059–1068

[28] Klaus PeterJochum, Denis Scholz, BrigitteStoll, Ulrike Weis, Stephen A.Wilson, QichaoYang, Antje Schwalb, NicoleBörner, Dorrit E.Jacob, Meinrat O.Andreae (2012), Chemical Geology, 15, 31-44

[29] E.J.Llorent Martinez, P.Ortega Barrales, M.L.Fernandezde Cordova, A.Dominguez Vidal, A.Ruiz Medina (2011), Food Chemistry, 127, 1257-1262

[30] Taner Boraa, Cagdas Aksoy, Zeki Tunay, Fırat Aydın (2015), Microchemical Journal, 123, 179-184

[31] S. Kilic, M. Soylak (2020), Journal of Food Science and Technology, 57, 927–933

[32] Amruta Balekundri, Vinodhkumar Mannur (2020), Future Journal of Pharmaceutical Sciences, 6:67

[33] Rajasamarsen K Modi, Arjun N Shetty, Pratima Mathad, Kallurmath R.S. (2020), International Journal of Plant, Animal and Environmental Sciences 10: 116-126.

[34] Amrita Mishra, Arun K. Mishra, Om Prakash Tiwari, Shivesh Jhab (2013), J Young Pharm. Sep; 5(3): 77–82.

[35] VivekSingh, A.N.Garg (1997), Applied Radiation and Isotopes, 48, I, 97-101

[36] Sudhir S. Kamat, R.P. Suryawanshi (2015), Journal of Academia and Industrial Research, 3, 577

[37] A N Garg, A Kumar, A G C Nair, A V R Reddy (2005) J Radioanal Nucl Chem. 263: 751-758

[38] R Paul Choudhury, A Kumar, A V R Reddy, A N Garg (2007) J Radioanal Nucl Chem 274: 411–419

[39] Nilanjan Ghosh, Rituparna Ghosh, Vivekananda Mandal, Subhash C. Mandal (2011), Pharmaceutical Biology, 49(9), 970-988,

[40] Ghosh N., Ghosh R, Bhat Z A, Mandal V, Bachar S C, Nima N D, Mandal S C (2014), Communications, 9(7) 1045.

[41] Ammar Mubark Ebrahim, Etayeb M. A., Khalid H. Manale Noun, Roumie M., Michalke B (2014), App. Rad. Isotopes, 90, 218–224.

[42] Maciej J. Bogusz, Huda Hassan, eid Al Enazi, Zuhour Ibraim, Mohammed AlTufail (2006), J.Pharm. Biomed. Anal. 41,554

Chapter 2

Tools and Techniques for Trace Elemental Analysis

2.1 X-ray Fluorescnce (XRF) Spectroscopy

2.1.1 Introduction

XRF is a well-established analytical technique for qualitative and quantitative analysis of samples which enables simultaneous detection of many elements in solid or liquid state with high-detection sensitivities [1]. XRF is routinely applied for several interdisciplinary problems in environmental science, material science, biomedicine, archaeology etc [2], [3], [4], [5]. XRF is based on the principle that individual atoms when excited by an external energy source, emit X-ray photons of characteristic energy or wavelength. By counting the number of photons of each energy emitted from the sample, the elements present in it can be identified and quantified. In 1914 Mosely laid the foundations of X-ray spectrometry by recording the spectra of different elements using a diffraction crystal spectrometer and a photographic plate. Mosely had formulated a mathematical relationship between X-ray frequency and its atomic number. Mosely used electrons as excitation source whereas Coster and Nishina used primary X-rays instead of electrons for excitation. The quantitative analysis of materials

done by Schreiber et al. [6], and later the development of detector technology led to the development of commercial XRF spectrometers. XRF is useful for the analysis of trace elements in molecules of solid, liquid, and thin-film samples. The sensitivity of the XRF depends on the energy of the incident radiation, the geometry of the instrument used and the efficiency of the detector.

The working principle of XRF analysis is the measurement of energy or wavelength and intensity of the characteristic X-ray photons emitted from a sample. Since the characteristic X-rays give the unique signature of the elements present, identification and quantification of the elements in the analyte sample can be done using the recorded spectrum. Based on the measurement of the spectrum of the emitted characteristic X-rays, there are two domains in XRF spectroscopy, namely wavelength dispersive (WD) and energy dispersive (ED) spectrometers. In wavelength dispersive X-ray fluorescence analysis (WDXRF), a wavelength versus intensity spectrum is obtained from a Bragg single-crystal dispersion medium which diffracts X-rays depending on their wavelength followed by counting performed by a proportional or scintillation counter. Energy-dispersive X-ray fluorescence (EDXRF) the spectrometer consists of a solid-state detector and associated multichannel analyzer (MCA). The detector acquires the photon counts and MCA sorts them according to the energy to get energy versus intensity spectrum. WD XRF has better resolution compared to EDXRF. However, the presence of additional optical components like rotating crystal and collimators reduce efficiency and increase the cost of analysis. Moreover, the ability to analyze most of the elements in the periodic table, simultaneously makes ED XRF a better choice than WDXRF.

When a primary X-ray from an X-ray tube or a radioactive source strikes a sample, the X-ray can either be absorbed by the atom or can be scattered by the material [1]. The process in which an X-ray is absorbed by the atom by transferring all its energy to an innermost electron is called the "photoelectric effect". During this process, if the primary X-ray had sufficient energy, electrons are ejected from the inner shell creating vacancies leading to an unstable con-

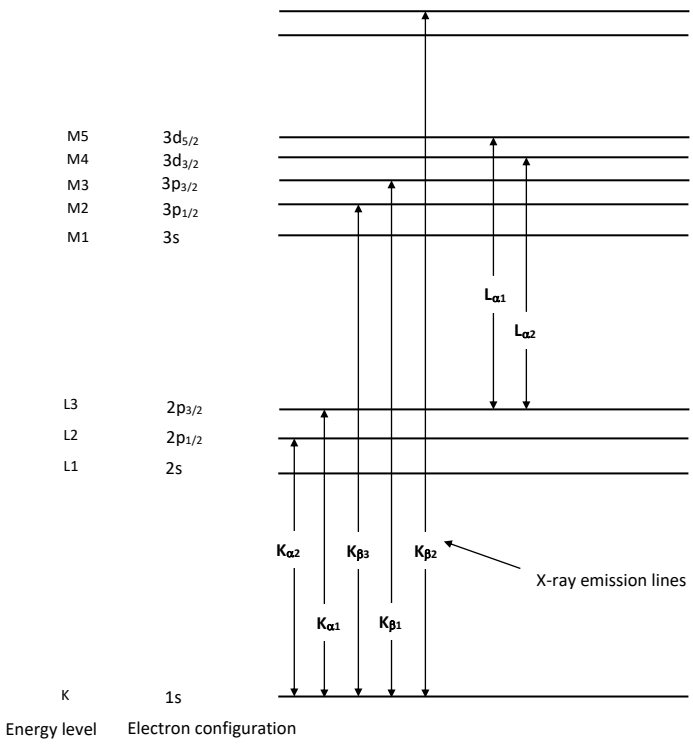

Figure 2.1: Energy level diagram showing X-ray transitions and notations

dition for the atom. As the atom returns to its stable state, electrons from the outer shells are transferred to the inner shells and the excess energy is emitted as electromagnetic radiations whose magnitude will be equal to the difference between the levels particular to the element excited. Hence, this acts as a signature of the element. The process of emission of characteristic X-ray is called X-ray Fluorescence (XRF). In addition to the radiative process of relaxation, a competing process of the Auger electron emission can also occur. The probabilities of X-ray emission and Auger emission are Z-dependent with the Auger yield higher for light elements and the fluorescence yield higher for heavy elements.

In most cases, the innermost K and L shells are involved in XRF detection. The characteristics X-rays are labelled as K, L, M, or N to denote the shells from which they originate. The energy level diagram showing the transitions and corresponding notations is given in Fig. 2.1 Another designation α, β *or* γ is made to mark the X-ray that originates from the transition of electrons from higher

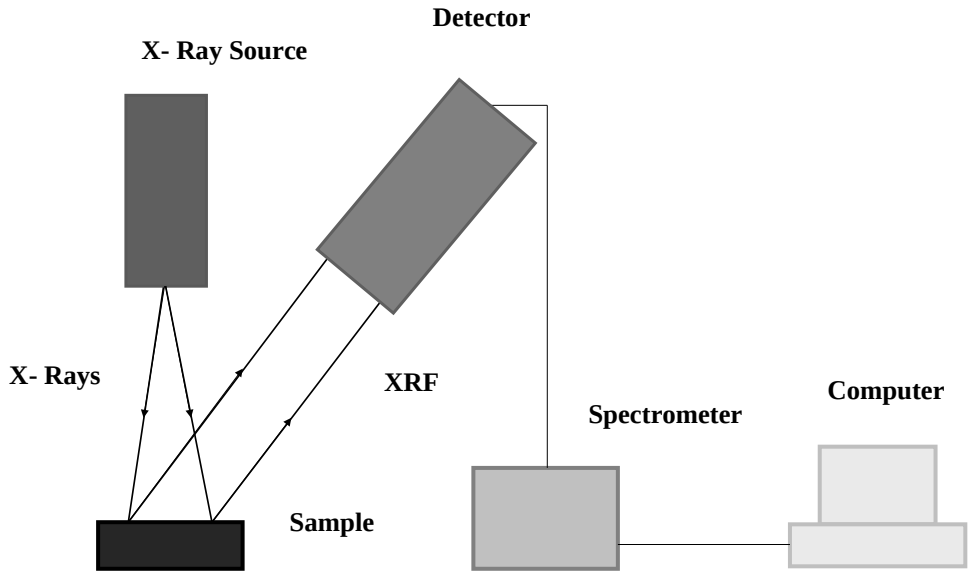

Figure 2.2: Schematic diagram of XRF setup

shells. Hence K_α X-ray is produced from a transition of an electron from the L to K shell, and a K_β X-ray is produced from a transition from an electron from the M to K shell, etc. While exciting the K-shell ($1s_{1/2}$), electron transition can occur between any of the two subshells, $2p_{3/2}$ or $2p_{1/2}$ subshells of L shell, leading to $K_{\alpha 1}$ and $K_{\alpha 2}$ respectively. Similarly, β_1 corresponds to the transition from subshells of M shell and so on. The detection system allows the determination of the energies of the emission lines and their intensities. Elements in a specimen are identified by their spectral line energies or wavelengths for qualitative analysis, and intensities are related to concentrations of elements providing the opportunity for quantitative analysis. A schematic diagram of the XRF setup is given in Fig. 2.2. Generally, the light and medium-mass elements are identified by their K X-rays ($20 < Z < 50$) and the heavy elements by L X-rays, as the detector efficiency, is lesser for K X-rays of heavy elements. The spectral data is converted into elemental concentrations by advanced software based on fun-

damental parameter methods or by empirical quantification method. The XRF method is widely used to measure the elemental composition of materials. Since this method is fast and non-destructive for the sample, it is the method advisable for analytical applications and industrial production.

2.1.2 Theory of XRF

When a beam of monochromatic, parallel X-rays of energy E_0 and intensity I_0 is incident on a sample of thickness x at an angle of incidence is 90^0, various interactions can take place [7]. A detailed description is given below.

Incident Radiation Absorption Effects

The incident beam is attenuated while traveling a pathlength x to reach the target. Therefore, the net intensity that reaches the sample volume is given by

$$I = I_0 \exp^{-\mu\rho x} \tag{2.1}$$

Here, μ is the mass absorption coefficient of the sample and ρ is the sample density. A fraction of the radiation that reaches the sample gets absorbed. The fraction of radiation intensity (dI) absorbed by the sample is given by

$$dI_s = \mu_s \rho dx \tag{2.2}$$

When there is more than one element in the sample, The intensity of radiation absorbed by the element i is given by

$$dI = \sum_i C_i \mu_i \rho_i dx \tag{2.3}$$

where C_i is the concentration of element i

The incoming intensity that is absorbed by element i in the volume element under consideration and thus available to produce K_α is given by

$$dI = I_0 C_i \mu_i \rho dx \exp^{-\mu_s \rho x} \tag{2.4}$$

Photoelectric Emission

The K_α fluorescence of element i is determined by the number of absorbed photons, as given in equation 2.4, and the probabilities associated with three atomic events: The probability that a K-shell electron will be ejected rather than an L or M shell electron, the probability of K_α emission in preference to other K lines, and the probability of K_α radiation rather than an Auger electron.

Absorption Jump Ratio

The first factor, the probability that a K shell electron will be ejected rather than an L- or M-shell electron, is given by K-shell "absorption jump ratio J_K:

$$J_k = \frac{r_K - 1}{r_K} \tag{2.5}$$

Here, r_K is the K-shell absorption jump defined as the ratio of the mass absorption coefficients at the K absorption edge $r_K = \mu_{max}/\mu_{min}$

Transition Probability

The probability that $K\alpha$ radiation will be emitted rather than another K line is called $g_{K\alpha}$ and is given by

$$g_{K\alpha} = \frac{I(K\alpha)}{[I(K\alpha) + I(K\alpha\beta)} \tag{2.6}$$

$$g_{K\alpha} = \frac{\frac{I(K\alpha)}{I(K\beta)}}{I(K\alpha)I(K\beta) + 1} \tag{2.7}$$

Fluorescence yield

The probability of emission of $K\alpha$ radiation rather than the production of an Auger electron, is called the fluorescence yield ω_K. Fluorescence yields have been determined both experimentally and theoretically.

Excitation factor

The product of the three probabilities gives us the excitation factor

$$Q = J_K g_{K\alpha} \omega_K = \frac{r_K - 1}{r_K} g_{K\alpha} \omega_K \tag{2.8}$$

Fluorescence Radiation Absorption

The fluorescent radiation (E_i) from element i in the volume element is attenuated while travelling the path length x to the detector. The fraction transmitted is given by $e^{-m_{s,E_i}\rho x}$

Since the fluorescence radiation is emitted uniformly in all direction, the fraction that enters the detector is given by $\frac{\Omega}{4\pi}$ where Ω is the solid angle defined by the detector which is approximately equal to $\pi a^2/d^2$. The intensity of primary fluorescence for i^{th} element is given by

$$I_i = I_0 C_i J_K g_{K\alpha} \omega_K \frac{\Omega}{4\pi} \frac{\mu_i}{\mu_s + \mu_{s,E_i}} \tag{2.9}$$

2.1.3 Advantages

XRF is an analytical technique that enables non-destructive analysis of materials in diverse sample types. The analysis of samples at low cost, with a wide elemental range is also an important advantage. Portable, handheld EDXRF instruments allow easy operation and better accessibility. The maintenance cost is also significantly lesser as compared to other nuclear analytical techniques.

2.2 Particle Induced X-ray Emision (PIXE)

2.2.1 Introduction

In 1970, Johanson et al. presented PIXE as a novel and powerful analytical method for elemental analysis. It involves the emission of characteristic X-rays from target atoms by the bombardment of 2-3 MeV proton beams. The characteristic X-rays acquired by suitable detectors provide a signature of the element qualitatively and quantitatively. The physical process behind PIXE is the creation of a vacancy in one of the core levels (K and L) of an element by the ion beam and its subsequent decay with the emission of characteristic X-ray. α- particles can also be used as probes in PIXE but the increase in background and complexity of spectra limit the applicability. PIXE is suitable for elements with Z>15. PIXE analysis can be done in the air directly, for larger samples like archaeological objects in external PIXE setup [8]. PIXE analysis of different sample types are available in the literature [9], [10], [11], [12], [13].

2.2.2 Theory of PIXE

When a charged particle (proton or heavier ion) enters a target material, it interacts inelastically with the sample atoms, thereby losing a fraction of its energy in each collision. As the particle moves forward through the medium, its energy decreases continuously, and the fractional loss depends on the nature of the medium, incident energy, type of the particle, all together called the stopping power. Typical stopping powers are available as atomic data sheets or coded programming. When high-energy protons or alpha particles collide with the target atoms, the atoms in the material get ionized. This results in the creation of vacancies in the inner shells, and the atom tries to regain its stability by filling the vacancy by a transition of electrons from outer shells. The probability of X-ray emission or the fluorescence yield is close to 1 for the heavy elements but less for the light elements. The notations of X-rays and transitions are already described in XRF. The characteristic X-ray produced were

acquired by a semiconductor detector, generally a Si-Li detector. This method is identified as a sensitive method for elemental analysis and depth profiling with much acceptability.

In PIXE, proton beam or helium ions are used as a projectile. In contrast to an electron beam, protons have certain advantages. In the case of electrons, momentum transfer is large, resulting in the loss of a larger fraction of energy wider scatter angle, and lesser penetration depth. In this case, as the mass is larger, a small fraction of momentum and energy is transferred, leading to a lesser angle of scattering and higher penetration depth. This increases the number of fluorescent radiations produced and hence get better counts.

The proton beam in PIXE is produced by accelerators where the negative charge for acceleration is supplied by a Multi-Cathode SNICS (Source of Negative ion by Caesium Ion Sputtering) source or by alpha-emitting sources like Cm-244. A schematic representation of the accelerator is given in Fig. 2.3. The ion gains energy due to the presence of an electric field within the accelerator due to the high potential difference between the terminals. The beam coming from the accelerator passes first through a bending magnet and is stabilized by passing through a slit. The beam is then directed axially down the beam-line using electrostatic and magnetic steering elements to the scattering chamber. The targets are loaded in the target ladder of desired geometry to avoid frequent opening and evacuation. The beam is incident generally at an angle 45^0 with respect to the target face. This ensures the detection of the fluorescent beam scattered at an angle 90 ^{0} with respect to the incident beam. In order to monitor the incident flux, the transmitted beam is directly fed to the Faraday cup that will provide information on the total charge collected, thereby act as charge integrator.

In PIXE, X-ray detectors like lithium drifted silicon, Si (Li) detector can be used to detect the X-rays produced. Si-Li is a detector with high energy resolution (about 160 - 180 eV for 5.9 keV photon). It comprises a cylindrical section of a single crystal of P-type silicon. Lithium is drifted into it under

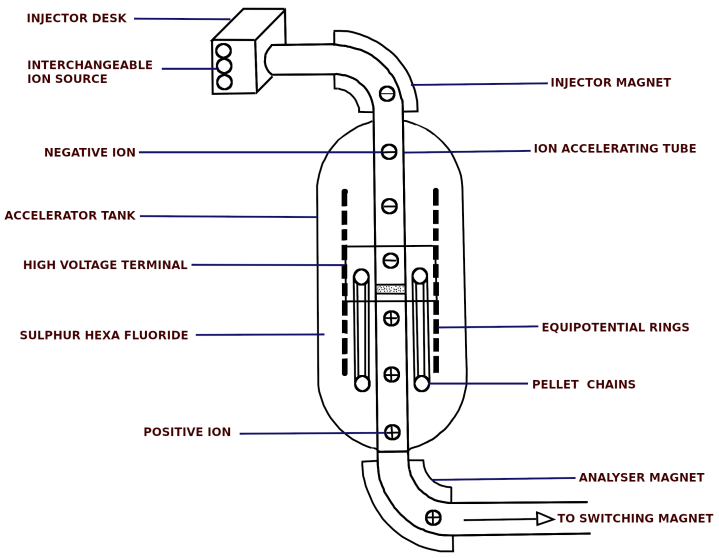

Figure 2.3: Schematic diagram of pelletron accelerator

high temperature so that a charge free volume called sensitive region depleted of charges is formed. The sensitive volume ranges from 4 to 16 mm in diameter, and 3 to 5-inch thickness, depending on the derived application. The smaller diameter detectors provide better energy resolution at low energies, and the thicker detectors have higher detection efficiency at energies approximately above 20 keV. When an X-ray photon reaches the detector, a cloud of electron hole pairs will be generated. The number of electron-hole pairs created is proportional to the energy of the detected photon. The detector bias voltage sweeps the charge to a charge sensitive pre-amplifier. The preamplifier collects this charge to produce an output pulse whose voltage amplitude is proportional to the original X-ray photon energy. The Si(Li) detector along with the first stage and feedback elements of the preamplifier are mounted in cryostats and operated at the liquid nitrogen temperature (77K) to minimize the electronic noise added to the signal. The X-rays from the target sample enter the detector through a thin beryllium

window of typically 8-25.4 pm thickness. The thickness of the window sets the lower energy limit for photons that can be detected by the detector.

The sensitivity of PIXE depends on various factors. For low Z elements, the higher X-ray production cross-section increase the sensitivity. For high Z elements, lower background increases the signal to noise ratio and improves sensitivity. But the efficiency of semiconductor detectors like Si-Li is low for high X-ray energies above 25 keV. Hence L X-rays, which have lower intensity are used for the detection of low Z elements. At higher beam energies, sensitivity is reduced for low Z elements due to background produced by projectile induced nuclear reactions. But at higher Z better sensitivity is achieved. Johansson et al. showed the variation of the minimum detectable concentration as a function of atomic number [14].

2.2.3 Background

A PIXE spectrum usually consists of two major components namely the peaks due to characteristic x-rays and the background continuum. The identification of characteristic X-rays produced by an interaction between a heavy charged particle and a solid target in elemental analysis of complex matrix, depends heavily on the background [15]. Secondary electron bremsstrahlung, primary proton bremsstrahlung, and nuclear reaction gamma rays are the three important factors that contribute to the background. Secondary electron bremsstrahlung is the major component of the continuous background in PIXE. The intensity of secondary electron Bremsstrahlung is very strong at low energies but it decreases rapidly when the photon energy becomes larger than the maximum energy that can be transferred from a projectile to an electron. Projectile bremsstrahlung background is produced as a result of the incident beam getting slowed down in the target, due to Coulomb interaction between the electron and the nuclei. Classically, the bremsstrahlung intensity emitted by a charged particle is proportional to the square of its deceleration. As the mass of the proton is smaller by a factor of 1836, the intensity of proton bremsstrahlung will be reduced by a

factor of $1/(1836)^2$. Hence it is negligible, in the energies of interest. In PIXE, there is a possibility of nuclear reactions to occur in the light elements (Z<20) resulting emission of gamma rays. The gamma rays interact with the detector through Compton scattering in the detector. This background depends on the particular elements present in the specimen and on the cross-sections of the reactions induced. This will be important in the analysis of a system containing multielement composition.

2.2.4 Data analysis Softwares

The determination of X-ray yield from the PIXE spectrum and its correlation to the corresponding elemental concentration forms the basis of quantitative PIXE analysis. Extraction of X-ray intensities from the PIXE spectrum is the first step in the quantification procedure which involves the least square fitting of a model spectrum to the experimental one. There are different software for the conversion of X-ray intensity to elemental concentrations namely GUPIX [8], PIXAN [17], GEOPIXE, [18], DATTPIXE [19], SAPIX[20], etc. The main difference between them arises from the different approaches in the treatment of background and peak shape. In addition to the fitting routines, most of the present PIXE software packages calculate elemental concentrations directly from a PIXE spectrum. One of the most used software is the GUPIX software package that includes spectrum fitting and quantitative analysis. The digital top hat filter removes the background and doubly differentiates Gaussian peaks. Using the complete fundamental parameter database and by appropriate modelling of the peak line shape, the number of parameters is reduced to one per element. Filtered data are compared to a model spectrum using the nonlinear least squares fit.

2.3 Neutron Activation Analysis (NAA)

2.3.1 Introduction

NAA is a physical technique based on nuclear reactions. When a neutron interacts with a target nucleus through inelastic collision, a compound nucleus is formed in the excited state. The compound nucleus will de-excite almost instantaneously to a more stable configuration through the emission of one or more characteristic prompt gamma rays. In many cases, this new configuration yields a radioactive nucleus that decays by emission of β particles with its particular half-life. The nucleus thus formed due to β emission will be excited, which will de-excite by the emission of γ rays. These gamma rays act as a delayed γ ray of the parent nucleus. This γ rays act as the signature of the element in the sample. A schematic diagram of the process of NAA is shown in Fig. 2.4.

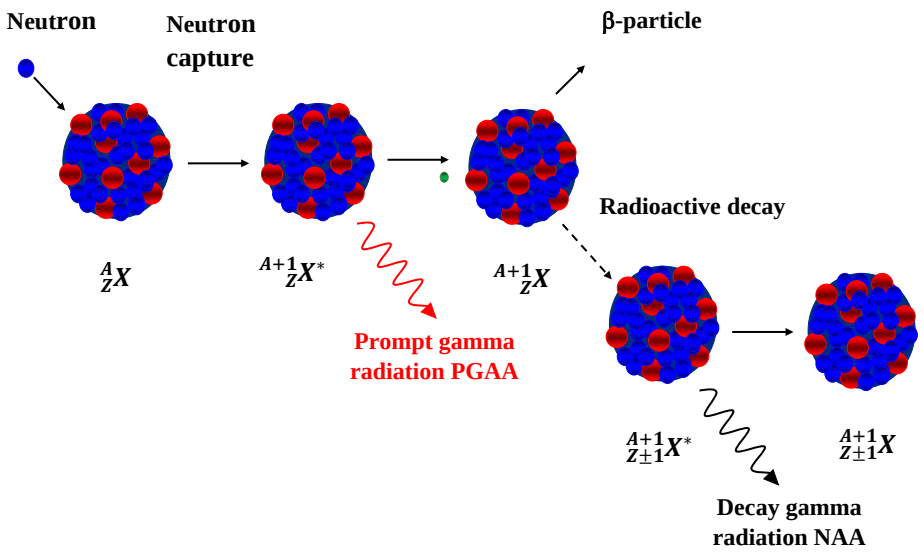

Figure 2.4: Basic processes underlying in NAA

In 1936, G. Hevesy and H. Levi determined the sub milligram quan-

tities of Dy in a rare earth sample by bombarding it with neutrons obtained from radium-beryllium source [21]. This marked the era of activation analysis for the determination of elemental composition in diverse sample types with high sensitivity and accuracy. The development of highly sensitive detectors like HPGe improved the detection limits. NAA can enhance the quality assurance capabilities of products non-destructively compared to ICPMS. It is considered as a 3-dimensional spectroscopic technique where alternative nuclides, alternate gamma rays, various decay lines, and multiple counting can be used to eliminate interferences and enhance analytical parameters.

2.3.2 Theory of NAA

Consider a sample with N_t number of target nuclei is exposed to neutrons of flux ϕ. The neutron capture cross section of the target element is given by σ. The rate at which the nuclei in the sample get activated is given by

$$\left[\frac{dN_p}{dt}\right] = N_t\sigma\phi - \lambda N_p \tag{2.10}$$

Where N_p is the number of product nuclei formed and λ is the decay constant of the product nucleus. Consider that the sample was irradiated for a duration t_1. During this time, the process of simultaneous excitation and decay occur until the activity reaches saturation. After time t_1 the induced activity will be

$$A = N_t\sigma\phi(1 - exp(-\lambda t_1)) \tag{2.11}$$

Here $S = 1 - exp(-\lambda t_1)$ is called the saturation correction factor. Let t_2 and t_3 be the cooling and counting times respectively. Considering the decay of nuclei during the cooling period

$$A = (N_t\sigma\phi)\{1 - exp(-\lambda t_1)\}\{exp(-\lambda t_2)\} \tag{2.12}$$

where $D = exp(-\lambda t_2)$ is called the decay correction

$$A = (N_A \theta \frac{m}{M} \sigma \phi)\{1 - exp(-\lambda t_1)\}\{exp(-\lambda t_2)\} \tag{2.13}$$

where N_A is the Avogado number, θ is the abundance of the isotope of interest, m is the mass of the element and M is the atomic mass of the element. The count rate (cps) acquired by a detector of efficiency ϵ under a photo peak is given by,

$$cps = (N_A \theta \frac{m}{M} \sigma \phi \epsilon \gamma)\{1 - exp(-\lambda t_1)\}\{exp(-\lambda t_2)\}\frac{\{1 - exp(-\lambda t_3)\}}{\lambda t_3} \tag{2.14}$$

where γ is the branching ratio of the γ ray. Then, the quantity of the element in the target sample can be obtained using the equation,

$$m = \frac{cpsXM}{(N_A \theta \sigma \phi \epsilon \gamma)\{1 - exp(-\lambda t_1)\}\{exp(-\lambda t_2)\}\frac{\{1-exp(-\lambda t_3)\}}{\lambda t_3}} \tag{2.15}$$

where, cps represents the counts per second, M is the atomic mass, N_A is the Avogadro number, θ is the abundance , σ is the neutron capture cross-section, ϕ is the incident thermal neutron flux, ϵ geometry dependent efficiency of the detector for the given gamma-ray energy, γ is the branching ratio of the particular gamma-ray, λ is the decay constant of the particular residual nucleus, t_1, t_2 and t_3 are the irradiation time, the cooling time and the counting times respectively.

2.3.3 Different methodologies in NAA

Depending on whether sample analysis is carried out with or without chemical separation, the NAA is classified into different types. If elements of interest can be determined without any chemical treatment, the process is called instrumental neutron activation (INAA). The advantage of this method is its non-destructive nature, minimal sample handling, multi-element capability, and no reagent-blank correction. When the concentration of elements of interest is below the detection limit of INAA, pre-or post-chemical separation is needed. In pre-concentration NAA (PNAA), the element of interest is separated before the

irradiation whereas in Radioisotopic NAA (RNAA), the radioisotope of interest is separated post-irradiation. Derivative NAA (DNAA) is used when the elements of interest are poorly determined by conventional NAA or does not have any characteristic gamma line, the elements are chemically complexed with an element that is amenable to NAA. When a radioisotope is short-lived, the cycle of cooling is repeated several times and the cumulative activities improve the signal to background ratio and discriminate long lived interfering nuclei. This is called cumulative instrumental neutron activation (CINAA) and is carried out using automated equipment that can control short irradiation, quick transfer of sample, and short counting of the sample. For an improved signal to back ground ratio and detection limit, the process can be repeated several times.

The simplest of these which can be non-destructively used with simpler sample preparation procedures is INAA. As the neutron energy distributions are quite broad and consist of three principal components thermal, epi-thermal, and fast, INAA can be divided into three types accordingly. The thermal neutron component consists of low-energy neutrons (0.025 eV- 0.55 eV) in thermal equilibrium with atoms in the reactor's moderator. In irradiation positions of most of the reactors, 90-95% of the neutrons that bombard a sample are thermal neutrons (energy of the order of 0.025 eV). In general, a one-megawatt reactor has a peak thermal neutron flux of approximately 10^{13} ncm^{-2} s^{-1}. If the energy of neutron spans from 0.2 to 500 keV it is epithermal NAA (ENAA). In ENAA, the total activity due to Na, K, Mn, Cl, Al, Br and La are suppressed. Nuclides of elements with high resonance integral to thermal neutron capture cross-section ratio, $Q_0\rangle 10$ such as Ag, As, Ba, Br, Cd, Cs, Ga, Gd, In, Mo, Ni, Pd, Pt, Rb, Sb, Se, Sm, Ta, Sr, and W can be detected effectively with this method. Here the samples are kept in thick boron or cadmium box and irradiated. Cd/B absorbs thermal neutrons and filter out the high energy neutrons. The detection limit is higher than the thermal neutron activation. FNAA can determine the concentration of O, N, F, Mg, Si, and P which are otherwise difficult with TNAA. The fast neutron component of the neutron spectrum (energies above 0.5 MeV)

consists of the primary fission yielding neutrons which still have much of their original energy following fission. In a typical reactor irradiation position, about 5% of the total flux consists of fast neutrons. NAA technique that employs nuclear reactions induced by fast neutrons is called fast neutron activation analyses (FNAA). The (n, γ) reactions of thermal neutrons and the $(n, x\gamma)$ reaction of fast neutrons are quite complementary to each other.

2.3.4 Standardization methods in NAA

There are different standardization methods adopted for the determination of elemental concentrations in NAA. In the absolute method of standardization, the mass of analyte element is directly determined using nuclear reaction-based data. Details of this method are discussed in section 2.3. The expression of mass of the element m in the sample can be obtained by equations 2.15. This method is not commonly practiced, as the determination of absolute values of σ and ϕ is difficult. Both parameters vary significantly with neutron energy. Moreover, the uncertainties associated with the absolute value of epi-thermal (n,γ) cross-sections, θ, and M contribute to the final result. Hence relative methodology is commonly used in NAA.

In this method an elemental standard is co-irradiated with the sample and the activities from both the sample and the standard are measured in identical conditions with respect to the detector. This method is simple as it does not need nuclear and reactor-based input parameters. The number of particles of element x in the target sample, denoted by $N_{t,(x,s)}$ is given by the equation,

$$N_{t,(x,s)} = \frac{A_{(x,s)}\lambda\Big[exp(\lambda t_2)\Big]_{(x,s)}}{\sigma\phi\theta\epsilon K\Big[1-exp(-\lambda t_1)\Big]_{(x,s)}\Big[1-exp(-\lambda t_3)\Big]_{(x,s)}} \tag{2.16}$$

where,

$N_{t,(x,s)}$ is the number of the target isotope per unit area of the irradiated sample,

S=$\left[1 - exp(-\lambda t_1)\right]_{(x,s)}$ represents the saturation correction of the sample,

D=$\left[exp(-\lambda t_2)\right]_{(x,s)}$ represents the decay correction of the sample,

C=$\frac{\left[1-exp(-\lambda t_3)\right]_{(x,s)}}{\lambda_{t3}}$ represents the counting correction of the sample,

The number of target particles in the referecnce sample $N_{t,(x,s)}$ is given by

$$N_{t,(x,r)} = \frac{A_{(x,r)}\lambda\left[exp(\lambda t_2)\right]_{(x,r)}}{\sigma\phi\theta\epsilon K\left[1 - exp(-\lambda t_1)\right]_{(x,r)}\left[1 - exp(-\lambda t_3)\right]_{(x,r)}} \tag{2.17}$$

Here the term (x,r) represents the values for the same quantities for element x in the reference sample.

Taking the ratios of the two equation, we get the expression to determine the number of particles in the unknown sample as,

$$N_{t,(x,s)} = N_{t,(x,r)}\frac{A_{(x,s)}\left[exp(\lambda t_2)\right]_{(x,s)}\left[1 - exp(-\lambda t_1)\right]_{(x,r)}\left[1 - exp(-\lambda t_3)\right]_{(x,r)}}{A_{(x,r)}\left[exp(\lambda t_2)\right]_{(x,r)}\left[1 - exp(-\lambda t_1)\right]_{(x,s)}\left[1 - exp(-\lambda t_3)\right]_{(x,s)}} \tag{2.18}$$

Single comparator or k_0 method

k_0 NAA involves the simultaneous irradiation of sample and neutron flux monitor and use of composite nuclear constant k_0 . Generally, Au is used as the flux monitor. It obviates the preparation of standards for each element. Prior knowledge of constituents in the sample is not needed. It includes the counts under a peak (CPS), sub cadmium to epi-thermal neutron ratio (f)m, epi-thermal neutron flux shape (α), absolute/relative efficiency of the detector, and two nuclear constants k_0 and Q_0. (f)m and α depends on the irradiation facility.

k_0 is defined as,

$$k_0 = \frac{M'\Theta\sigma_0\theta}{M\Theta'\sigma_0'\theta'} \tag{2.19}$$

M and M' are the atomic weights of the elements and monitor, Θ is the isotopic abundance of the target nucleus, σ_0 is the thermal neutron activation cross section for the (n,γ) reaction, θ is the branching ratio of the gamma energy, Here the primed quantities refer to the comparator sample. k_0 method is based on the Hogdahl convention [22] and the expression for the k_0 is given by

$$k_0 = \frac{\frac{\frac{N_p}{t}}{SDCW}}{\frac{\frac{N_p}{t}}{SDCw}} \frac{1}{k_0} \frac{(f + Q_0(\alpha)'\epsilon'}{(f + Q_0(\alpha)\epsilon} \tag{2.20}$$

Here w and W are the mass of the comparator and mass of the sample and t is the live time of counting.

$$Q_0(\alpha) = \frac{Q_0 - 0.429}{E_\gamma^\alpha} + \frac{0.429}{(2\alpha + 1)E_{Cd}^\alpha} \tag{2.21}$$

k_0 factor is available in literature [23]. The final expression of the concentration of element i with respect to the mono-standard is given by,

$$\frac{m_i}{m_i'} = \frac{[SDC(f + Q_0(\alpha))]_i'}{[SDC(f + Q_0(\alpha))]_i} \frac{P_A i}{P_A i'} \frac{\epsilon_\gamma}{\epsilon_\gamma i} \frac{(k_{0,Au}(i)')}{(k_{0,Au}(i))} \tag{2.22}$$

The relative concentration is converted into absolute concentration by using the mass of the mono-standard.

2.3.5 Advantages and Limitations

NAA is very well suited for the detection of trace elements in diverse sample types with high sensitivity. This method possesses inherent accuracy as the elemental concentration obtained can be verified by using multiple gamma rays of the same element. The detection of more than one isotope for the same element also improves the reliability of the method. As the gamma rays from the

excited nuclei are detected, the uncertainty due to matrix effects will be minimal. Moreover, the use of the relative method gives better results by making the results independent of variations in neutron flux. Irrespective of the various advantages of NAA, there are some limitations. Neutron flux of the order of 10^{13} ncm$^{-2}s^{-1}$ is needed to get better sensitivity which requires reactor facilities. Neutron self-shielding at resonance energies reduce the neutron flux due to absorption and scattering. Gamma-ray spectral interferences and self-attenuation in the sample material, also influence the quality of the results. The time required to conduct analysis is also significantly high. This limits the application of NAA at industrial and commercial levels.

2.4 Photon Activation Analysis (PAA)

2.4.1 Introduction

A photo-nuclear reaction is characterized by giant dipole resonance. When the wavelength of the photon becomes similar to the diameter of the nucleus, the photon can be absorbed by the target through electric dipole resonance and there occurs a collective oscillation of all the protons against all neutrons. Photons produced by Bremsstrahlung is preferably used for activation in photon activation analysis. With elements of high atomic number (W, Pb) as bremsstrahlung converter, photon flux can be efficiently generated with the help of high energy electronic accelerators. When a high energy electron interacts with matter, energy is lost as radiation whose magnitude is proportional to Z^2. Elements with higher atomic numbers like W, Pb, etc. produce efficient bremsstrahlung suitable for photon activation. The pioneering work in the field of photonuclear reactions is credited to Chadwick and Goldhaber [24]. They used 2.62 MeV γ rays from ^{208}Tl as excitation source for photo-disintegration of deuterons. Later microtrons, synchrotrons and betatrons were used to induce photonuclear reactions.

High energy bremsstrahlung photons from electronic accelerators used for radiation therapy can induce photo-nuclear reactions. $(\gamma, \gamma'), (\gamma, n), (\gamma, p)$

and (γ, α) are found to be the prominent nuclear reactions possible in this energy range. Bremsstrahlung photons are produced when electrons are decelerated by Coulomb repulsion. It is directed in the forward direction with a continuous energy distribution with a maximum energy equal to the electron acceleration energy. Bremsstrahlung photons interact with the nucleus and the cross sections of these reactions are about hundred times larger than that of nuclear reactions induced by electrons of same energy. These reactions produce radioisotopes which emit γ radiation and act as signature of that element.

Photonuclear cross section depends on probability of photon absorption. At energies lower than a few MeV, inelastic(γ, γ') reactions are possible, but the cross-section integrals for these isomeric transition reactions are very small. The cross-sections for (γ, n) reaction is sufficiently larger compared to the direct process. The most suitable energy range for photon activation is 20 MeV as it covers the giant resonance of most of the nuclides.

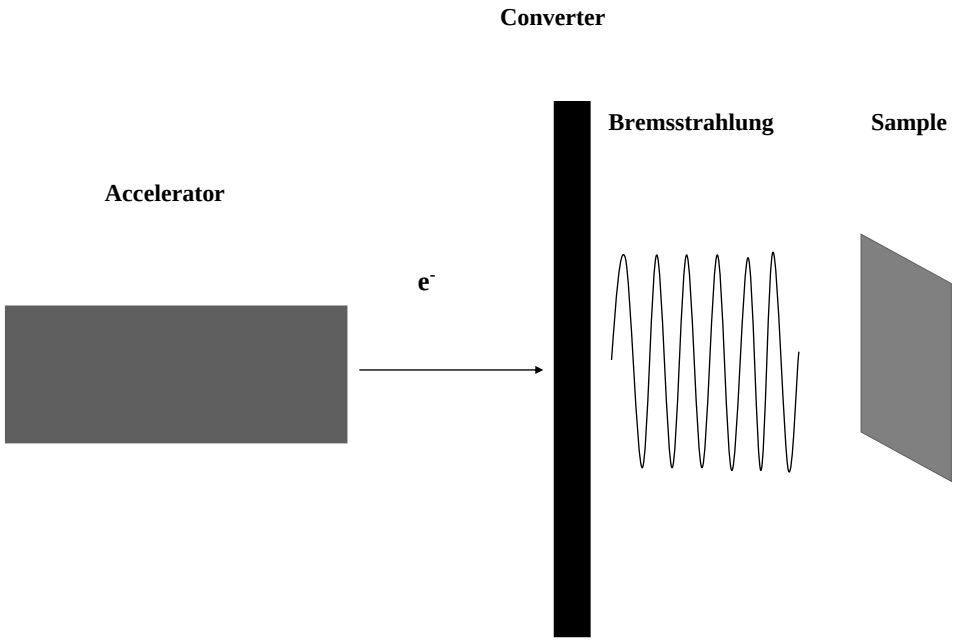

Figure 2.5: Schematic diagram of Photon Activation

Radio isotopes like ^{124} Sb were used as excitation source in the analysis of samples like beryllium, deuterium, etc. But the photon flux is not sufficient for practical application where the elements of interest are of ppm levels and the cross-sections are low. Photon activation has several advantages compared to neutron activation. Elements such as Be, C, N, O, F, Si, P, Ni, Tl, Pb and Bi which are difficult to detect by NAA can be quantified with high detection power in PAA [25]. Excessive matrix activity, inhomogeneous activation due to large absorption cross-sections, etc. are significantly reduced in PAA. Moreover, the uncertainty caused by self-shielding due to the resonance behaviour of neutron spectrum at the epithermal region [26] is eliminated. Compared to NAA, the penetration power is high for PAA. Photons penetrate deeper into the medium and hence larger samples can be analyzed without destruction of the sample [27]. Moreover, the limited availability of NAA facilities, as it requires reactor set up in order to impart high flux of neutrons of the order of $10^{13} ncm^{-2}s^{-1}$, poses a severe constraint for NAA. Considering these aspects, a method of trace elemental analysis of multi-elemental samples using medical LINAC (Linear Accelerator) is a promising technique. Canel et al. (2016) and Chaoa et al. (2009) and Stamatelatos (2016) et al. reported the application of medical LINAC for the analysis of different sample types [28], [29], [30]. The growing demand for medical LINACs for treatment purposes provides better accessibility to the photon source for activation analysis. Application of PAA for the quantitative determination of elemental composition of herbal samples is also an emerging area of research.

2.4.2 Theory of PAA

In PAA, the nuclides present in the target sample are made radioactive through exposure to high energy photons. The nuclei undergo radiative decay and emit characteristic gamma lines. The elemental concentration is calculated from the reaction yield corresponding to the respective energies using the for-

mula,

$$C_m = \frac{mN_A\epsilon\theta\Theta}{A}\frac{(1-\exp^{-\lambda t_1})(1-\exp^{-\lambda t_2})\exp^{(-\lambda t_3)}}{\lambda t_2}\int_{E_{th}}^{E_{max}}\sigma(E)\phi(E)dE \quad (2.23)$$

where m is the mass of the sample, N_A is the Avogadro number, ϵ is the energy-dependent efficiency of the detector, θ is the branching ratio, Θ is the abundance of the natural isotope, A is the atomic mass of the target isotope, σ is the spectrum averaged cross-section, ϕ is the normalized flux of photons, λ is the decay constant of the particular isotope, t_1 is the irradiation time, t_2 is the cooling time, and t_3 is the counting time in seconds. For the monitor In, the number of particles per unit area undergoing exposure is calculated from the weight of the sample. The ratio method is used to find the number of particles present in the sample belonging to each element. A schematic diagram of the photon activation setup is shown in Fig. 2.5

2.5 Inductively Coupled Plasma Mass Spectroscopy (ICPMS)

2.5.1 Introduction

ICP-MS is a powerful analytical technique for the determination of trace and ultra-trace elements in biological materials. It measures the mass-to-charge ratio of ions, generated by a high-temperature argon plasma. ICPMS offers very high sensitivity over a wide range of elements. This technique is highly expensive but offers the best characteristics of all the atomic spectrometry methods in terms of sensitivity, throughput, and multielement measurement. A schematic diagram of the setup of ICPMS is shown in Fig. 2.6

2.5.2 Theory of ICPMS

The basic principle behind mass spectrometry is the transport of charged particles in an electromagnetic field. When a charge of q moves in a crossed electromagnetic field, Lorentz force, F comes in to play which deviates the path

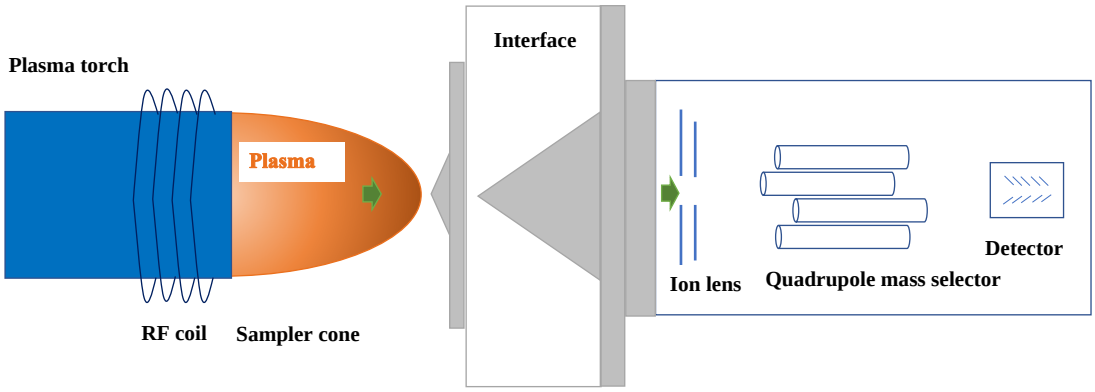

Figure 2.6: Schematic diagram of ICPMS spectrometer

of the ion, whose magnitude is given by,

$$F = qvB \tag{2.24}$$

The ion follows a circular path whose radius is defined by the formula,

$$r = \sqrt{\frac{2mV}{qB^2}} \tag{2.25}$$

For a given electromagnetic field, in case of singly charged ion species, the radius of the trajectory depends only on m/q of the ion. Hence the number of ions of each species in the plasma can be determined by using a suitable detector and associated circuitry.

Microwave-assisted sample digestion method utilizing solvents like HNO_3, H_2SO_4, HCl and HF are used for efficient sample digestion [31]. The liquid samples are first nebulized in the sample introduction system, creating a

fine aerosol, that is subsequently transferred to the argon plasma. The high-temperature plasma atomizes and ionizes the sample, generating ions of the species. The ions transport is optimized by electrostatic quadrupole and Einzel lenses and the stream of ions enter the mass analyzer. The mass analyzer separates ions according to their mass-charge ratio (m/q), and these ions are measured at the detector.

Most elements form singly charged positive ions; however, some elements may also form a small fraction of double-charged ions. The degree to which an element is ionized depends on the temperature of the plasma and the ionization potential of the element. Fortunately, most elements have a first ionization potential much lower than argon and are therefore efficiently ionized in the plasma. Hence ICP-MS is suitable to measure nearly all elements in the periodic table. The concentration of elements present in the sample can be determined through calibration of the detector with certified reference materials consisting of the elements of interest.

2.6 Other Techniques for Trace Elemental Analysis

Atomic Absorption Spectrometry (AAS)

AAS uses the electronic absorption characteristic of an element. This technique uses a wavelength of light specifically absorbed by an element. Atoms absorb UV or visible light and make transitions to higher electronic states. The energies correspond to the energy needed for electronic transition in the element. The analyte concentration is determined from the amount of absorbed radiation. Atoms of different elements absorb characteristic wavelengths of light. For determination of a particular element, that light which the element absorbs is made to fall on the sample. The magnitude of absorbed radiation will be directly proportional to the number of atoms in the sample. This method is very popular as it is cheaper compared to other techniques but, there are many drawbacks

to this method. The analysis of different elements is not simultaneous in AAS. Moreover, AAS is a destructive method and is less sensitive compared to ion beam techniques.

Rutherford Back Scattering Spectrometry (RBS)

It is based on the classical gold foil experiment of Rutherford [32]. RBS involves the measurement of energy and yield of ions backscattered from the atoms in a sample. In RBS, the projectiles elastically backscattered from nuclei of sample atoms are recorded. The measured energy depends on the mass of the target nucleus and thus on the isotope of the element and also on the depth of the scattering event beneath the surface. RBS is generally performed with 2-2.5 MeV α particles.

Elastic Recoil Detection Analysis (ERDA)

ERDA is a useful multi-element technique suitable for depth profiling of light elements. The basic principle governing ERDA is identical to RBS. It involves the bombardment of the target with an ion beam and detection and analysis of the recoils from the target in the forward direction. A particle filter of suitable thickness is placed in front of the recoil detector to prevent the ion beam scattered in the forward direction from being counted. Atoms of different elements with different masses recoiled from the surface appear at different energies that depend on the stopping power of the target and the thickness of the stopper foil.

Particle Induced Gamma Emission (PIGE)

PIGE involves the measurement of prompt γ rays emanating from a nuclear reaction induced by the incident ion beam of a few MeV protons from an accelerator. This technique provides sensitive determination of low Z elements such as B, Li, F, Na, Al, Mg, and Si. Hence it is complementary to PIXE.

Bibliography

[1] Ron Jenkins(1999) X-Ray Fluorescence Spectrometry, Volume 152, Second Edition, John Wiley & Sons, Inc. DOI:10.1002/9781118521014

[2] M Mantler, M Schreiner (2000) X-Ray Fluorescence spectrometry in Art and archaeology. X-Ray Spectrometry. 29: 3–17

[3] Khuder, MKh Sawan, J Karjou, A K Razouk (2009) Determination of trace elements in Syrian medicinal plants and their infusions by energy dispersive X-ray fluorescence and total reflection X-ray fluorescence spectrometry. Spectrochim. Acta B 64:721–725

[4] T Weizhi, B Ni, W Pingsheng, N Huiling (2000) Suitability of NAA for certification of reference materials for multi-elements. J Radioanal Nucl Chem. 245:51-56

[5] Cristache, O G Duliu, C Ricman, M Toma et al. (2008) Determination of elemental content in geological samples. Rom J Phys. 53: 941–94

[6] T. P. Schreiber; A. M. Wims (1982). Relative intensity factors for K, L and M shell x-ray lines X-ray spectrometry, 11(2), 42–45. doi:10.1002/xrs.1300110203

[7] Volker Thomson (2007) Spectroscopy, 22(5)

[8] V. Vijayan, R. K. Choudhury, B. Mallick, S. Sahu, S. K. Choudhary, H. P. Lenka, T. R. Rautray, P. K. Nayak (2003), External particle induced x-ray emission, Current Science, 85:6, 772

[9] B. Tripathy, Tapash R. Rautray, A.C. Rautray, V. Vijayan (2010), Applied Radiation and Isotopes 68, 454–458

[10] A.K. Mohanty, S.K. Das V. Vijayan, D. Sengupta, S.K. Saha (2003), Nuclear Instruments and Methods in Physics Research B 211, 145–154

[11] Oyuntsetseg Bolormaa, Jamsranjav Baasansuren, Katsunori Kawasaki, Makiko Watanabe, Toshiyuki Hattroi (2007), Nuclear Instruments and Methods in Physics Research B 262, 385–390

[12] P. Sarita, G. J. Naga Raju, M. Ravi Kumar, A. S. Pradeep, S. Bhuloka Reddy (2013), J Radioanal Nucl Chem, 297:431–436, DOI 10.1007/s10967-012-2398-2

[13] S. Bhuloka Reddy, M. John Charles, G.J. Naga Raju, V. Vijayan, B. Seetharami Reddy, M. Ravi Kumar, B. Sundareswar

[14] S. A. E. Johansson, and T. B. Johansson(1976), Nucl. Instr. Meth, 137, 473.

[15] F. Folkmann, G. Gaarde, T. Huus, and K. Kemp (1974), Nucl. Instr. Meth. 116, 487

[16] Maxwell, J. A., Campbell, J. L., Teesdale, W. J. (1989). Nuclear Instruments and Methods in Physics Research Section B: Beam Interactions with Materials and Atoms, 43(2), 218–230. doi:10.1016/0168-583x(89)90042-6

[17] CLAYTON, E., PIXAN (1986), The Lucas Heights PIXE Analysis Computer Package, AAEC/M113.

[18] Ryan, C. G., Cousens, D. R., Sie, S. H., Griffin, W. L. (1990). Nuclear Instruments and Methods in Physics Research Section B: Beam Interactions with Materials and Atoms, 49(1-4), 271–276. doi:10.1016/0168-583x(90)90259-w

[19] M.A. Reis and L.C. Alves (1992), Nuclear Instruments and Methods in Physics Research B68, 300-304

[20] Sera, K., Futatsugawa, S. (1996).Nuclear Instruments and Methods in Physics Research Section B: Beam Interactions with Materials and Atoms, 109-110, 99–104. doi:10.1016/0168-583x(95)01208-7

[21] G. Hevesy, Hilde Levi (1936) NATURE, 185

[22] OT. Hogdahl (1965), Proceedings of Symposium Radiochemical Methods of Analysis, IAEA, 1(23)

[23] Frans De Corte, Andras Simonits (2003), Atomic data and Nuclear data tables 85, 47-27

[24] J. Chadwick, M. Goldhaber (1934), Nature, 134,237

[25] Avino P, Petrucci A, Schulze D, Segebade C (2019), Encyclopedia of Analytical Science, 3rd Edn, 25.

[26] Pytel K, Jozefowicz K, Pytel B, Koziel A (2004), Radiat Prot Dosimetry, 110, 823.

[27] Ni J, Xu X G, Block R C, Bopp R F (2000), Int J Environ Anal Chem, 78, 117.

[28] Eke C, Boztosun I, Dapo H, Segebade C, Bayram E (2016), J Radioanal Nucl Chem, 309, 79.

[29] Chaoa J H, Liub M T, Yehc S A, Huangb S S, Wuc J M, Changa Y L, Hsua F Y, Chuange C Y, Liue H Y, Sune Y C (2009), Appl Radiat Isot, 67, 1121.

[30] Stamatelatoes I E, Vasilopoulou T, Filippaki E, Georgolopoulou P, Ntalla E, Bassiakos Y (2016), J Radioanal Nucl Chem, 309, 165.

[31] Stefania Gaudino, Chiara Galas, Maria Belli, Sabrina Barbizzi, Paolo de Zorzi, Radojko Jacimovi, Zvonka Jeran, Alessandra Pati, Umberto Sansone (2007) Accred Qual Assur12:84–93 DOI 10.1007/s00769-006-0238-1

[32] Rutherford E. (1919), Philosophical Magazine 6 th series, vol 37

[33] TENDL-2017, https:// tendl.web.psi.ch 2017

[34] https://www-nds.iaea.org/relnsd/vcharthtml/VChartHTML.html

[35] Kazuyoshi Masumoto, Christian Segebade, Encyclopedia of Analytical chemistry, R. A. Meyers (Ed.) Copyright John Wiley anfd Sons

Chapter 3

Materials and Methods

Samples of Triphala Churna, Amalakyadi Churna, Chaturbhadrika Churna, and Nishakatakadi Decoction are analyzed using different techniques like XRF, PIXE, NAA, PAA, and ICPMS. Details of the samples and their preparation are discussed in this chapter. The detailed description of the experimental setup and measurement are also discussed in the following sections.

3.1 Sample Details

Herbal sample Phyllanthes emblica was selected for study as it is widely used in many herbal preparations. Four simple herbal formulations namely, Triphala Churna, Amalakyadi Churna, Chaturbhadrika Churna, and Nishakatakadi Decoction are selected for the study. Three of the formulations contain P.emblica as an essential ingredient[6], [7]. As per the Ayurvedic Pharmacopoeia of India (API), Triphala Churna contains three herbs namely Phyllanthes emblica, Terminalia chebula, Terminalia bellirica. Further, the addition of the herb Glycyrrhiza glabra is also referred to in the AFI. Amalakyadi Churna contains four herbs Phyllanthes emblica, Terminalia bellirica, Plumbago zeylanica, Piper longum, and a mineral ingredient. The non-herbal mineral ingredient of Amalakyadi Churna, the rock salt in crystal form is also used in the study. The ingredients of Chaturbhadrika Churna contain four herbs namely Aconitum heterophyllum, Pistacia integerrima, Piper longum, and Cyprus ro-

tundus. Nishakatakadi is a liquid preparation prescribed in reference text Sahasrayoga, one of the authentic documents based on which the API is being compiled. It contains eight herbs namely Curcuma longa, Strychnos potatorum, Aerva lanata, Symplocos racemosa, Chrysopogon zizanioides, Phyllanthus emblica, Salacia reticulata, Ixora coccinea. Details of herbs and Parts used are given in Table 3.1. All the samples were collected from local markets in Malappuram and Calicut district of Kerala. Commercial samples of Triphala Churna is procured from six different manufacturers and were coded as T1, T2, T3, T4, T5, T6. Three different batches of T6 were collected and named T6a, T6b, T6c, and kept in airtight containers. Commercial samples of Nishakatakadi from different manufacturers were procured from dealers in Calicut and Malappuram districts and coded as C1, C2, C3, C4, C5, C6, C7, and C8 out of which C1 to C6 were in decoction form and C7 and C8 were in tablet form.

3.2 Certified Reference Samples

Certified reference samples are generally used as monitor and control samples. The calibration of the detector with the certified samples of a comparable matrix in XRF helps to reduce matrix related uncertainties. The analysis of certified reference samples is an important step to establish quality control of analytical results. Analysis of reference samples serves as calibration data to make the results independent of variations in beam flux and detector efficiency provides an effective way to identify the extent of uncertainty by evaluating how much the certified value deviated from the observed values. NIST apple leaf (NIST1515), NISTpeach leaf (NIST1547), NIST tomato leaf (NIST1573a) IAEA rye flour (IAEA-V-8), milk powder (IAEA153), hay powder (IAEA-V-10), animal blood (IAEA A-13) [1], [2], [3], [4], [5] procured for calibration and quality checking of the obtained results. In photon activation analysis, 99.7% In-115 was used as a monitor sample.

Table 3.1: Details of herbs

Code name	Botanical name	Sanskrit /Common name	Part used
Triphaladi churna			
AA	Phyllanthus emblica	Amlaki/Amla	Pericarp
AK	Terminalia chebula	Abhaya/Katukka	Pericarp
TT	Terminalia bellirica	Bibhitaka/Thannikka	Pericarp
TI	Glycyrrhiza glabra	Yashtimadhu/Irattimadhuram	root
Nishakatakadi Decoction			
H1	Curcuma longa	Nisha /Manjal	Root tuber
H2	Strychnos potatorum	Kataka /Thettambaral	Seed
H3	Aerva lanata	Bhadrika /Cheroola	Root
H4	Symplocos racemosa	Lodhra/Pachotti	Stem bark
H5	Chrysopogon zizanioides	Useera /Ramacham	Root
H6	Phyllanthus emblica	Amalaka /Nellikka	Pericarp
H7	Salacia reticulata	Vairi /Ekanayaka	Root
H8	Ixora coccinea	Paranti / Kattuthechi	Root
Amalakyadi Churna			
AC	Plumbago zeylanica	Chitrak/Vellakoduveli	Root
AA	Phyllanthus emblica	Amlaki/Amla	Pericarp
AK	Terminalia chebula	Abhaya/Katukka	Pericarp
AP	Piper longum	Pippali/Tippali	Fruit
Chaturbhadrika Churna			
CA	Aconitum heterophyllum	Athivisha/Athividayam	Root tuber
CS	Pistacia integerrima	Sringi/Karkatashringi	Leaf gall
AP	Piper longum	Pippali/Tippali	Fruit
CM	Cyperus rotundus	Musta/Muthanga	Root tuber

3.3 Sample preparation

Sample preparation is an important step in trace elemental analysis to provide good quality data. The raw samples are to be made in fine powder form for analysis after removing the impurities. The samples were thoroughly washed in double-distilled water and were dried at 60^0 for 24 hr. For fruit samples, seeds were removed. The samples were oven-dried in a vacuum for 6 hours at110^0C. Freeze drying was also done for selected formulations and their ingredient herbs. The dried samples were ground into fine powder by stainless steel grinder and agate mortar and pestle. The samples were further passed through sieve no: 80. The fine powder of the samples was kept in a desiccator till further analysis. The sample for the compound formulation of Churna was prepared by taking equal parts by weight of each sample followed by thorough mixing to maintain homogeneity. The reference sample for Nishakatakadi decoction was prepared by taking all herbs in equal proportion and extracting the water-soluble part of the herbs as per the reference text. The residue remaining was filtered out and the decoction was freeze-dried to remove the water content and kept in dissector till further analysis.

3.4 Analysis Using XRF

3.4.1 Sample preparation for XRF

The samples for XRF analysis have been prepared by taking, 400 mg of each herb, and subsequently pressing into pellets of 20mm diameter and 1mm thickness using a manual hydraulic press. A pressure of 10 tons was applied for all the samples. Binder material was required since the pellets obtained were hard and self-sustaining. Three to ten replicate pellets were prepared for each sample. Pellets of NIST and IAEA standard reference samples were also prepared following the same procedure for the purpose of calibration. For PIXE analysis, 140 mg of sample was mixed with 60 mg 99.9999 % graphite powder. The role of graphite powder is to give mechanical strength to the pellet by acting as

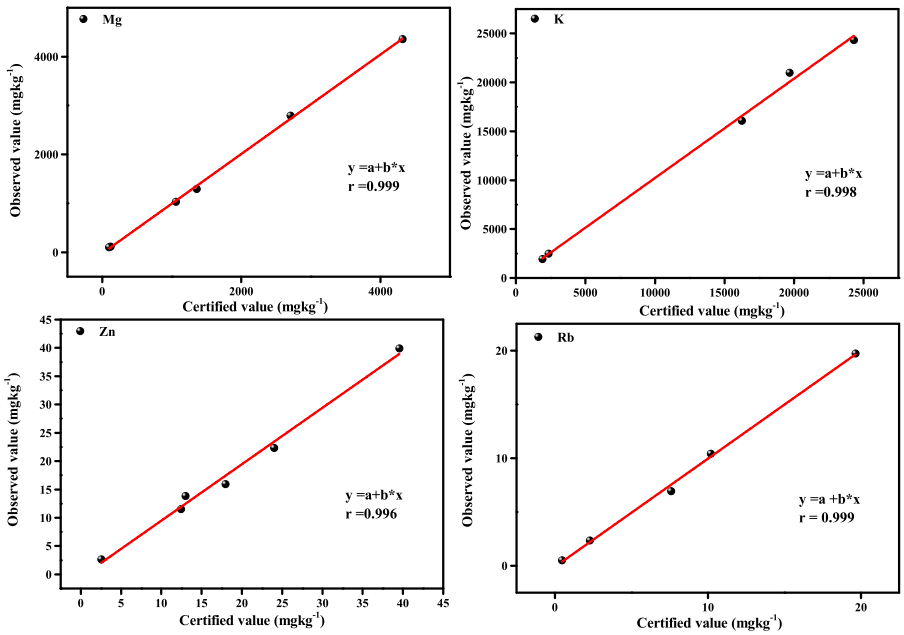

Figure 3.1: XRF Calibration plots for pressed pellets

a binder, improve conductivity, and to reduce the bremsstrahlung background. The samples were made into pellets of 13 mm in diameter and 1 mm thickness by applying a pressure of 8 ton in a hydraulic press. Pellets of each herb samples and the compound formulation has been made for irradiation. The sample for the compound formulation was prepared by taking equal parts by weight of each herb followed by thorough mixing for ensuring homogeneity as prescribed in the reference texts. The decoctions were freeze-dried and ground into fine powder and pelletized in the same manner as described above.

3.4.2 Calibration of XRF spectrometer

In the present study, XRF measurements were performed using Spectro XEPOS ED XRF spectrometer, at Central Sophisticated Instrumentation Facility (CSIF) at the University of Calicut. The spectrometer uses polarized X-rays for atomic excitation with a 50-Watt Pd end-window X-ray tube. The Bremsstrahlung target consists of Rh and a Co/Pd binary alloy. It produces

maximum energy of 50 keV which irradiates the sample. The Incident beam is a combination of polarized and direct beam. The polarized beam is produced from a crystal of highly annealed pyrolytic graphite, which helps to reduce the noise signal. A Peltier cooled Silicon Drift Detector (SDD) of active area 20 mm^2 and resolution less than 130 eV for MnK_α is used to acquire the x-ray photons produced from each element of the sample. Counts are converted into elemental concentrations by Turbo Quant II software. The energy and efficiency calibration of the spectrometer was performed using six reference standards namely, apple leaf (NIST1515), peach leaf (NIST1547), rye flour (IAEA-V-8), milk powder (IAEA153), hay powder (IAEA-V-10), animal blood (IAEA A-13).

To calibrate the XRF spectrometer for detection efficiency and the x-ray energies, NIST-IAEA samples were analyzed. As a representative case, the measured data and the certified data along with percentage error for NIST 1515 and NIST1547 has been shown in Table 3.2. The uncertainty reported in the measured data is the sum of errors due to statistics of counting and the standard deviation of the repeated measurements. Calibration curves were plotted, and the plots for Mg, K, Zn, and Rb were shown in Fig. 3.1. The figures showed good linearity with r$>$ 0.994. The variation in the efficiency of the detector with energy has been plotted for NIST 1515 and shown in Fig. 3.2.

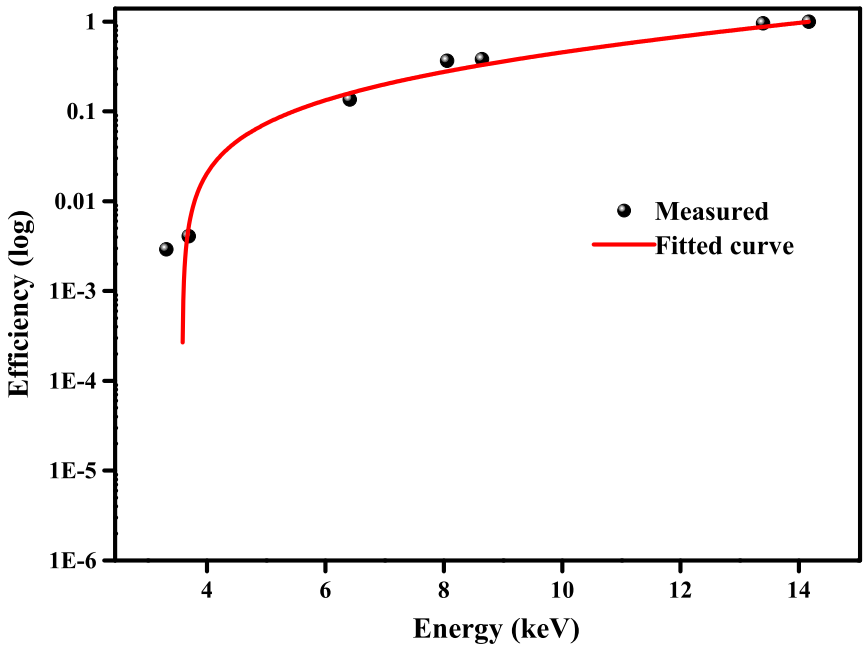

Figure 3.2: Energy dependant efficiency of SDD detector

Table 3.2: Elemental profile of NIST 1515 and NIST 1547 ($mgkg^{-1}$)

	NIST1515			**NIST1547**		
Element	**Measured**	**Certified**	**%error**	**Measured**	**Certified**	**%error**
Mg	2890±10	2710±120	6.74	4356±13	4320±150	0.83
Al	293±2	284.5±5.8	3.14	256.05±0.65	248.9±6.5	2.87
P	1719±6	1593±68	7.89	1365±3	1371±82	0.66
Cl	603±5	582±15	3.68	370±1	361±14	2.66
K	15953±101	16080±210	0.79	24155±25	24330±380	0.72
Ca	15330±22	15250±100	0.52	15610±20	15590±160	0.13
Mn	52.3±0.2	54.1±1.1	3.15	94.385±0.9	97.8±1.8	3.49
Fe	79.1±0.2	82.7±2.6	4.39	216.3±0.4	219.8±6.8	1.59
Cu	5.4±0.25	5.69±0.13	3.56	4.06 ±0.03	3.75±0.37	8.36
Zn	11.36±0.81	12.45±0.43	8.7	15.94±0.46	17.97±0.53	9.88
Br	1.69±0.4	1.8	5.82	11.04±0.1	11	0.36
Rb	9.69±0.67	10.2±0.89	5.02	18.79±0.4	19.65±0.89	4.37
Sr	23.61 ±0.33	25.1±5.0	5.92	50.935±0.2	53±5	3.89

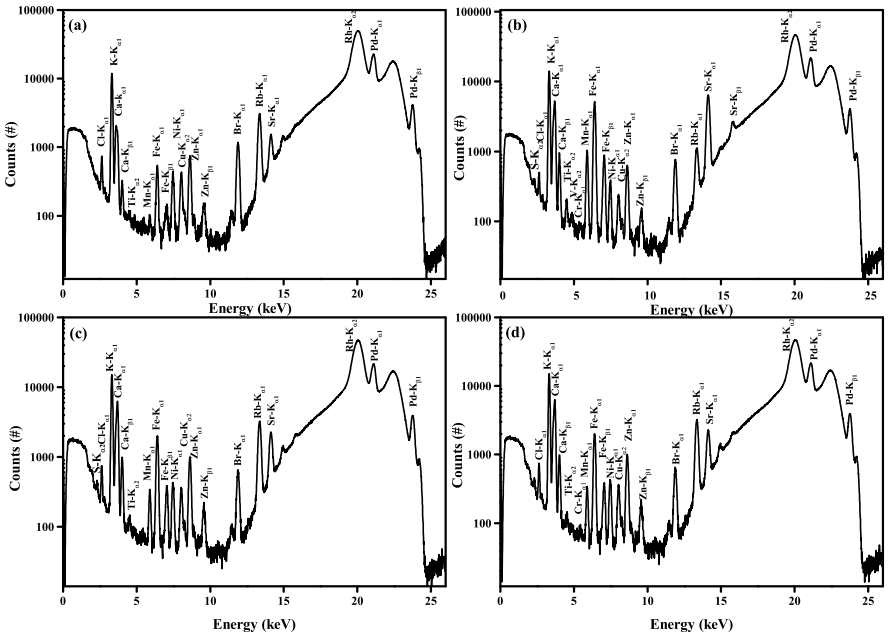

Figure 3.3: XRF spectra of (a) P. emblica, (b) T. bellerica, (c) T. chebula and (d) Triphala churna

3.4.3 XRF analysis of Triphala Churna

XRF measurement was performed for pellets of individual herbs in Triphala Churna and the combination formulation, prepared as per API (REF). Typical XRF spectra observed for the samples P. emblica, T. bellerica, and T. chebula are shown in Fig. 3.3 a-c. The fluorescence spectra of the compound formulation prepared is shown in Fig. 3.3 d. Distinct peaks corresponding to energies of K_α lines of X-ray were used to identify all the elements except Ba and Pb. L_α line at 4.47 keV confirmed the presence of Ba. The broad peaks around 20 keV correspond to the contribution of Rayleigh and Compton scattering from anode material of the X-ray tube.

3.4.4 XRF analysis of Nishakatakadi decoction

The XRF spectra of individual herbs in Nishakatakadi decoction are shown in Fig. 3.4 and Fig. 3.5 and the K lines of X-rays are marked in the spec-

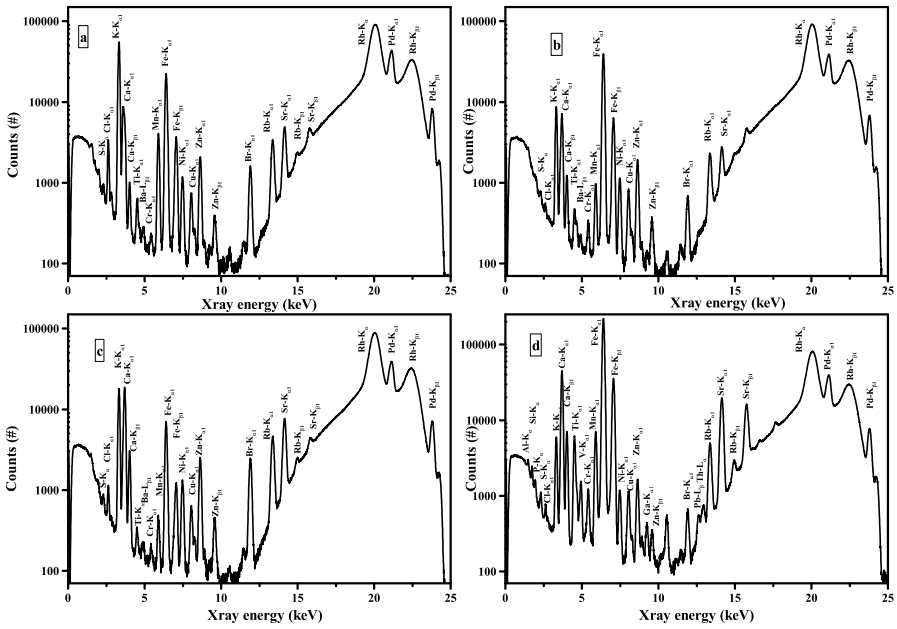

Figure 3.4: XRF spectra of (a) C. longa, (b) S. potatorum, (c) A. lanata, and (d) S. racemosa

trum. The spectra corresponding to the prepared reference sample, REF1, and REF2 are shown in Fig. 3.6. The spectra of commercial samples of Nishakatakadi using XRF are shown Fig. 3.7 and Fig. 3.8

3.4.5 XRF analysis of Amalakyadi Churna

The Fig. 3.9 bottom shows the XRF spectra of the compound formulation Amalakyadi churna, and the K lines of X-rays are marked in the spectrum.

3.4.6 XRF analysis of Balachaturbhadrika Churna

The Fig. 3.9 top shows the XRF spectra of Balachaturbhadrika Churna.and the K lines of X-rays are marked in the spectrum.

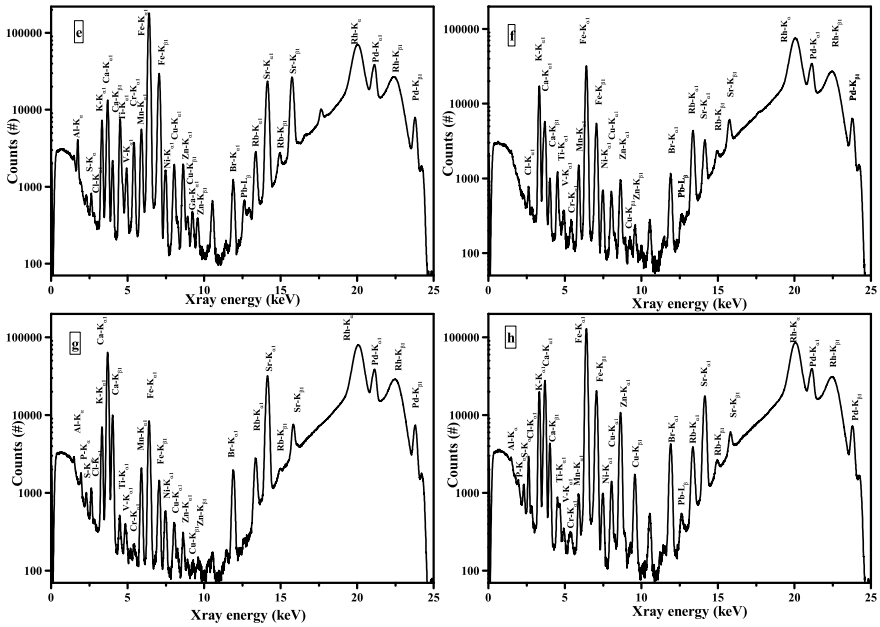

Figure 3.5: XRF spectra of (e) S. reticulata, (f) P. emblica, (g) C. zizanioides and (h) I. coccinea

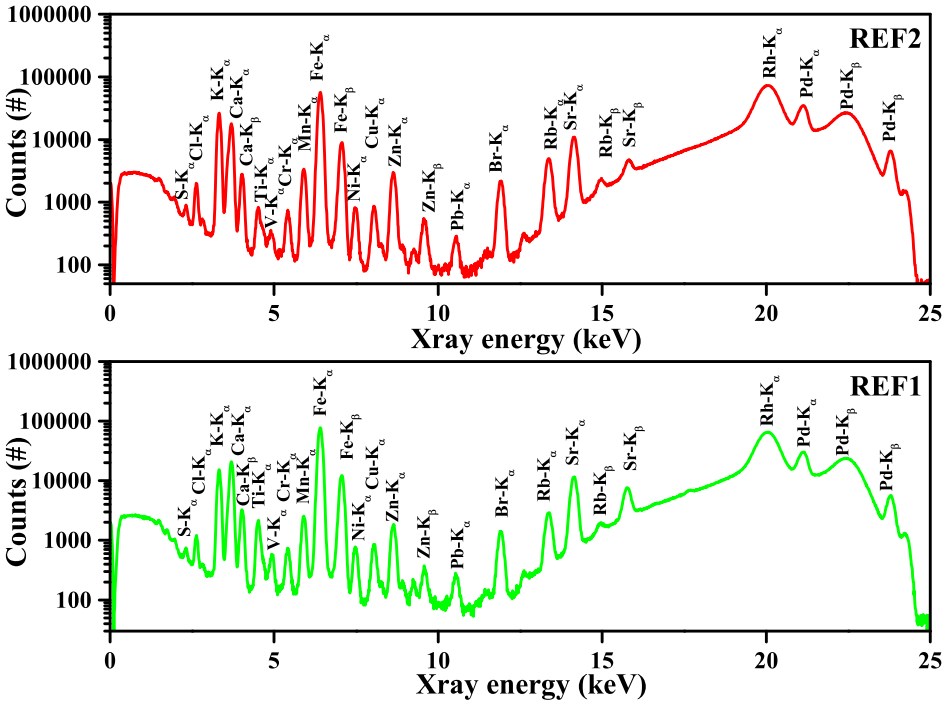

Figure 3.6: XRF spectra of Nishakatakadi-Powder and Decoction

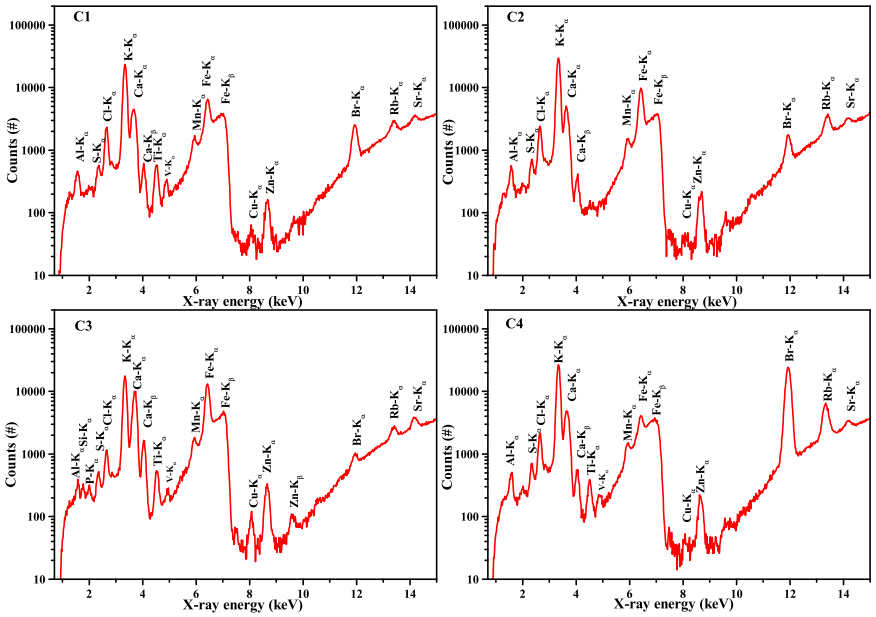

Figure 3.7: XRF spectra of commercial samples of Nishakatakadi decoction C1-C4

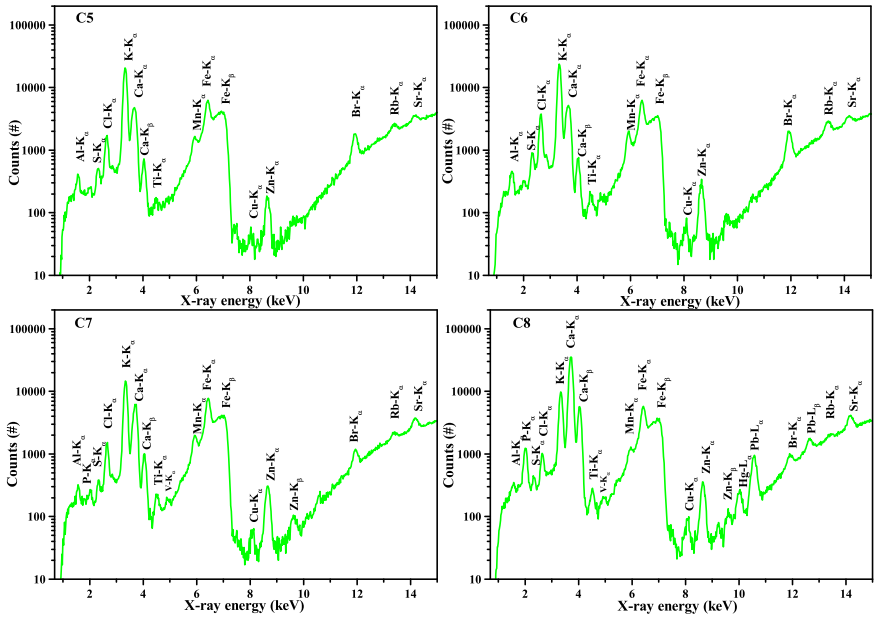

Figure 3.8: XRF spectra of commercial samples of Nishakatakadi decoction C5-C8

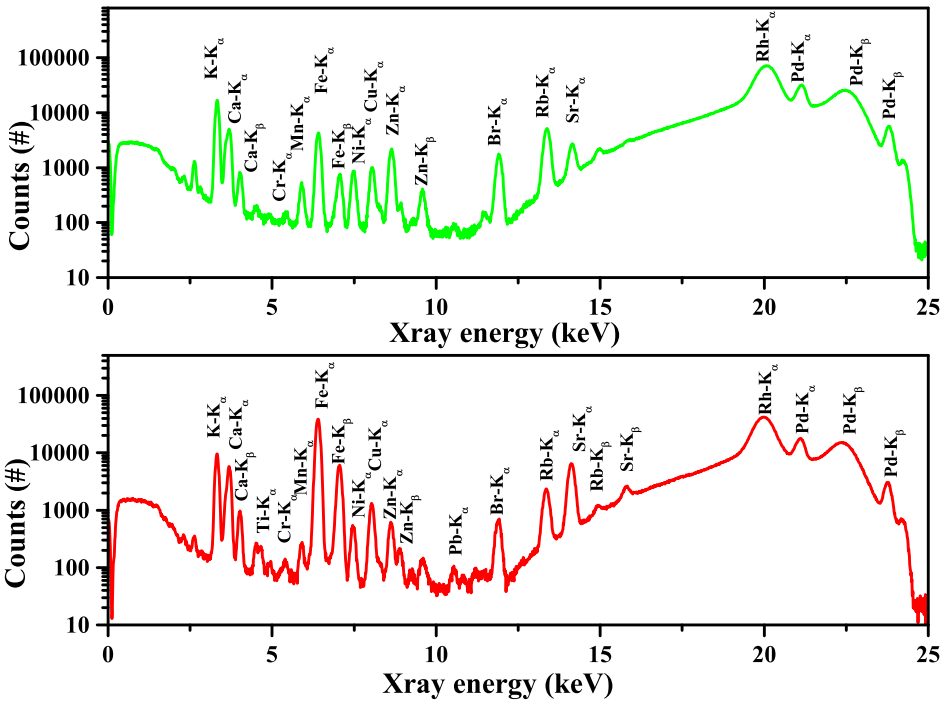

Figure 3.9: XRF spectra of Amalakyadi Churna and Balachaturbhadrika Churna

3.5 PIXE

3.5.1 Sample preparation for PIXE

Pellets for PIXE analysis were prepared by using the powdered samples and graphite powder. 160 mg of powder sample is mixed with 40 mg of 99.999% graphite powder using mortar and pestle, and pressed into pellets of 13 mm diameter, by applying a pressure of 8-10 ton in a manual hydraulic press. The role of graphite powder is to give mechanical strength to the pellet by acting as a binder, to improve conductivity, and to reduce the bremsstrahlung background. Pellets of each herb samples, the compound formulation prepared as a reference, and the commercial samples of the formulation have been made for irradiation. The freeze-dried decoctions were also ground into a fine powder and pelletized in the same manner as described above.

PIXE measurements were done at the tandem pelletron accelerator

in the Ion Beam Laboratory of Institute of Physics, Bhubaneswar, India. This facility consists of a 3MV tandem pelletron accelerator (National Electrostatic Corporation, USA, model 9SDH-2) with six beamlines. The ion source includes an Alphatross source and a SNICSs source. A schematic diagram of the setup is given in Fig. 3.10.

The proton beam used in this experiment were produced by the SNICS (Source of Negative ion by Caesium Ion Sputtering) source with TiH_2 as cathode material to produce protons. In the SNICS source, Cs atoms were ionized to forms Cs^+ ions and were accelerated to the cathode tip. The Cs ions sputtered the cathode material and the sputtered hydrogen atoms were ionized and accelerated through an aperture to the pre-acceleration section. The selection of the desired ion species was done by the injector magnet. Einzel lenses and magnetic steerers collimate the beam and lead it to the accelerator. The negative ions on entering the accelerator get accelerated towards the positive terminal at the center of the accelerator tube. The terminal can hold a maximum voltage of 3MV. Two nylon chains containing steel pellets on each link delivers charge to the terminal. Electrons are stripped off the beam by introducing nitrogen gas at the mid terminal. The collision of a negative beam with the nitrogen gas results in neutral as well as single and multiple positive charged ions. The accelerated beam at the positive terminal sees the ground potential at the far end of the accelerator and gets further accelerated. The whole accelerating column is insulated by SF_6 gas at 65-70 psi pressure. A switching magnet steers the desired charged species to the respective beamlines. Magnetic quadrupole lens and steering magnets focus the beam into the target chamber. The energy of the proton beam at the target is a function of the voltages at the pre-acceleration stage, the terminal voltage of the accelerator, and the charge of the ion selected by the switching magnet. 2 mm proton beam, with a beam current of 20-30 nA was used in the experiment. A fully automated system controls the beam production and transport to the target which simplified the tuning procedures

Proton beam of approximately 3 MeV with a beam diameter of 2-3

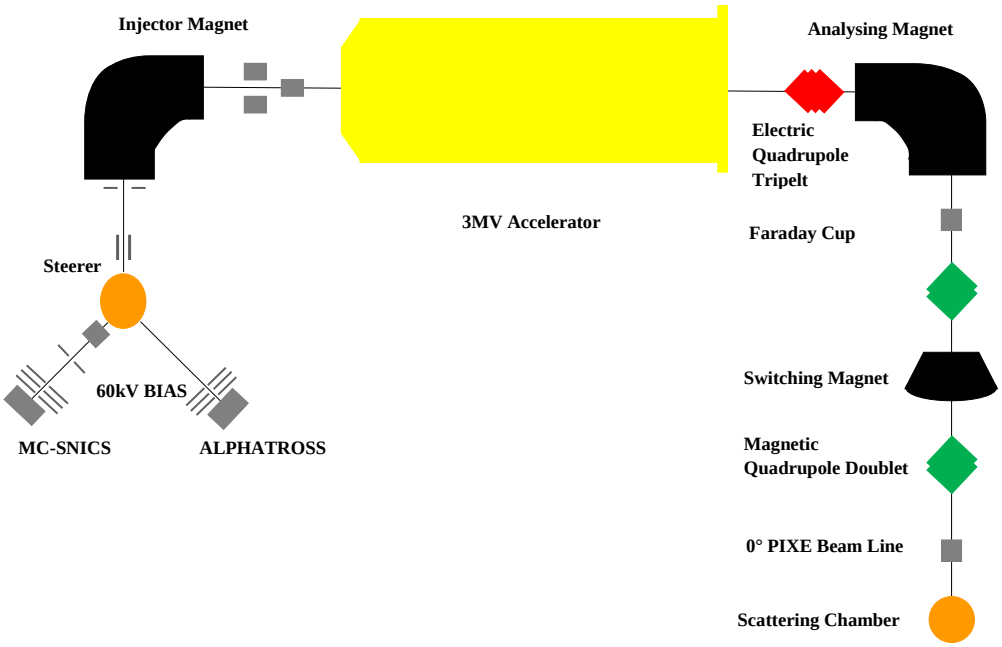

Figure 3.10: PIXE beam line

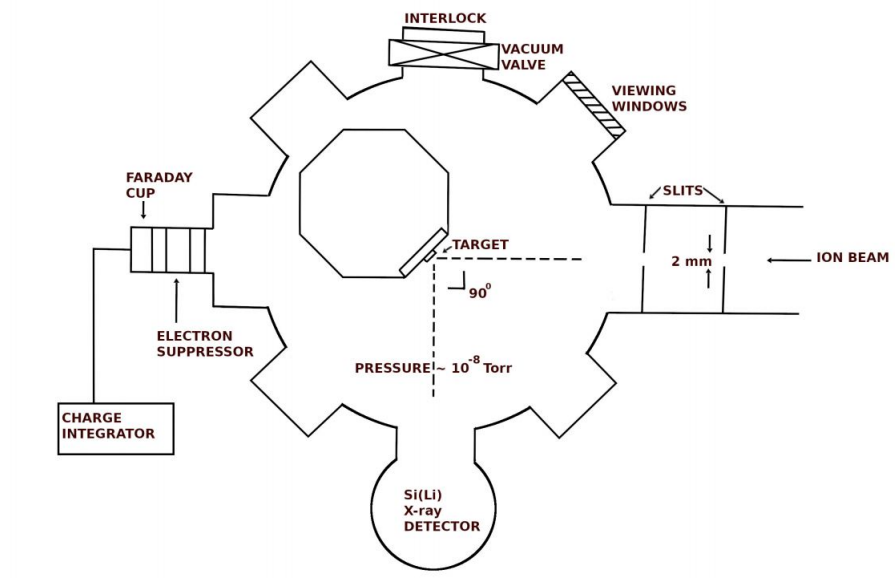

Figure 3.11: PIXE scattering chamber

mm falls on the target kept in the octagonal-shaped scattering chamber of 20 inch diameter and 15 inch height. A schematic diagram of the scattering chamber

is given in Fig. 3.11. To detect X-rays, a Si-Li detector is placed close enough to the target to provide a large solid angle. A viewing window facilitates visual indication of beam position and size of the beam spot on the target. The target was placed at an angle 45^0 to the beam direction and the X-ray detector was placed at an angle 45^0 to the target position. The chamber was maintained at a pressure of 10^6 torr) during the measurements using rotary and diffusion pumps. Since the thick target samples are electrically conductive, the charge integrator was coupled directly to the target holder to monitor the beam current. The samples were loaded on an octagonal shaped aluminium target ladder which can hold 48 samples at a time. This avoids the need for frequent opening and re-evacuation of the scattering chamber. The target holder was mounted on a sample manipulator attached through the top port of the chamber. The position of the beam on the target could be changed manually from outside without breaking the vacuum by rotating the sample manipulator in the desired direction.

The characteristic X-ray spectra were recorded using 30 mm^2 Canberra Si-Li detector with 8 μm thick Be window and energy resolution 165 eV FWHM at 5.9 keV, coupled to FAST COMPTEC model multichannel analyzer. Three aluminium windows of 25 μm thickness were used as X-ray absorbers in the detector to reduce background. For each sample, the total charge collected and the average beam current were noted. The acquired spectra were analyzed using GUPIX software package [8]. GUPIX is an interactive software that utilizes the most updated databases for cross-sections, stopping powers, attenuation coefficients. Here, the elemental concentrations have been extracted from peak intensities via standardization technique involving fundamental parameters, predetermined instrument constants, and input parameters such as solid angle and charge collected. This avoids the need for an internal standard for the samples for determining absolute concentrations. The energy-dependent efficiency of the detector was determined using the X-rays from a standard source of Am-241.

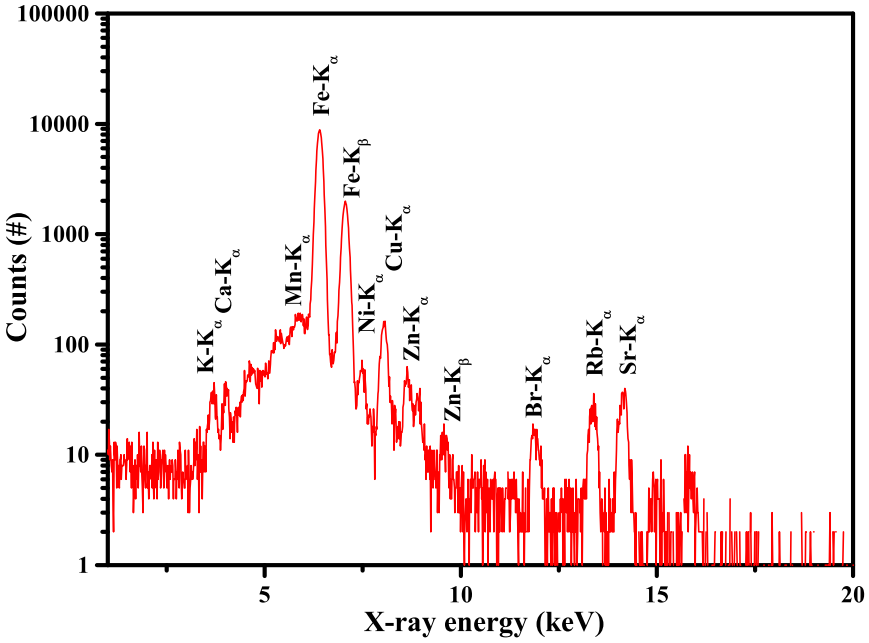

Figure 3.12: PIXE spectrum of reference sample of Triphaladi Churna

3.5.2 PIXE analysis of Triphaladi Churna

For PIXE analysis, individual samples in Triphaladi Churna and the prepared reference sample were irradiated with the proton beam at IOP Bhubaneswar. The spectra of the samples were obtained and plotted in Fig. 3.12. The spectrum obtained in the PIXE experiment is the sum of contributions of different elements in the target irradiated. It consists of K X-rays from light elements, K and L X-rays from medium Z elements, and L X-rays from high Z elements. The Gaussian peaks are superimposed on a continuous background originating from secondary Bremstahlung and Compton scattering of γ rays. To compute the intensities of each characteristic X-ray computer-assisted programming approach is adopted. The PIXE spectrum shows that the peaks corresponding to Fe-K_α and Fe-K_β are the highest intensity peaks. The low energy peaks, for K and Ca are less intense and the background is more in this region compared to the high energy side.

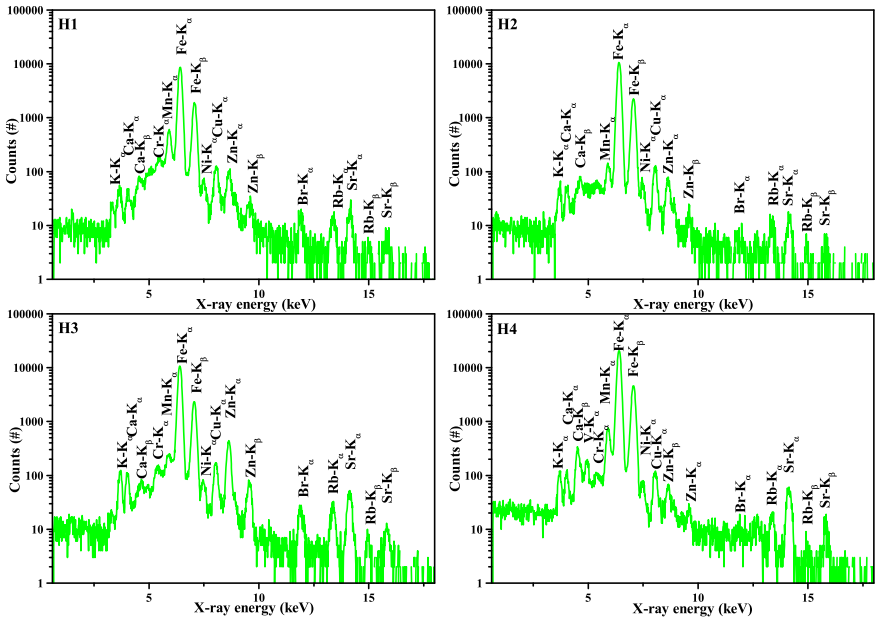

Figure 3.13: PIXE spectrum of herbs in Nishakatakadi H1 to H4

3.5.3 PIXE analysis of Nishakatakadi decoction

Pellet samples of individual herbs in Nishakatakadi, reference samples, and the commercial preparations were mounted on the sample ladder and irradiated with proton beam at 1.478 MV terminal voltage. Typical PIXE spectrum for individual herbs in Nishakatakadi irradiated with a proton beam from tandem pelletron accelerator is shown in Fig. 3.13 and Fig. 3.14. The spectrum of reference samples prepared is shown in Fig. 3.15. For all elements except Pb and Ba, K lines of X-rays have been used and for Pb and Ba L_α lines have been used. Trace elemental concentration of the individual herbs and the compound formulation were tabulated.

3.5.4 PIXE analysis of Amalakyadi Churna

The PIXE spectrum of Amalakyadi Churna is given in Fig. 3.16 and the peaks are marked. The PIXE spectrum of mineral ingredient, rock salt is given in Fig. 3.17. The spectrum is significantly different from the herbal samples.

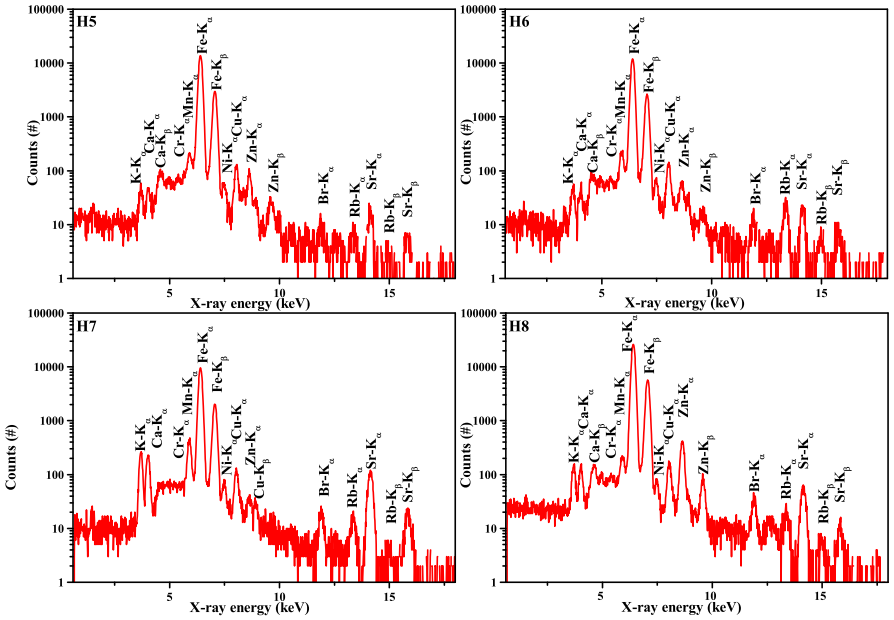

Figure 3.14: PIXE spectrum of herbs in Nishakatakadi H5 to H8

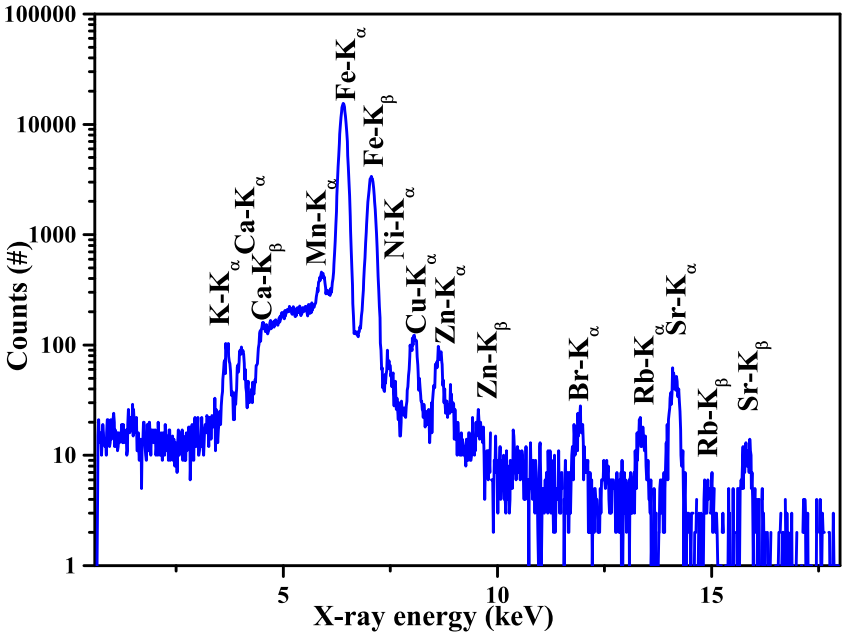

Figure 3.15: PIXE spectrum of reference sample of Nishakatakadi

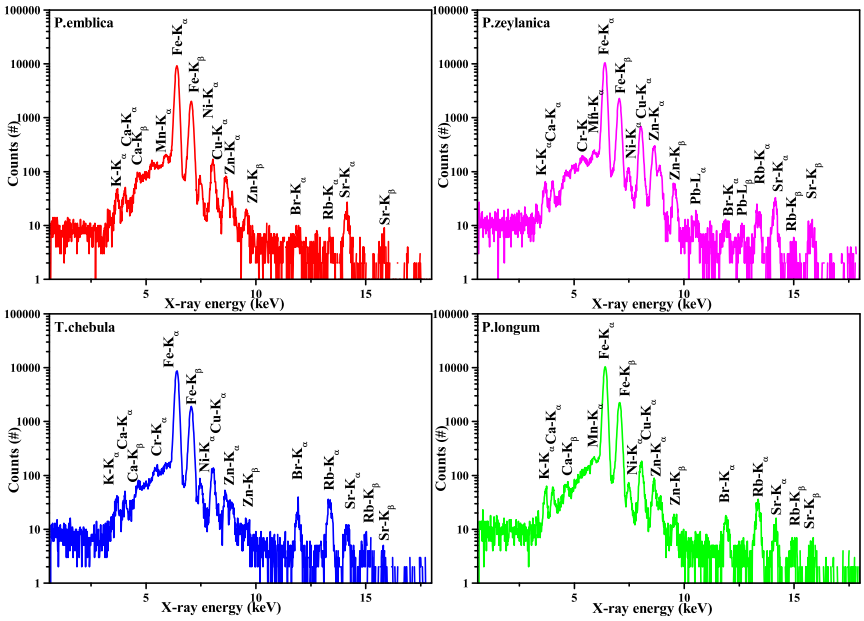

Figure 3.16: PIXE spectrum of herbs in Amalakyadi churna

Peaks corresponding to trace elements like K, Ca are absent in this spectrum.

3.6 NAA

3.6.1 Sample preparation for NAA

Samples for NAA were prepared by packing, samples, standard and blank together and keeping in polypropylene rabbits. Samples of known quantities were taken in polythene cover, tightly folded and made compact, further sealed in another polythene bag to avoid any spillage of sample. Samples of the certified reference standard, NIST 1515 apple leaf or NIST Tomato leaf was also packed in the same manner as described above. Sample blanks were prepared in the same manner without the sample for blank correction. The samples, standard, and blank have been inserted in the polypropylene rabbits and kept for neutron irradiation.

NAA has been done at the KAMINI (Kalpakkam Mini) reactor at

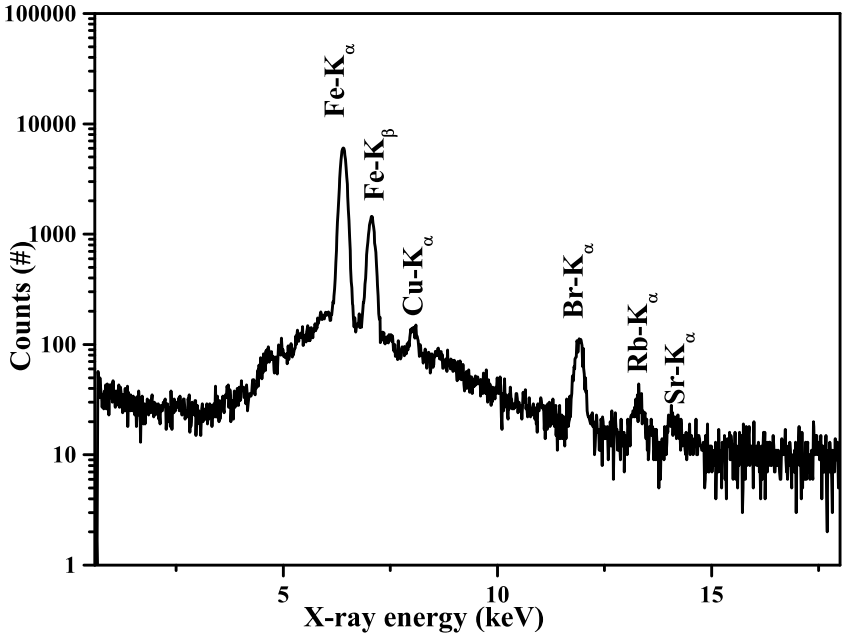

Figure 3.17: PIXE spectrum rock salt

Indira Gandhi Centre for Atomic Research (IGCAR) Kalpakkam. KAMINI is a 30 kW tank-type research reactor in which the fuel, ^{233}U is situated in a pool of light water. A 20 % ^{233}U with Al clad constitutes the core of the reactor which is cooled by natural convection. Zircalloy canned BeO reflector is arranged on all sides of the reactor core to minimize fuel and improve neutron economy. For reactor power control and shut down, two control rods made of cadmium sandwiched in aluminium is used. A gravity drop mechanism is employed for rapid shut down of the reactor. A pneumatically operated fast sample transfer system is provided for shooting and retrieving the samples. The samples are put in polypropylene rabbits of 20 mm diameter and 30 mm height and shot to reach the irradiation location adjacent to the core reflector boundary. Thermal neutrons flux of $10^{12} ncm^{-2}s^{-1}\ m^{-2}$ is available at the PFTS position.

The samples packed in the rabbits were irradiated at the PFTS position of the reactor at 20 KW power for 5 hrs for long half-life elements and 5 minutes for short half-life elements. The short irradiated sample was counted

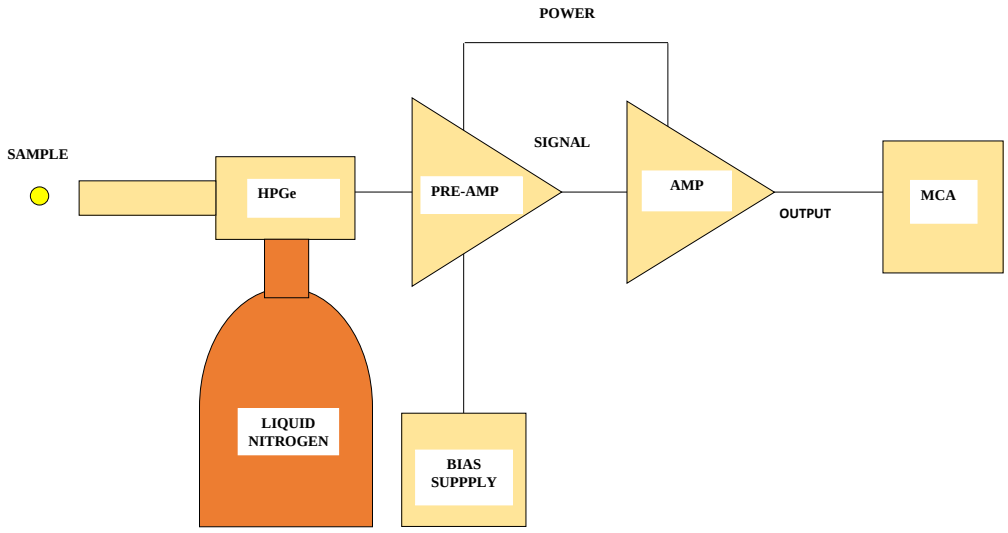

Figure 3.18: Schematic diagram of gamma spectroscopy setup

immediately to get short-lived nuclei. The long irradiated samples were kept overnight in the fume hood to reduce the activity to acceptable levels. The activities induced in the samples, standard and blank were analyzed by detecting the gamma rays using a coaxial HPGe detector of 30 % efficiency by keeping the sample at a fixed distance from the detector. A schematic diagram of the gamma spectroscopy setup is shown in Fig. 3.18. Counting times were optimized depending on the half-lives of the expected elements. The detector was pre-calibrated using standard ^{152}Eu source and gamma spectrum is given in Fig. 3.19 the energy-dependent efficiency is plotted in Fig. 3.20. The efficiency of the detector is shown in Table 3.3. The counting and cooling times were optimized depending on the half-life of each element. The details of the identified elements are shown in Table 3.4. Here the relative method is used for determination elemental concentration in the herbal samples.

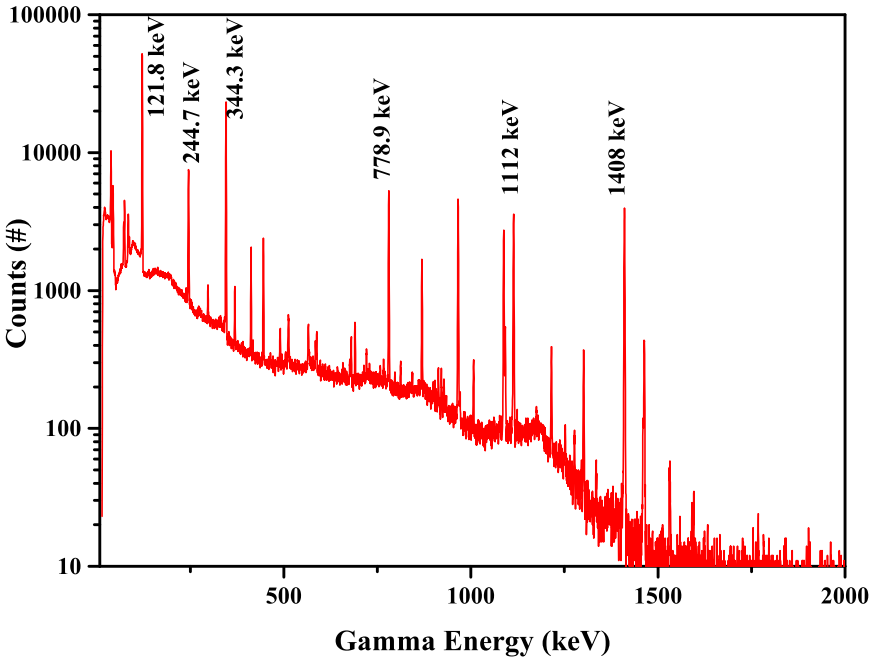

Figure 3.19: The gamma spectrum of ^{152}Eu source

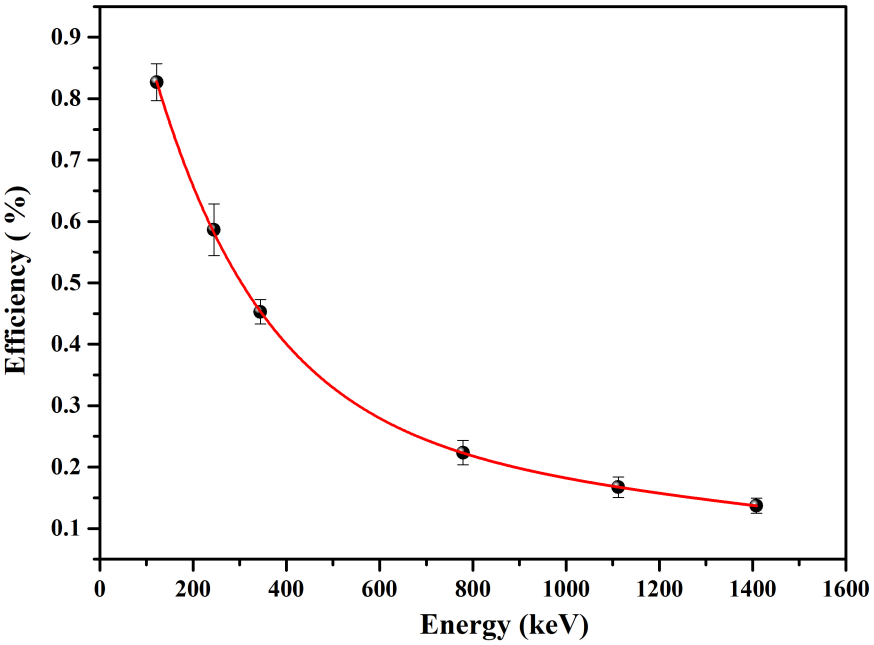

Figure 3.20: The energy dependent efficiency plot of HPGe detector using ^{152}Eu source

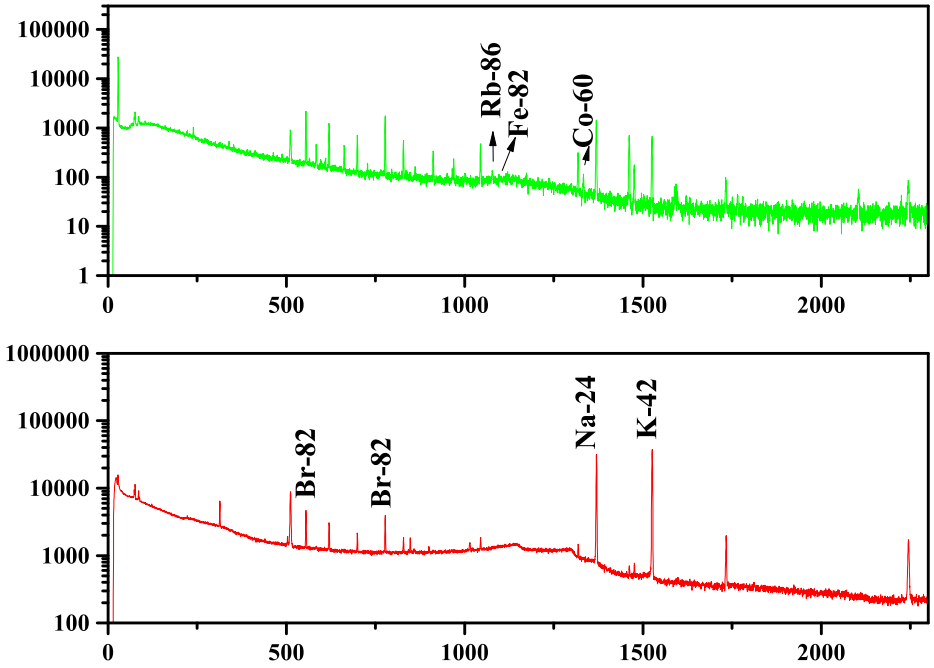

Figure 3.21: NAA spectrum of Triphaladi Churna

3.6.2 NAA of Triphaladi Churna

The typical gamma spectrum of Tripahladi Churna by thermal neutron activation is shown in Fig. 3.21. Twelve elements, viz., Br, Fe, Rb, Na, Zn, Co, K, La, Mn, W, Sm and Cl were identified by NAA in different herbs and the corresponding peaks are marked.

Table 3.3: The energy dependent efficiency of HPGe detector using ^{152}Eu source

Energy (keV)	Counts/ second	Efficiency
121.78	10.35	0.827±0.03
244.67	1.93	0.586±0.04
344.30	5.28	0.453±0.02
778.90	1.27	0.223±0.02
1112.07	1.00	0.167 ±0.02
1408.08	1.25	0.137±0.01

Table 3.4: Details of the identified nuclides

Element	**Reaction**	$\mathbf{t}_{\frac{1}{2}}$ (s)	**Abundance** (%)	σ**(n,** γ**)** (mb)	E_γ (keV)	I_γ (%)
Na	^{23}Na(n,γ) ^{24}Na	5.39*10^5	100	0.525	1368.6	99.99
				0.525	2754	99.86
Cl	^{37}Cl(n,γ)^{38}Cl	2.24*10^3	24.24	0.433	2167	44
				0.433	1643	33
K	^{39}K(n,γ)^{40}K	3.9*10^{16}	93.26	38	1460	10.66
K	^{41}K(n,γ)^{42}K	4.45*10^4	6.7	1.46	1524	18
Ca	^{46}Ca(n,γ)^{47}Ca	3.91*10^5	0.004	0.74	1297	67
				0.74	489	5.9
Mn	^{46}Mn(n,γ) ^{56} Mn	9.23*10^3	100	13.36	846.8	98.9
					1810.7	26.9
Fe	^{58}Fe(n,γ)^{59}Fe	3.8*10^6	0.28	1.32	1099	56.5
Co	^{59}Co(n,γ)^{60}Co	1.67*10^8	100	37.18	1332.5	99.98
Rb	^{85}Rb(n,γ)^{86}Rb	1.6*10^6	72.17	0.49	1077	8.64
Ni	^{64}Ni(n,γ)^{65}Ni	9.07*10^3	0.92	1640	1481.84	23.59
Cu	^{63}Cu(n,γ)^{64}Cu	4.57*10^4	69.15	500	1345.77	0.48
Zn	^{64}Zn(n,γ)^{65}Zn	2.1*10^7	49.2	0.73	1115	50.04
	^{68}Zn(n,γ)^{69m}Zn	4.95*10^4	18.45	1.07	438	94.85
Br	^{81}Br(n,γ)^{82}Br	1.2*10^5	49.31	2360	776.52	83.6
					554	71.7
Ba	^{138}Ba(n,γ)^{138}Ba	9.9*10^5	71.69	4040	123.8	89.9
La	^{139}La(n,γ)^{140}La	1.45*10^5	99.9	9.2	329	20.3
					487	45.5
					816	23.28
					1596	95.4
Eu	^{153}Eu(n,γ)^{154}Eu	2.7 *10^8	52.19	312	123	40.4
					1274	34.8
					723	20.06
W	^{186}W(n,γ)^{187}W	8.64*10^4	28.43	38.1	618.4	7.6
					479.53	26.6
					685.8	33.2
Sm	^{152}Sm(n,γ)^{153}Sm	1.67*10^5	26.75	206	103.18	29.25
Au	^{197}Au(n,γ)^{198}Au	2.32*10^5	100	98.65	411.8	95.6

3.6.3 NAA of Nishakatakadi decoction

The typical gamma spectrum of S.potatorum and P.emblica under thermal neutron activation is shown in Fig. 3.22, and 3.23. Twelve elements, viz., Br, Fe, Rb, Na, Zn, Co, K, La, Mn, W, Sm and Cl were identified by NAA in different herbs and the corresponding peaks were marked in the spectrum. Activity of Na is very high due to its high thermal neutron cross sections which is evident from the sharp peak at 1369 keV. This highly increases the dead time of the detector. Once the activity of Na is subsided, the spectra are acquired with dead times less than 3%. Gamma spectrum of Nishakatakadi decoction under thermal neutron activation is shown in Fig. 3.24

3.7 Photon Activation Analysis Using Medical LINAC

3.7.1 Sample preparation for PAA

The sample for photon activation was by pressing 15 g of the dried sample using a hydraulic press with a pressure of 9 tons. A compact cylindrical pellet of 20 mm diameter and 50 mm thickness was obtained. The sample was covered with Al foil to avoid any spillage. ^{115}In foil of known weight was used for monitoring the photon flux.

The photon activation analysis has been done using a medical linear accelerator (LINAC). A 20 MeV electron beam with a beam current of 35μA from Varian CLINAC-iX, medical LINAC, falling on a thick Pb target produces the high-intensity bremsstrahlung photons with endpoint energy of 20 MeV. The sample was attached to the bottom of the Pb bremsstrahlung target, along with the flux monitor to get the maximum bremsstrahlung flux. Irradiation was done for 20 minutes with this configuration for achieving a measurable level of induced activity. Gamma spectrum from the irradiated samples was acquired using Kromeck-CZT (Cadmium Zinc Telluride semiconductor detector) gamma

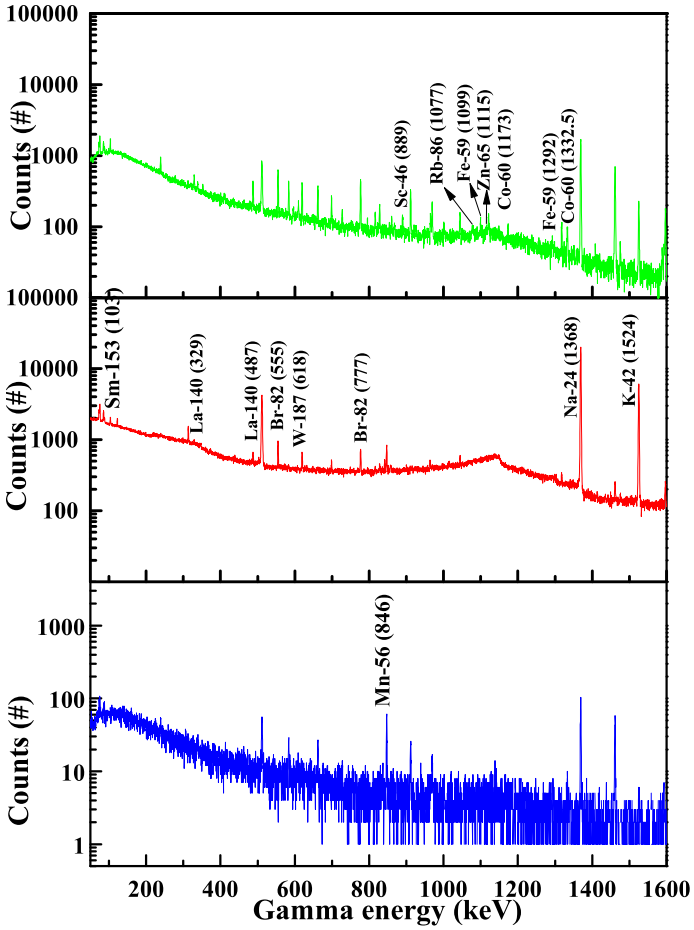

Figure 3.22: Gamma spectrum of S. potatorum under thermal neutron irradiation

spectrometer, having a crystal size of 1cm x 1cm x 1cm and resolution of 32 keV at 661 keV. Counting was performed for different intervals after sufficient cooling, to get good statistics for both short and long-lived nuclides. Separate counting of the monitor was done, to minimize the random coincidence effects. The energy and efficiency calibration of the CZT detector was done using standard calibration sources of known activity viz. ^{22}Na, ^{137}Cs, ^{133}Ba and ^{60}Co and the details are given in Table 3.5.

The gamma spectra of standard sources were shown in Fig. 3.25. The energy-dependent efficiency was calculated and the plot was shown in Fig. 3.26.

Table 3.5: Details of the Standard Sources

Source	Source Strength(Bq)	Half Life(s)	Total Activity(A)
^{133}Ba	118400	3.32*10^8	40249
^{60}Co	148000	9.48*10^8	101367
^{22}Na	74000	8.20*10^7	931
^{137}Cs	118400	9.48*10^8	13678

Table 3.6: Calibration details of CZT detector

Line No.	Gamma Line(keV)	I_γ	counts
^{133}Ba	80.9979	0.329	30000
	276.3989	0.0716	10992
	302.8508	0.1834	19968
	356.0129	0.6205	41993
	383.8485	0.0894	7484
^{137}Cs	661.657	0.851	260000
^{22}Na	1274	0.9994	900
^{60}Co	1173.228	0.9985	11000
	1332.496	0.9998	7300

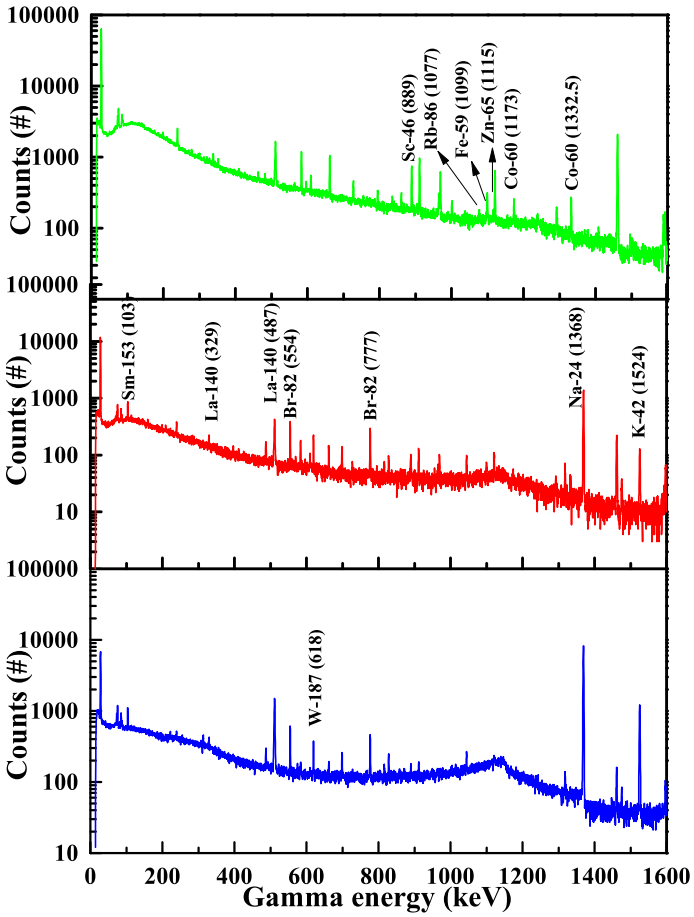

Figure 3.23: Gamma spectrum of P. emblica under thermal neutron irradiation

The curve was fitted by the least square curve fitting with appropriate function for the interpolation of efficiency. The TENDL-2017 recommended cross-sections were used for the analysis, for both the sample as well as the monitor [33]. Half-life, gamma energy, intensity, and abundance data were taken from the IAEA chart of nuclides [34]. The details of the observed reaction channels, gamma energies, half-life, efficiency, cross-section, decay constant, and Q values are given in Table 3.7. Proper normalization has been done for energy averaged flux for different isotopes having different Q values.

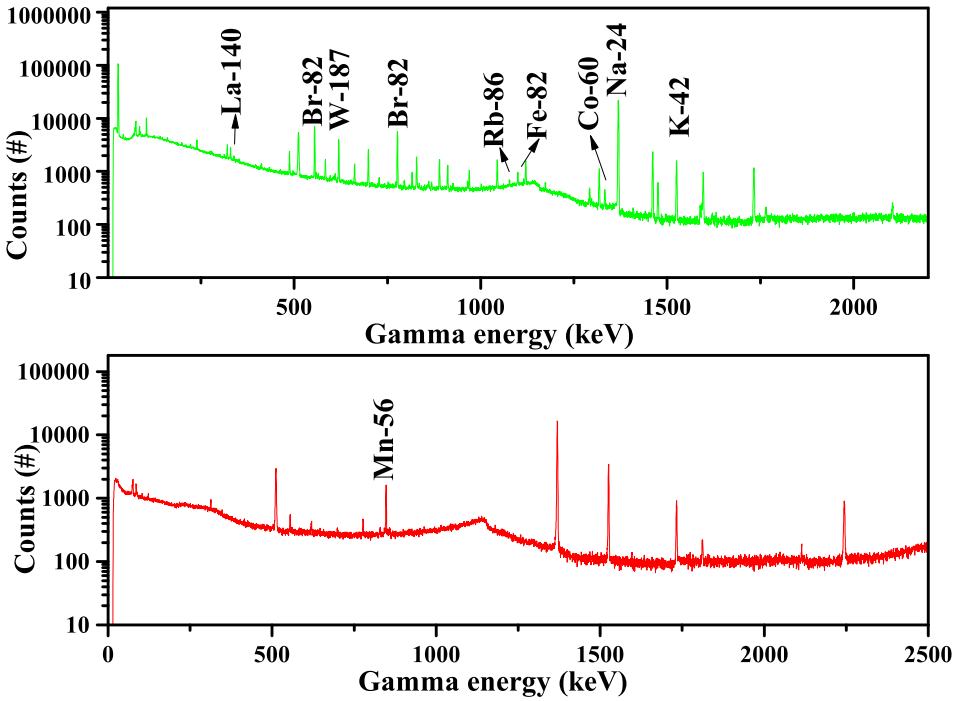

Figure 3.24: Gamma spectrum of Nishakatakadi decoction under thermal neutron irradiation

3.7.2 Photon Activation Analysis of P. emblica

Compact cylindrical sample of the herb P.emblica has been irradiated in Bremsstrahlung photons produced from 20 KV electronic accelerator. The typical gamma spectrum of the irradiated sample is shown in Fig. 3.27. The elemental identification was done from the centroid of the observed peaks. Accordingly, elements like Fe, Sr, Zn Mn, Cl, Br, and Rb were identified. For Rb, two peaks were identified at energies 248 keV and 464 keV resulting from the reaction $^{85}Rb(\gamma, n)^{84m}Rb$. The spectrum showed an intense peak at 511 keV also, which can be attributed to pair annihilation. This is an indication of the predominance of C, N, and O in the sample matrix which produces (γ, n) reaction products that are pure β^+ emitters instead of nuclide specific gamma rays.

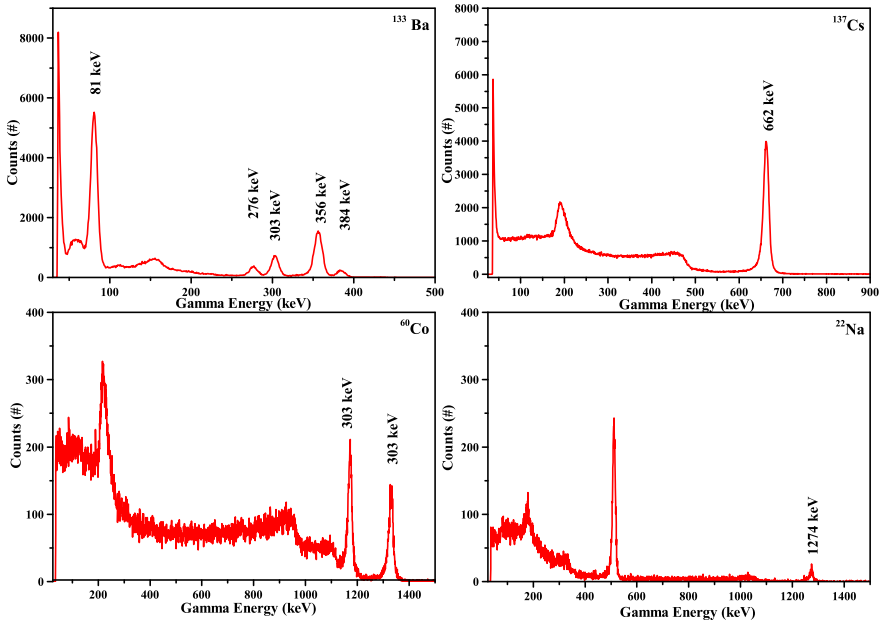

Figure 3.25: Gamma spectra using standard sources

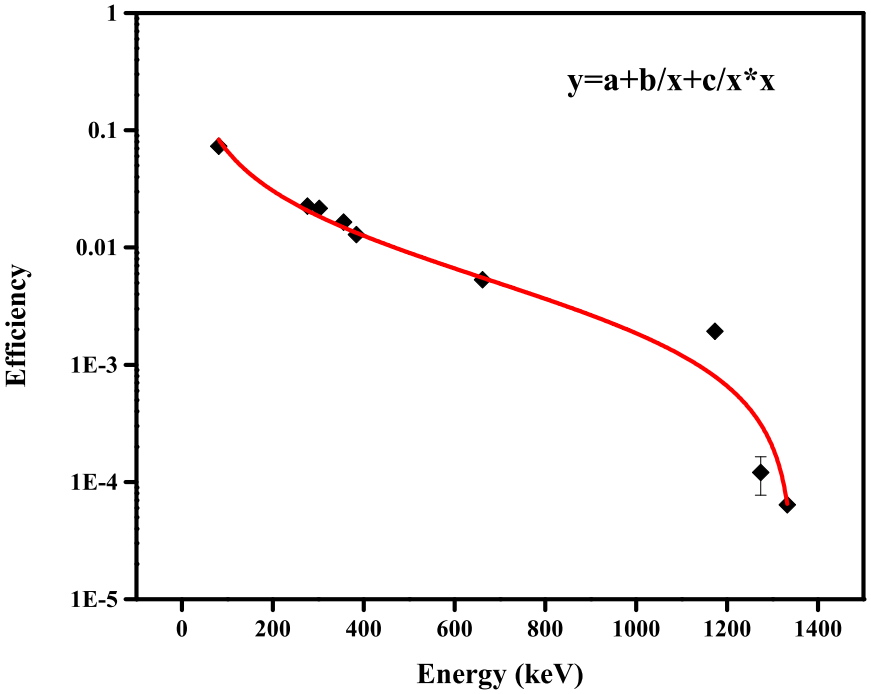

Figure 3.26: Efficiency calibration of CZT detector

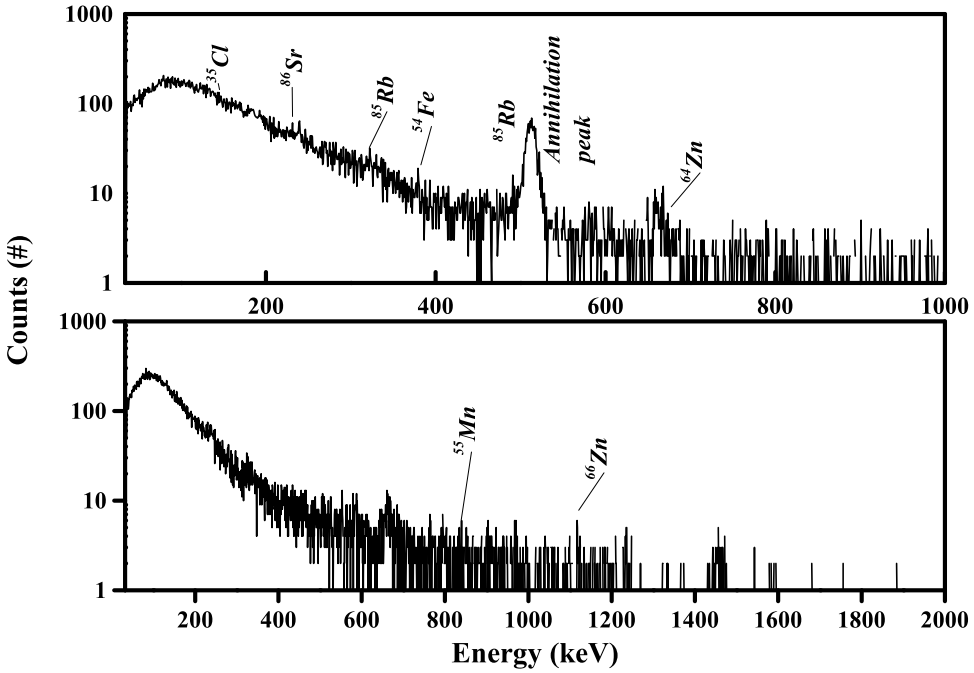

Figure 3.27: Gamma spectrum of P. emblica under photon irradiation

Table 3.7: Details of the observed reaction channels

Reaction channel	**Q value**	E_γ **(I%)**	**Half-life**	**Efficiency**	**Abundance**
	(MeV)	(keV)	(s)		(%)
$^{54}Fe(\gamma,n)^{53}Fe$	13.38	377.9 (42)	510.6	0.0151	5.845
$^{86}Sr(\gamma,n)^{85m}Sr$	11.11	231 (83.9)	4.05*10^3	0.02738	9.86
$^{64}Zn(\gamma,n)^{63}Zn$	11.86	669.6 (8.2)	2.31*10^3	0.00665	49
$^{85}Rb(\gamma,n)^{84m}Rb$	10.48	248 (63)	1.22*10^3	0.02257	72.17
$^{55}Mn(\gamma,n)^{54}Mn$	10.23	834.8 (100)	2.70*10^7	0.00479	100
$^{35}Cl(\gamma,n)^{34m}Cl$	12.64	146.4 (38.3)	1.92*10^3	0.04415	75.76
$^{81}Br(\gamma,n)^{80}Br$	10.16	616.3 (6.7)	1.06*10^3	0.00746	49.31

3.8 ICPMS

3.8.1 Sample preparation for ICPMS

The wet digestion method was adopted in sample preparation for ICPMS. The powdered sample was digested in a Milestone Ethos UP microwave digester.

Supra pure HNO_3 (Carlo Erba), ultra-pure H_2O_2 (Fisher Scientific) were used for sample digestion. ICP multi-element standards from Sigma Aldrich were used for the calibration of ICPMS. Pre-digestion was done at room temperature. For this, 10 mg of the sample was taken in a digestion vessel and 7 ml of concentrated HNO_3 and 3 ml of H_2O_2 were added to it. After 30 minutes of pre-digestion, the vessel was closed and kept inside the microwave digester at 483K. After complete digestion, clear sample solutions were allowed to cool and then filtered using Whatman 42 filter paper. The samples were transferred to a standard flask and diluted to 50 ml with high purity milli-Q water. For elemental calibration, standard stock solutions of As, Cd, Co, Cr, Cu, Hg, I, Mn, Ni, Pb, Pd, Ti, V, Zn, and Zr were prepared from the ICPMS standards and the standard mix solution was prepared from them. The mix solution was diluted to get six multi-element standards of different concentrations used for instrument calibration. Diluent 2% HNO_3 was taken as the blank solution.

The ICPMS analysis of the individual herbs was done for trace elements with Agilent 7800 mass spectrometer. The details of the instrument setup are given in Table 3.8. The calibration curves for each element showed good linearity over the entire range of concentrations, with an r value higher than 0.999. The content calculation was done using the equation,

$$C = \frac{(S - B)V}{Wx1000} \tag{3.1}$$

where C is the concentration in $mgkg^{-1}$, S is the sample concentration, B is sample blank concentration, V is the made-up volume and W is the weight of the sample.

3.8.2 ICPMS analysis of Triphala churna

In ICPMS, a known quantity of samples of Triphala Churna and its constituent herbs were digested into liquid form and diluted with Millipore water. The samples are introduced through the nebulizer, to form a fine aerosol for analysis.

Table 3.8: Optimal operating conditions of ICP-MS

Instrument parameter	Conditions	Instrument parameter	Conditions
RF Power	1500 V	Extraction2	-165 V
RF matching	1.80 V	Omega bias	-80V
Sample depth	8.0mm	Omega lens	7.3V
Nebulizer gas	1.10l/min	Cell entrance	-40 V
Nebulizer pump	0.10rps	Cell exit	-60 V
S/C temp	20C	Deflect	-1.2V
Nebulizer gas	1.10 l/min	Plate bias	-55V
Extraction 1	0 V	He-gas flow rate	3.4 ml/min

3.8.3 ICPMS analysis of Nishakatakadi decoction

Analysis of constituent herbs in Nishakatakadi decoction was done using ICPMS. A known quantity of the powdered sample, about 100 mg each, were taken for digestion. The digested samples were diluted further and used for analysis. All the eight constituent herbs of Nishakatakadi decoction were taken for sample analysis by ICPMS.

3.8.4 ICPMS analysis of Amalakyadi Churna

ICPMS analysis was done for Amalakyadi Churna and its ingredient herbs. As Amalakyadi Churna contains P. emblica and T. chebula as common ingredients as Triphala Churna, the result was taken for those samples.

3.8.5 ICPMS analysis of Balachaturbhadrika Churna

For samples analysis, the liquid samples of constituent herbs in Balachaturbhadrika Churna are made into aerosol and fed through the inlet tube. All the four herbs in Chaturbhadrika formulation were analyzed in this method.

Bibliography

[1] Apple Leaves, Standard Reference Material 1515, National Institute of Standards and Technology, https://www-s.nist.gov/srmors/certificates/1515.pdf

[2] Peach Leaves, Standard Reference Material 1547, National Institute of Standards and Technology, https://www-s.nist.gov/srmors/certificates/1547.pdf

[3] https://nucleus.iaea.org/rpst/Documents/rs_iaea-v-8.pdf

[4] https://nucleus.iaea.org/rpst/Documents/rs_iaea-a-13.pdf

[5] https://nucleus.iaea.org/rpst/Documents/rs_iaea-v-10.pdf

[6] The Ayurvedic Formulary of India Part I Second Edition (2003) National Institute of Science Communication and Information Resources, CSIR, ISBN 81-901151-4-6, The Controller of Publications, Delhi.

[7] Ayurvedic Pharmacopoeia of India, Part-I and II -Formulations(2007) Government of India, Ministry of Health and Family Welfare, Department of Ayurveda, Yoga and Naturopathy, Unani, Siddha and Homoeopathy, New Delhi

[8] Maxwell, J. A., Campbell, J. L., Teesdale, W. J. (1989). Nuclear Instruments and Methods in Physics Research Section B: Beam Interactions with Materials and Atoms, 43(2), 218–230. doi:10.1016/0168-583x(89)90042-6

Chapter 4

Results and Discussion

Detailed analysis of the elemental profiles for the formulations of Triphaladi Churna, Nishakatakaadi decoction, Amalakyadi Churna, and Chaturbhadrika Churna, along with the constituent herbs and selected commercial formulations has been carried out using various techniques. Triphaladi Churna and Nishakatakadi decoction have been done using XRF, PIXE, NAA, and ICPMS where as Amalakyadi Churna and Chaturbhadrika Churna are done by XRF, ICPMS and PIXE. As a sample case, the analysis of P. emblica has been done by PAA.

4.1 Analysis of Triphala Churna

Analysis of Triphala Churna is done using XRF and PIXE, NAA and ICPMS for the individual herbs, and the compound formulations. The concentration of major and trace elements obtained from XRF are shown in Table 4.1. All the concentrations in the tables are expressed in mgkg $^{-1}$ units and uncertainty reported in each result includes the statistical error and systematic error. K and Ca were found to be the major elements in all the samples. The concentration of minor elements like Al, Cl, Mg, P, and S and trace elements like, Cr, Cu, Br, Fe, Mn, Nb, Ni, Sr, Rb, Ti, Y, Zn, and Zr are also tabulated. It was observed that, the elemental concentration of different herbs varies widely with respect to each other. For example, P. emblica has a high contribution of

Fe (289 ± 17 $mgkg^{-1}$) whereas T. chebula has the least contribution (11.6 ± 0.2 $mgkg^{-1}$). Mn has a contribution of 71 ± 2 $mgkg^{-1}$ in P. emblica, 19.04 ± 0.7 $mgkg^{-1}$ in T. bellirica and the least contribution of 2.6 ± 0.8 $mgkg^{-1}$ in T. chebula. Sr is present with the highest concentration of 44.6 ± 0.80 $mgkg^{-1}$ in P. emblica and with the lowest concentration of 0.9 ± 0.6 $mgkg^{-1}$ in T. chebula and so on. The relative quantity of each trace element will be the characteristic representation of the herb.

Analysis of the elemental profile of Triphala Churna shows that a good contribution of trace elements comes from P. emblica. Mn and Fe are the trace elements with the highest contribution in P. emblica. Mn concentration varies from 3 to 71 in different herbs contributing to the formulation. Concentration of Zn varies between 8 to 15 $mgkg^{-1}$. P. emblica contains only 4 $mgkg^{-1}$ of Rb whereas T. bellirica and T. chebula contain around 20-27 $mgkg^{-1}$ of Rb. The major contribution of Mn and Fe comes from P. emblica. The contribution of Rb is less significant in P. emblica. Cu and Ni concentrations are of less than 5 $mgkg^{-1}$ in all the samples.

To generate the characteristic elemental profile of the Triphala Churna, data for the XRF analysis of the compound formulation, are prepared in equal weight of the constituent herbs, as per the prescription of API. The obtained elemental profile is compared with the sum of relative fractions of the respective herb for each element and is also tabulated in Table 4.1.

Table 4.1: Elemental concentration of Triphaladi Churna in mgkg^{-1} using XRF

Elements	**Herbs**				**Formulations**	
	P. emblica	**T. chebula**	**T. bellirica**	**G.glabra**	**Triphaladi**	**Triphala**
Al	280±20	117.2±0.4	158±3	124.3±8	135±11	175±13
Br	6.40±0.05	10.3±0.57	5.3±0.17	3.44±1.6	4.81 ± 1.30	7.58±0.33
Ca	6600±136	1911±29	7790±133	2265±34	5439 ±17	5814±109
Cl	110±42	1950±70	2150±42	974±46	1210±21	1788±34
Cr	1.81±0.21	NA	1.72±0.3	0.99±0.16	NA	NA
Cu	2.03±0.29	5.12±0.06	4.22±0.23	6.67±0.53	6.11 ±0.38	4.21±0.38
Fe	289±17	11.6±0.2	118±17	135±54	112 ±6	139±15
K	13203±56	11400±212	14700±210	9851±203	10212±79	13453±45
Mg	1090±47	770±24	1655±3	1103±14	938±42	1162±10
Mn	71±2	2.6±0.8	19.04±0.7	18.57 ±3.9	22.7±1.5	27.2±0.68
Ni	1.05±0.62	1.1±0.8	1.1±0.23	NA	NA	NA
P	132±25	443±26	1082±15	623±13	432±18	569±34
Rb	3.92±0.07	22.4±1.7	26.63±1.3	1.45±1.2	9.82±0.7	19±1.1
S	1594±36	1233±14	1832±51	1434±28	1410±36	1588±24
Sr	44.6±0.80	0.9±0.6	8.3±0.7	349±52	98.36±12.9	19±1.2
Zn	7.9±1.7	11.2±0.5	15.3±0.8	5.65±0.75	8.09±0.6	10.32±0.81

[1]

[1]NA-Not Analyzed or Detected

It can be seen that the variation in the concentration of any element is less than the measurement uncertainties. This is strong support for the reliability of the measurements. Hence it can be assumed that the elemental profile of any compound herbal formulation can be prepared on the basis of its relative herbal contribution from individual constituent herbs. The difference between the deduced values and the measure values is less than 3 % for all elements except Cu and Sr in Triphala Churna. This indicates that the pellets prepared for analysis are more or less homogeneous. The elemental profile of Triphaladi Churna and the herb, G. glabra are also tabulated in Table 4.1.

The elemental profiles of Triphaladi Churna obtained using PIXE is tabulated in Table 4.2. The results or PIXE is comparable to XRF for most of the elements. PIXE analysis of Triphala Churna was able to identify elements like, Cr, Ni, and Ba, which were not obtained using XRF due to lesser sensitivity of these elements at low concentrations. The concentration of Cr was found to be the highest in T. bellirica. Fe, Mn, Zn were found to be the prominent trace elements in P. emblica. Concentration of Rb was found to be the highest in T. chebula and that of Br was the highest in T. bellirica. It was observed that the concentrations of low Z elements like Ca and Fe were found to be underestimated in PIXE. This may be due to the absorption of characteristic X-rays by the Al filter at the detector. The concentration of Ba was found to be 89 $\pm$ 14.86 mgkg^{-1} in T. chebula. The presence of Cr was not detected in P. emblica. Highest concentration of Cr was found in T. bellerica and lowest in T. chebula . The presence of Cr was not detected in the prepared formulation of Triphala Churna using PIXE.

The elemental profile of the samples obtained using NAA analysis is given in Table 4.3. In addition to the common elements determined by XRF, the concentration of elements like Co, La, Na, Sc, Sm and W were also quantified in NAA. The concentration of Co, La, Sm, and W are below 1 mgkg^{-1}. Na detection was not possible by XRF whereas a significantly high counts are obtained for Na in NAA. This is primarily due to the high thermal neutron cross

section of Na. Na was found to be of highest concentration in G. glabra and the lowest in P.emblica. Na concentration was found to be slightly overestimated in the prepared formulation of Triphala Churna as observed from Table 4.3. The elemental concentration of Triphala Churna using ICPMS are given in Table 4.4. It was observed that, Ti and Mn were found in highest concentration in P. emblica. The presence of Cu and Ca was observed in T. bellirica only. Presence of Co was detected only in P. emblica and T. bellerica where as presence of Zn was observed in all the herbs with a highest concentration in T. chebula

Table 4.2: Elemental concentration of Triphaladi Churna in $mgkg^{-1}$ using PIXE

Elements	**Herbs**				**Formulations**	
	P. emblica	**T. chebula**	**T. bellirica**	**G. glabra**	**Triphaladi**	**Triphala**
Ba	NA	89±14.86	NA	NA	NA	NA
Br	4.1±0.12	6.4±0.69	11±0.83	NA	7.6±0.77	6.9±0.74
Ca	67.7±5.3	153±7.5	50.5±10.7	226±8	55.9 ±4.8	61.5±5.2
Cu	15.2±0.44	13.7±0.42	14.3±0.41	15.6±0.44	6±0.4	12.7±0.41
Fe	211±0.63	144±0.38	15±0.3	NA	116±0.34	107±0.32
Mn	60.8±2.4	23.8±2.67	6.3±1.0	18.1±3.2	28±3.2	10.9
Ni	6.6±0.35	6.2±0.40	6.4±0.36	4.6±0.37	4.5±0.35	4.7±0.35
Rb	3.8±1.2	32.5±1.77	26.7±1.6	NA	25.2±1.55	23.7±1.5
Sr	42.4±1.65	24.3±1.65	10.6±1.24	280.1±4.8	67.3±1.32	16.9±1.36
Zn	9±0.34	8.3±0.1	9.10±0.29	6.0±0.36	5.2±0.31	4.8±0.31
Cr	NA	2.9±0.18	17.8±3.5	8.8 ±2.6	5.4±.0.25	NA

[2]

As ICPMS shows good sensitivity even at sub-ppm levels, the trace elements like Ti, V, Cr, Mn, Co, Ni, Cu, Zn, Br, Cd, Zr, As, Hg, Pb are quantified using ICPMS. The results of ICPMS analysis for Triphala Churna and its constituent herbs are shown in Table 4.4. Zr was detected in T. bellirica with a concentration of 1.24 ± 0.04 $mgkg^{-1}$. A significantly high concentration Sr was

[2]NA-Not Analyzed or Detected

observed in G. glabra in the ICPMS and PIXE. This leads to a higher concentration of Sr in Triphaladi formulation compared to Triphala formulation. The ICPMS results also indicate that toxic heavy elements like Hg, Cd, Pb and As are below the feasible limit of daily intake.

To evaluate the current status of the herbal formulations available in the market, analysis has also been carried out for a set of commercially available samples of Triphala Churna. In the present analysis, nine different samples of Triphala Churna, out of which three were the samples of different batches of the same manufacturer, have been analyzed using XRF. The data is shown in Table 4.5. It was observed that, the measured elemental profile of the prepared compound formulation as obatined from and the deducted profile had a remarkable similarity. Detailed analysis shows that the variation in elemental profiles with respect to the reference prepared may be due the excess or deficiency of certain herbs. The excess of Rb in T1 may be due to an increased proportion of T. bellirica or T. chebula. In commercial sample T5, Mn concentration is compared to the reference. This may be due to a decrease in the proportion of P. emblica which contain Mn at a significant amount. The highest concentration of Zn indicates an increase in the contribution of T. bellirica in T5. Excess concentration of Br in T4 indicates a higher percentage of T. chebula.

Table 4.3: NAA analysis of Triphaladi churna in $mgkg^{-1}$

Elements	**Herbs (dry mass)**				**Triphaladi**
	P. emblica	**T. chebula**	**T. bellirica**	**G. glabra**	
Ba	NA	2.84 ± 0.7	NA	NA	NA
Br	3.48±0.45	11.15±0.41	16.04±1.88	2.38±0.11	10.98±0.28
Ca	NA	NA	5527±240	NA	NA
Cl	73.2±12	NA	NA	NA	NA
Co	0.63±0.11	NA	0.12±0.33	NA	NA
Cu	NA	NA	13.7±7.3	NA	NA
K	16148±159	19073±357	15658±240	14352±632	NA

La	NA	0.664±0.011	NA	0.2±0.006	0.15±0.004
Mn	37.2±4	11.1±1.88	3.982±3	13.81±3	12.5±1
Na	19.7±2	30.35±3	40.07±3	46.11±4	45.68±4
Rb	NA	24.37±7	27.69±8	NA	NA
Sc	NA	NA	0.02±0.001	NA	0.015±0.001
Sm	NA	0.101±0.006	NA	0.052±0.006	0.024±0.004
W	0.017±0.004	NA	0.111±0.008	NA	0.04±0.002
Zn	7.7±2.2	63.46± 13	17.64±5.9	5.22±19	NA

Table 4.4: Elemenetal concentration of Triphala Churna in $mgkg^{-1}$ using ICPMS

Elements	**Herbs (Dry mass)**			**%Uncertainity**
	P. emblica	**T. chebula**	**T. bellirica**	
Br	3.02	3.55	6.24	14
Cd	0.02	0.01	0.002	10
Co	0.15	0.55	0.05	07
Cr	1.32	NA	0.14	04
Cu	1.72	4.26	4.82	2
Hg	0.04	0.06	0.03	8
Mn	67.1	21.3	3.07	5
Ni	0.27	1.35	0.49	5
Pb	0.52	0.13	0.11	10
Pd	0.2	0.05	0.02	3
Rb	2.55	44.77	36.24	3
Sr	9.40	28.05	6.45	9
Ti	19.5	12.3	0.07	5
V	0.52	0.35	0.03	6
Zn	10.3	14.2	9.4	10
Zr	1.62	1.24	NA	1

Table 4.5: Elemental concentration of commercial samples of Triphala Churna in $mgkg^{-1}$

Elements	T1	T2	T3	T4	T5	T6
Mg	1161±86	1080.67±54	1101±32	1053±10	1005±43	1110±22
Al	366±17	320.60±36	305±9	446±22	387±93	336±24
Si	1163±44	1001.27±28	947±83	1965±63	1851±83	1000±50
P	570±15	328.00±17	348.0±27	489±14	705±33	365±14
S	1537±21	1327.00±82	1387.6±95	1468±15	1388±12	1353±213
Cl	3010±20	1996±57	2539±88	2386±52	2303±73	2131±22
K	14530±184	10760±74	12033±180	11580±40	12110±86	11246±104
Ca	7052±20	6437±20	6136±6	6122±22	4727±35	6614±39
Cr	2.4±0.37	113±24	745±17	1.7±0.5	3±1	116±2
Mn	24.4±0.6	44.8±0.3	37.1±10	34.5±1.4	4.7±0.3	46±0.7
Fe	704±27	789±14	685.87±15	996±13	324±18	829±15
Ni	3±0.08	7.95±0.7	6.04±2	2.56±0.17	2.87±0.5	7.86±0.6
Cu	4.6±0.75	5.78±0.5	5.58±0.7	17.29±0.84	3.83±0.3	5.55±0.8
Zn	3.9±0.09	3.02±0.67	2.69±0.5	32.71±0.57	0.51±0.3	2.55±0.09
Br	7.95±0.15	7.43±0.02	7.84±0.7	11.47±0.49	7.08±0.1	7.94±0.19
Rb	39.78±0.61	20.95±0.8	23.52±4.8	25.75±.78	32.77±0.2	22.40±0.64
Sr	11.89±0.5	9.5±0.3	13±1.2	7.4±0.74	9.5±0.2	11.8±0.4

4.2 Analysis of Nishakatakadi decoction

Analysis of Nishakatakadi decoction was done for the formulation as well as the individual constituent herbs using XRF, PIXE, NAA, and ICPMS. Analysis of commercial samples was also done using XRF and PIXE. The concentration of major, minor, and trace elements in the individual herbs obtained using XRF is tabulated in Table 4.7. Wide variation has been observed in the elemental concentrations in different herbs. K and Ca were found to be the important major elements in all the samples. Al, Cl, Mg, P, and S were also found at varying concentrations. Essential trace elements like Cu, Cr, Fe, Mn, and Zn were observed in all the herbs constituting the formulation, but at varying concentrations. Nishakatakadi is a formulation administered for the treatment of diabetes mellitus. It is reported that Ca, Cr, Cu, K, Mn, and Zn plays a pivotal role in the secretion of insulin and are involved in the potentiation of insulin in glucose metabolism [39, 40, 41, 42, 43, 44]. It was observed that the highest and lowest concentration of Cu were present in C. zizanioides and S. reticulata with 16.0 ±

Table 4.6: Variation in same commercial sample of differerent batches by XRF ($mgkg^{-1}$)

Elements	T7-a	T7-b	T7-c
Mg	1161±31	1039±33	1202±18
Al	518±47	393±19	437±23
Si	1965±42	1931±	1508±36
P	562±52	358.7±12.6	438±50
S	1429 ±32	1380±18	1476±49
Cl	2810±42	2126±39	2561±78
K	12587±86	12306±106	12376±217
Ca	5517±29	5790±67	6133±60
Cr	6.37±0.44	6.7±1.66	5.53±1.17
Mn	27.97±0.63	28.8±0.8	25.51±1.05
Fe	1582±30	820±14	1027±28
Ni	2.83±0.08	3.99±0.3	3.32±0.5
Cu	5.20±0.31	4.4±0.4	4.78±0.41
Zn	5.55±0.76	4.8±1.2	3.00±1.30
Br	8.6±0.1	7.2±0.6	6.9±0.2
Rb	29.5±0.2	24.71±0.17	23.98±0.88
Sr	9.59±0.12	7.79±0.10	7.75±0.57

1.8 $mgkg^{-1}$ and 2.3 ± 0.20 $mgkg^{-1}$ respectively. Except for S. reticulata, all the samples were found to contain Zn at a moderate concentration with the highest value of 78 ± 15 $mgkg^{-1}$ in I. coccinea. S. reticulata was found to contain the least concentration of Zn with 1.20 ± 0.20 $mgkg^{-1}$. S. reticulata contributed the highest percentage of Ca with a concentration of 21500 ± 370 $mgkg^{-1}$, whereas the same was found to be lowest in C. longa (1900 ± 20 $mgkg^{-1}$). C. zizanioides and I. coccinea were found to be rich in Fe with 4000 ± 110 and 5000 ± 160 $mgkg^{-1}$ respectively. For Mn, the highest concentration was observed in S. racemosa (260 ± 7 $mgkg^{-1}$), while the least concentration of 9.8 ± 0.2 in A. lanata. An exceptionally high concentration of Si was observed in root sample of C. zizanioides (39000 ± 5900 $mgkg^{-1}$) and stem bark of S. racemosa (20000 ± 150 $mgkg^{-1}$). Ti concentration was also significantly high in C. zizanioides and S. racemosa. Br concentration was found to vary from 2 to 25 mgkg-1 in different samples. Ba, Cr, Cs, Cu, and Pb were found to be highest in C. zizanioides. Toxic heavy metal pollutants like Cd and Hg were not detected in these herbs.

Table 4.7: Elemental concentration of Nishakatakadi in $mgkg^{-1}$ using XRF

Elements	**Herbs**								**Formulations**	
	H1	**H2**	**H3**	**H4**	**H5**	**H6**	**H7**	**H8**	**REF1**	**REF2**
Al	650±60	185±8	199±3	5770±270	3250±410	500±300	13500±200	1360±170	3060±310	2520±330
Ba	62±29	53.1±2.8	48.7±6.3	168±26	248±14	53±28	158±23	27±10	110±20	90±10
Br	9.00±1.20	2.18±1.48	17.8±2.4	2.95±1.45	4.45±0.79	7.45±1.46	13.5±1.1	25.9±1.1	10.4±0.2	15.5 ±0.9
Ca	1890±20	2690±30	7460±60	14800±300	4650±90	1990±740	21460±370	10040±250	8780±190	8270±70
Cl	5040±10	190±10	1300±60	490±10	920±80	950±90	1770±30	4720±70	2200±90	3700±10
Cr	1.9±2.4	12±3	3.5±0.8	74 ±4	320±30	8.6±2.7	4.4±1.0	5.0±0.40	58.0±2.0	59.0±2.0
Cs	18.6±0.6	24.8±3.0	14.8±5.5	12.5±11.1	21.8±0.3	NA	15.7±1.8	15.6±4.9	23.0±9.0	23.0±9.0
Cu	4.77±0.22	5.00±0.26	4.08±0.45	9.50±0.19	16.7±1.8	8.20±5.00	2.27±0.20	11.17±0.44	7.7±0.3	7.7±0.3
Fe	610±10	610±160	186±5	4720±130	3980±110	1070±380	255±7	5020±160	1800±90	1800±90
K	26900±100	4170±140	9240±140	2730±60	3220±120	9100±1400	4140±90	9260±380	8500±300	16000±300
Mg	5410±40	1010±60	1190±30	4990±150	1560±60	600±100	2060±30	1740±190	2300±30	3800±400
Mn	160±10	26±1	9.8±0.2	255±7	180±10	43±28	100±1	28±0.1	108±4	165±4
P	3480±20	1050±80	590±20	276±1	690±50	680±30	254±3	960±80	1200±100	1420±10
Pb	NA	0.73±0.11	NA	5.67±0.11	6.12±0.62	2.68±0.12	1.24±0.12	5.40±0.20	3.2±0.3	3.2±0.3
Rb	11.82±0.03	7.60±0.23	17.14±0.51	19.24±0.88	9.50±0.17	14.60±8.00	11.32±0.38	11.99±1.02	12.4±0.2	24±2
S	1140±30	710±30	1030±30	1740±50	910±10	460±90	1480±20	2450±150	1400±40	1595±10
Si	3400±300	620±60	320±20	19500±150	39000±5900	7170±70	800±30	3500±700	6900±500	4600±300
Sr	15.0±0.3	7.12±0.06	25.1±0.7	71.1±2.4	82.6±3.4	10.9±1.3	137±7	58.0±4.0	50±1	50±5
Zn	16.8±1.0	14.2±0.9	20.14±1.74	14.3±0.8	16.0±1.8	11.0±3.8	1.20±0.20	78±15	18.0±0.5	31.6±3.3

The elemental concentration of the compound powder formulation and the decoction formulation are tabulated in Table 4.7. It has been observed that the sum of the fraction of the concentration of any particular element determined from each herb is consistent with the concentration obtained for the prepared powder formulation for the corresponding elements given. This ensures the homogeneity of the pellets prepared for compound formulation in powder form. In the reference decoction, Al, Ba, Ca, Cs, Fe, La, Si, and Ti showed a significant reduction in concentration compared to powder formulation as indicated by the ratio of the concentration of the two reference samples. This may be due to the formation of insoluble compounds which get filtered during the preparation. Br, Cl, Co, Cr, Cu, K, Mn, P, and Pb showed an increase in the extracted decoction. Hence, water-soluble compounds of elements may show higher concentration and insoluble ones may show a lesser concentration in the decoction. The estimation of filtration loss is important while determining the daily intake of elements in processed formulations like decoction and fermented liquid extracts. The method of decoction preparation is supposed to reduce the unwanted accumulation of certain non-essential elements while ensuring the availability of essential trace elements like Cu, Cr, Fe, Mn, Mg, Rb, Zn, of specific interest, in the drug. The correlation between the trace elemental concentration and the therapeutic effect of the combined formulation in the treatment of diabetes mellitus is yet to be revealed.

Table 4.8: Elemental concentration of Nishakatakadi in mgkg^{-1} using PIXE

Elements	**Herbs**								**Formulations**	
	H1	**H2**	**H3**	**H4**	**H5**	**H6**	**H7**	**H8**	**REF1**	**REF2**
Ba	54.8 ±11	32.9 ± 12	75.2 ±14	362.6± 26	NA	75.7 ± 14	98.2 ± 11	93.1 ± 12	NA	187.5± 20
Br	6.7±1.0	0.24±0.01	12.8±1	0.18±0.01	3.1±0.7	5.9±0.7	11.2±0.8	17.5±1.1	12.8±1.0	9.5 ±1.1
Ca	89.6±6.5	97±5.6	230 ±8	47.5±6.9	84.8±5.5	84.1±5.4	515.5±10.6	269.4±8.8	230.1±7.9	163.5±19
Cr	15.7±2.1	7.3±1.9	26.6±2.8	55.02±3.7	NA	11.5±2.0	NA	13.6±2.4	26.6±2.8	NA
Cu	15.3±0.5	12.9±0.4	17.4±0.05	3.3 ±0.5	12.3±0.4	13.7±0.4	11.8±0.4	16.1±0.5	17.4±0.5	11.7±0.8
Fe	160.5±0.4	139.6±0.4	141±0.4	164±0.6	181.4±0.4	157.4±0.4	123.8±0.4	350.6±0.6	141.1±0.4	203±8
Mn	210.5±3.0	30.1±1.6	9.89±2.6	220±4	31.1±2.2	50.4±2.1	122.3±2.5	38.8±2.2	27.8±2.6	63.9 ±7
Mo	5 ±1.3	NA	NA	NA	NA	NA	NA	NA	NA	NA
Ni	5±0.4	4.8±0.4	6.3 ±0.62	1.4 ±0.03	4.3±0.4	5.2±0.4	5.2±0.4	5.7±0.4	6.3±0.4	4.3±0.6
Rb	11.1±1.7	10±1.0	26.2±1.6	12.9 ±1.3	NA	22.6±1.5	12±1.4	13.6±1.6	26.2±1.6	14 ±1.8
Se	NA	0.22	NA	NA	NA	NA	NA	NA	NA	NA
Sr	22.6±1.6	13.5±1.8	23.5±5.6	67.26±2.8	18.8±1.5	12.7±1.6	144.7±3.4	71.3±2.5	56.5±2.3	60.5±3.6
Zn	12.1±0.4	8.1±0.3	17.5±0.7	2.3±0.1	8.7±0.4	5.6±0.4	3.2±0.3	50.3±0.7	51.8±0.7	14.9 ±1

Elemental profile of the herbal samples of Nishakatakadi, obtained from the PIXE analysis is given in Table 4.8. Elemental concentration of Ba, Br, Ca, Cr, Cu, Fe, Mn, Mo, Ni, Rb, Sr, and Zn were obtained. As the sensitivity of PIXE is lesser for low Z elements, analysis of low Z elements is not done here. The Table 4.8 shows that the concentration of Ca varies between 47 to 515 $mgkg^{-1}$ in different herbs. Even though K and Ca are generally considered as the major elements in herbal samples, the concentration of both the elements is under estimated in the PIXE results. The presence of trace quantities of Ni was observed in all the herbs with an average concentration less than 6 $mgkg^{-1}$. Mo was found in P. emblica at 5 $mgkg^{-1}$ with an uncertainty of 26 %. The presence of Pb was identified in the PIXE spectrum. But, reliable results for the concentration of Pb is not obtained due to the presence of large uncertainty. PIXE results show that, Ni concentration is almost similar in all the herbs of Nishakatakadi except S. recemosa. The concentration of Ba shows wide variation in the constituent herbs of Nishakatakadi.

The trace elemental profiles of the compound formulations and its constituent herbs, obtained from NAA, are presented in Table 4.9. It was observed that, Na had a significant contribution in all the herbs even though its presence was not detected in XRF. Na concentration was found to vary between 11 to 620 $mgkg^{-1}$ in different herbs. Co and Sc were found to be less than 1 $mgkg^{-1}$ in all the samples whereas La concentration varies between 0.2 to 5 $mgkg^{-1}$. The high thermal neutron captures cross-section, suitable gamma energies, and convenient half-lives enable the detection of these elements at very low concentrations. The analysis of reference samples shows that K is a major element both in the powder and in the decoction. The process of extraction to form decoction increases the concentration of K from 10600 $mgkg^{-1}$ to 19000 $mgkg^{-1}$. The presence of Fe was decreased considerably after extraction which is attributed to the filtration loss as previously discussed.

In order to have a better knowledge of trace elemental content expected in Nishakatakadi decoction, ICPMS studies for individual herbs were done and

the results are tabulated in Table 4.9 . Cu, Cr, Mn, Rb, Sr and Zn are the elements identified using ICPMS. In addition, heavy trace elements like, Hg, Cd, Pb, As, Bi were detected in the constituent herbs of Nishakatakadi. The accurate determination of the concentration of these elements was difficult in X-ray methods, due to poor efficiency of X-ray detector and the low intensity of observable X-ray. The analysed sample of P. emblica was found to contain 1.178 mg of Hg per kg. The lowest concentration of Hg was observed to be 0.18 mgkg^{-1} in P. emblica and a comparable concentration of 0.187 mgkg^{-1} was observed in I. coccinea. The presence of Cd was not detected in ICPMS results for S. potatorum and P. emblica. Cd concentration was found to the highest in S. recemosa with a concentration of 0.646 with an uncertainty of 10 % . The concentration of As was also found to be the highest in S. recemosa. However, the large uncertainty in the determination of As (26 %) makes the observation less reliable. The WHO recommended concentration of trace elements in these herbs fall well above the observed values for Hg, Cd, and As. The presence of Pb was found to vary from 231 μgkg^{-1} to 3571 $\mu g kg^{-1}$ with an uncertainty of 10 %

As a representative case of primary analysis of marketed samples, the analysis of elemental concentrations in some commercially available formulations of Nishakatakadi is carried out. The result is presented in Table 4.11. A good correlation between commercial samples C1, C2, C3, C4, C5, C7, and prepared decoction sample, is observed with a Pearson correlation coefficient r >.92 at a significance level of 0.01. The samples C6 and C8 showed poor correlation as evident from the correlation coefficient which indicated a significant deviation of the sample from the prepared decoction.

Table 4.9: Elemental concentration Nishsakatakadi in mgkg^{-1} using NAA

Elements	Herbs								Formulations	
	H1	**H2**	**H3**	**H4**	**H5**	**H6**	**H7**	**H8**	**REF1**	**REF2**
Br	8.44±0.25	2.70±0.15	17.6±1.3	2.7±0.4	7.5±0.9	6.6±0.3	11.77±0.09	26.0±0.5	9.9±0.2	15.0±0.7
Co	0.08±0.02	0.13±0.02	0.17±0.35	0.01±0.06	0.08±0.1	0.52±0.05	NA	0.59±0.65	0.531±0.02	0.529±0.03
Fe	NA	710±120	170±15	NA	NA	1020±240	NA	5400±100	1869±370	1360±340
K	30850±500	4590±70	16710±250	2970±120	4590±70	12390±200	4465±87	11550±410	10600±270	19000±440
La	0.56±0.10	0.67±0.01	0.26±0.01	3.13±0.10	2.31±0.10	1.06±0.10	1.556±0.42	4.76±0.10	2.0±0.55	1.2±0.35
Mn	160±	23.0±0.3	10±3	NA	NA	NA	111.7±6.4	NA	129±11	176±14
Na	85±7	54±5	84±8	150±14	540±50	160±5	11.22±0.32	620±20	296±9	344±10
Rb	NA	NA	19±6	NA	NA	16.3±4	NA	13±4	26±5	24±4
Sc	0.064±0.013	0.06±0.02	0.10±0.03	0.14±0.04	0.07±0.03	0.88±0.05	NA	1.04±0.12	NA	NA
Sm	0.09±0.01	0.112±0.008	NA	0.480±0.034	0.41±0.02	0.24±0.03	0.098±0.008	1.20±.18	0.40±0.02	0.28±0.01
W	0.029±0.003	0.01±0.001	0.06±0.01	0.01±0.001	0.02±0.01	0.13±0.02	NA	NA	NA	NA
Zn	NA	NA	17±6	NA	NA	14±5	NA	80±7	27.9±3	28.0±3.1

[3]

[3]NA-Not Analyzed or Detected

Table 4.10: Elemental concentration of Nishsakatakadi in $mgkg^{-1}$ using ICPMS

Elements	**Herbs (dry mass)**								**Uncertainity in concentration**
	H1	**H2**	**H3**	**H4**	**H5**	**H6**	**H7**	**H8**	
As	0.0768	0.0230	0.0354	0.7223	0.3369	0.1742	0.2470	0.3905	0.26
Ba	28.29	8.25	24.20	87.6	17.3	32.07	101.02	10.01	NA
Bi	0.0040	0.0035	0.0005	0.0160	NA	NA	NA	NA	NA
Cd	0.0449	NA	0.0579	0.6464	0.0456	0.0489	NA	0.0384	0.10
Co	0.397	0.138	0.085	1.654	0.866	0.520	0.314	0.795	0.07
Cr	3.169	4.650	1.383	42.915	4.172	9.010	2.809	3.256	0.04
Cu	5.15	4.85	3.33	11.14	6.53	5.36	1.45	11.66	0.02
Mn	174	22.4	9.95	289	32.5	56.4	81.4	27.8	0.05
Hg	0.6198	0.3413	0.2636	0.2752	0.6017	1.1775	0.1636	0.1817	0.08
Mo	0.1627	0.0425	NA	0.3616	0.0828	NA	NA	NA	0.05
Ni	1.7894	3.6569	0.3924	7.0455	1.2592	2.1538	0.8861	3.0497	0.05
Pb	0.4606	0.5096	0.2311	2.6613	1.2107	2.2771	0.9040	3.5750	0.10
Pd	0.3378	0.1244	0.0150	0.0584	0.0614	NA	0.1217	0.0265	0.03
Rb	9.7	6.3	16.5	10.9	3.34	16.3	8.6	11.7	0.03
Se	0.0998	0.0665	0.0664	0.5440	0.2006	0.0220	0.0444	0.5772	0.04
Sr	14.3	6.6	25.5	71.4	9.69	9.66	128.	65.8	0.09
V	1.632	0.544	0.307	16.039	3.062	4.423	0.613	3.508	0.06
Zn	14.8	12.9	17.08	11.7	13.97	8.63	2.11	56.07	0.09

Table 4.11: Elemental concentration of commercial samples of Nishakatakadi decoction in $mgkg^{-1}$ using XRF

Elements	**Commercial samples**							
	C1	**C2**	**C3**	**C4**	**C5**	**C6**	**C7**	**C8**
P	1460±20	1470±80	1520±30	1550±10	1395±2	1520±50	1610±90	15440±440
S	2010±50	2740±60	2150±90	2770±40	2010±50	3510±120	3250±50	1110±40
Cl	13570±550	18300±800	5200±200	14700±300	9060±30	20670±630	8890±460	2530±80
K	22670±460	28710±560	16750±220	26060±370	20030±100	22000±400	16500±400	9370±100
Ca	3300±30	3910±70	5890±250	3780±40	3360±100	3570±60	5310±130	23670±340
Mn	120±10	129±7	137±4	117±2	108±5	210±6	147±4	69±3
Fe	710±40	1510±30	2020±120	210±2	596±20	700±40	830±20	610±10
Cu	2.2±0.3	1.8±0.7	6.7±0.7	2.2±0.4	3.3±1.2	2.9±0.8	4.6±1	6.7±1.1
Zn	5.6±1.4	12.5±1.5	22.0±1.0	12.6±0.6	11.0±0.9	20.2±0.6	16.0±1.3	24.0±3.3
Br	90±3	55±1	15±2	1211±33	56±1	69±2	39±3	14±3
Rb	38±3	75±3	34±2	192±3	22±2	42.5±0.8	23.4±0.3	9±1
Sr	34±2	28±1	57±4	34.8±0.5	33.0±0.7	36.2±0.5	50±4	70±5

[4]

[4]NA-Not Analyzed or Detected

4.3 Analysis of Amalakyadi Churna

Elemental profiling of Ayurvedic formulation Amalakyadi Churna and its constituent herbs using XRF, PIXE, and ICPMS have been performed. The elemental concentration obtained from XRF is tabulated in Table 4.12. The XRF results show that the concentration of major elements like, Cl and Ca has a concentration of the order of 3000 $mgkg^{-1}$ and K has a concentration of the order of 15000 $mgkg^{-1}$. Concentration of Rb and Sr in P. zeylanica was found to be 45.7 $\pm$ 1.1$mgkg^{-1}$ and 12.60 $\pm$ 1.8 $mgkg^{-1}$ respectively. Br concentration of P. zeylanica was found to be low when compared to P. longum. The presence of elements Fe, Cu, K and Zn act as a signature of P. zeylanica in the formulaton.

The Table 4.13 shows the concentration of elements for the constituent herbs and the compound formulation using PIXE. The analysis shows that P. zeylanica contains a relatively higher concentration of Sr and Zn. The concentration of Mn was found to be the same in both P. longum and P. emblica ($\approx$ 20 $mgkg^{-1}$) whereas, the lowest contribution comes from T. chebula ($\approx$ $mgkg^{-1}$). The concentration of Ni was found to the highest in P. zeylanica whereas, only a slight variation in the concentration of Ni for P. longum, P. emblica and T. chebula. PIXE result shows a significant concentration of Zn in P. zeylanica with 34.3 $\pm$ 1.38 $mgkg^{-1}$. The analysis of rock salt was done using PIXE. The presence of Br (56 $\pm$ 7 $mgkg^{-1}$) Cu (6 $\pm$ 0.24 $mgkg^{-1}$) and Fe (59 $\pm$ 4 $mgkg^{-1}$) was observed in the PIXE analysis.

The elemental profile for Amalakyadi Churna obtained from ICPMS is tabulated in Table 4.14. The table shows that, the major contribution of Br in the formulation is due to T. chebula. Cu concentration was found to be highest in P. zeylanica. T. chebula and P. longum contain an almost similar concentration of Rb, (26.7 $\pm$ 2.58 and 27.3 $\pm$ 2.80 $mgkg^{-1}$) which is far less than the concentration of Rb in the formulation (13.9 $\pm$ 2.2 $mgkg^{-1}$).

Table 4.12: Elemental concentration of Amalakyadi Churna in $mgkg^{-1}$ using XRF

Elements	**Herbs**				**Formulations**
	P. longum	**P. zeylanica**	**P. emblica**	**T. chebula**	
Br	16.16 ± 0.66	3.71± 1.3	7.45 ± 1.46	5.81 ± 1.26	24 ± 3.4
Ca	3486 ± 425	3200 ± 193	1990 ± 740	1638± 112	2203± 371
Cl	3326 ± 10.61	3238 ± 297	950 ± 90	NA	1841 ± 86
Cu	10.77 ± 0.24	28.4 ±6.7	8.20 ±5.00	7.38 ± 1.09	16.74 ± 0.6
Fe	64 ± 10.56	182 ± 5.1	1070 ± 380	174.21 ± 2.35	69.37 ± 2.5
K	10734 ± 1141	15225 ± 1066	9100 ± 1400	9809 ± 681	19872 ± 251
Mn	10.45 ± 0.94	14.5 ± 0.98	43 ± 28	4.89 ± 0.58	12.8 ± 1.4
P	1841 ± 105	290 ± 59	680 ± 30	379 ± 125	680 ± 84
Rb	29.93 ± 3.23	12.6 ± 1.83	14.60 ± 8.00	34.05 ± 3.29	18.7 ± 2.6
S	1336 ± 56	1955 ± 278	460 ± 90	NA	863 ± 48
Sr	3.69 ± 0.54	45.71 ± 1.1	10.9 ± 1.3	6.7± 3.38	16.71 ± 1.4
Zn	12.46 ± 0.21	41± 2.7	11.0 ± 3.8	7.20 ± 1.71	15.83 ± 1.3

[5]

[5]NA-Not Analyzed or Detected

Table 4.13: Elemental concentration of herbs in Amalakyadi Churna in $mgkg^{-1}$ using PIXE

Elements	**P. longum**	**P. zeylanica**	**P. emblica**	**T. chebula**	**Formulation**
Br	NA	NA	7.2 ± 1.25	11 ± 1.38	14.1 ± 1.46
Ca	90.8 ± 9.94	94.4 ±10.96	67.7 ± 9.48	50.5 ± 8.94	72.5 ± 1.7
Cr	NA	26.5 ± 6.02	NA	NA	NA
Cu	17.6 ± 0.99	73.1 ± 2.07	15.2 ± 0.88	14.3 ± 0.80	20.6 ± 0.68
Fe	121.3 ± 1.56	135.5 ± 3.46	115.2 ± 1.49	137.3 ± 1.75	109.6 ± 0.17
Mn	15.1 ± 2.2	14.7 ± 3.77	20.8 ± 4.94	6.3± 2.9	13.9 ± 3.4
Ni	5.4 ± 0.68	9.1 ± 0.91	6.6 ± 0.67	6.4 ± 0.70	5.1 2 ± 0.5
Pb	NA	5.3 ± 1.57	NA	NA	NA
Rb	27.3 ± 2.80	14 ± 2.10	NA	26.7 ± 2.58	13.9± 2.2
Sr	10.5 ± 1.97	30.6 ± 2.96	17.4 ± 2.52	10.6 ± 1.97	14.2 ± 2.18
Zn	8.4 ± 0.69	34.3 ± 1.38	9 ± 0.67	4.6 ± 0.53	10 ± 1.08

[6]

Table 4.14: Elemental concentration in Amalakyadi Churna in $mgkg^{-1}$ using ICPMS

Elements	**Herbs**				**Formulation**
	P. longum	**P. zeylanica**	**P. emblica**	**T. chebula**	
Br	NA	NA	3.02	3.55	NA
Cd	NA	NA	0.02	0.01	NA
Cr	2.083	0.952	9.10	0.49	NA
Cu	11.823	1.978	5.36	6.46	24.4468
Hg	0.103	0.0891	1.178	0.24	NA
Mn	11.098	17.453	56.38	1.89	6.265
Mo	0.1023	NA	NA	NA	NA
Ni	0.736	0.868	2.277	1.04	2.117
Pb	0.278	0.1404	2.277	1.04	NA
Rb	30.115	17.798	16.27	36.25	15.394
Sr	3.886	55.067	9.66	6.45	8.415
V	0.183	0.52	0.52	NA	0.35
Zn	11.975	53.278	8.63	6.8	23.69
Zr	NA	NA	1.62	1.24	NA

[7]

[7]NA-Not Analyzed or Detected

Table 4.15: Trace elements in Balachaturbhadrika Churna in $mgkg^{-1}$ using XRF

Elements	**Herbs (dry mass)**				**Formulation**
	C .rotundus	**P.longum**	**P. integerrima**	**A.heterophyllum**	
Al	87 ±4	114 ± 4	275 ± 47	116 ± 20	139 ± 21
Ba	34 ± 11	34.89 ± 5.3	46.05 ± 3.45	22.70 ±1.50	14 ± 21.31
Br	7.03 ± 0.38	16.16 ± 0.66	1.06 ± 0.04	7.10 ± 0.14	NA
Ca	450 ± 14	3490 ± 425	2020 ± 98.9	2560 ± 85	1970 ± 58
Cl	860 ± 1.66	3330 ± 10.60	2070 ± 63	640 ± 3.62	2160 ± 60
Cr	0.17 ± 0.12	0.11 ± 0.00	1.64 ± 1.33	0.11 ± 0.00	0.11 ± 0.00
Cu	9.91 ± 0.20	10.77 ± 0.24	4.86 ± 0.25	7.06 ± 0.33	7.97 ± 0.42
Fe	53.40 ± 2.72	64 ± 10.56	171 ± 9.67	105 ± 4.27	95.56 ± 9.40
K	6920 ± 87	10730 ± 1140	12760 ± 270	6640 ± 207	9640 ± 150
Mg	960 ± 32	1420 ± 74	915 ± 44.49	1200± 47	1070 ± 21
Mn	11.54 ± 0.81	10.45 ± 0.94	22.30 ± 0.63	14.5 ± 0.25	15.99 ± 0.30
Ni	2.51 ± 0.24	2.24 ± 0.08	2.64 ± 0.17	4.07 ± 0.80	2.59 ± 0.34
P	2920 ± 50	1840 ± 105	1020 ± 40	1730 ± 63	1910 ± 132
Rb	8.15 ± 0.10	29.93 ± 3.23	39.62 ± 2.20	9.66 ± 0.27	21.88 ± 1.10
S	1213 ± 23	1336 ± 56	706 ± 27	810 ± 26	1135 ± 103
Si	2380 ± 145	759 ± 76	1470 ± 316	334 ± 143	1410 ± 177
Sr	6.69 ± 0.43	3.69 ± 0.54	4.94 ± 0.64	10.85 ±0.36	7.68 ± 0.43
Ti	2.65 ± 0.13	4.48 ± 0.87	14.89 ± 0.35	9.91 ± 0.71	7.34 ± 0.68
Zn	64.34 ± 2.55	12.46 ± 0.21	9.43 ± 0.33	19.36 ± 0.89	19.36 ± 1.15

4.4 Analysis of Balachaturbhadrika Churna

Elemental profiles of Balachaturbhadrika Churna and its constituent herbs have been shown in Table 4.15 and 4.16. It was observed that the major element K was present with highest concentration in P. integerrima (12700 ± 269). P. longum was also found to contain comparable concentration of K (10700). A. heterophyllum and C. rotundus were found to contain comparable concentrations of K of the order of 6900 and 6600 . The XRF results show that, the Chaturbhadrika formulation contains Cu and Sr of comparable concentrations (7.97 ± 0.42 $mgkg^{-1}$ and 7.68 ± 0.43 $mgkg^{-1}$) respectively. Presence of Mn, Rb and Zn were observed with concentrations of 15.99 ± 0.30 mgk^{-1}, 21.88 ± 1.10 $mgkg^{-1}$ and 19.36 ± 1.15 $mgkg^{-1}$ respectively. In C. rotundus, the concentration of Zn was found to be significantly high (64 $mgkg^{-1}$). ICPMS result shows the concentration of toxic heavy metals Cd, Hg, and Pb accumulated in the herbs are within the permissible limit of intake.

Table 4.16: Trace elements in Balachaturbhadrika Churna in $mgkg^{-1}$ using ICPMS

Elements	**Herbs (dry mass)**			
	C. rotundus	**P. longum**	**P. integerrima**	**A. heterophyllum**
Ba	4.453	4.590	1.885	4.58
Cd	0.032	NA	0.004	0.0588
Co	0.062	0.025	0.118	0.062
Cr	2.027	2.083	0.074	0.296
Cu	8.805	11.823	4.119	6.382
Hg	0.22	0.103	0.089	0.082
Mn	8.42	11.10	3.10	12.8
Mo	NA	0.102	NA	NA
Ni	0.872	0.736	2.015	4.926
Pb	0.473	0.278	0.117	0.145
Pd	0.008	NA	NA	NA

Rb	11.288	30.115	30.033	8.536
Se	0.044	NA	0.022	NA
Sr	3.665	3.886	2.028	10.7270
V	0.416	NA	NA	0.082
Zn	78.198	11.976	4.842	16.822

[8]

4.5 Photon Activation Analysis of P. emblica

Analysis of compound herbal formulations and their ingredient herbs have been done using different methods like XRF, PIXE, NAA, and ICPMS, and the elemental fingerprints are generated. Out of the four selected formulations, P. emblica was a common herb in three of the formulations. Hence, P. emblica was taken as a representative sample, and taken for further analysis, using PAA. The concentration of various elements in P. emblica determined using PAA is tabulated in Table 4.17. The concentration of Fe was found to be 450 ± 17 $mgkg^{-1}$. PAA is expected to give a complementary result to other techniques like NAA and PIXE. It was observed that, there is a significant variation in the results of some elements in PAA. This may be due to the lesser cross-section for (γ, n) reactions for these elements, or variation in the detection characteristics of different methods.

Table 4.17: Elemental concentration obtained using PAA for P. emblica

Elements	**Concentration ($mgkg^{-1}$)**
Fe	450 ± 17
Sr	50.6 ± 7.9
Zn	9.35 ± 3.70
Rb	12.56 ± 2.6
Cl	71.67 ± 14
Mn	0.27 ± 0.03
Br	67.17 ± 5.9

[8]NA-Not Analyzed or Detected

Trace elemental analysis can be a better tool for standardization of herbal formulations as it can provide information of several parameters in each formulation by which classification of herbal formulations can be done. The elemental profiles of reference samples of powder formulations were comparable to the deduced elemental profile from the individual herbs. The identification of elements characteristic to a particular herb can indicate the presence or absence of that herb in the combined formulation, which can set be set as a referral standard for quality assurance.

Bibliography

[1] Maciej J. Bogusz, Huda Hassan, eid Al Enazi, Zuhour Ibraim, Mohammed AlTufail (2006) J.Pharm. Biomed. Anal. 41, 554

[2] Ari I De Ektessabi, M. Ariona, R A Bionet, Analytical Sciences 21 (2005) 885-892

[3] Antoaneta Ene, I V Popescu, Claudia Stihi, Anca Gheboianu, A. Pantelic Carmelia Petre (2010) Environmental and Earth Physics, Rom. Jour. Phys., 55, 78 806814

Chapter 5

Comprehensive Analysis of Different Techniques

Elemental analysis of herbal formulations namely Triphaladi Churna, Nishakatakadi decoction, Amalakyadi Churna, and Balachaturbhadrika Churna has been carried out using different techniques like XRF, PIXE, NAA, ICPMS, and PAA. The reliability of the results of each technique depends on the specific method of analysis. There are also practical difficulties in carrying out analysis of certain elements in any particular method adopted. A combination of elemental profiles obtained by different methods thus generates a reliable elemental fingerprint, especially at trace levels. A comprehensive analysis of the results discussed in the previous chapter is included in this chapter.

5.1 Comparison Between Different Techniques

Out of the five methods adopted for analysis, XRF, PIXE, NAA, and PAA are considered as non-destructive techniques. Even though the underlying process in both PIXE and XRF are same, there is certain pros and cons for both the techniques. In XRF, the identification of Na to U is typically possible, the quantity of the element in the sample selected limits the application. In general, the sensitivity of XRF is lower than that of PIXE for medium Z elements.

Hence PIXE will be comparatively better in this regard. The contribution from bremsstrahlung target of the X-ray source like Rh and Pd comes at energies greater than 20 keV, and characteristic peaks at this region are immersed in the background especially for Cd and In. PIXE can produce reliable results for elements with Z values ranging from 13 to 40. Beyond that, the energies of K X-rays fall in a region where the efficiency of conventional X-ray detector Si-Li detector is low. Hence L lines are used for elements of atomic number greater than 40 in both XRF and PIXE. The intensity of L lines is rather low which results in decreased counts for these elements and hence, increases the uncertainty in the results. Elements like Ba and Pb were detected by their $L\alpha$ lines and hence the X-ray results are less reliable for these elements in the case of both XRF and PIXE. PIXE spectra showed a marked decrease in the counts for elements like K and Ca. This can be attributed to the absorption of the major part of these X-rays by the Al filter at the detector, which absorbs the low energy X-rays and thus reduces the counts at the detector considerably. In the present detector, Al foil of total thickness 0.75 μ was used as an X-ray filter. Hence the results of K, Ca, and other low Z elements are not reliable quantitatively. Hence the concentration of these elements obtained from XRF is more dependable than PIXE. The concentration of Fe in XRF can also have interferences due to the target material Co which broadens the peaks of Fe. Hence for Fe, the PIXE results are more reliable. The detection limit of PIXE is higher than XRF. For the elements with very low concentrations of sub-ppm levels, like Cr, Co and Ni, XRF results give larger uncertainty due to less sensitivity at low concentrations. Hence results of PIXE can be considered as the better choice for quantification of Co, Cr, and Ni.

Activation methods are far more sensitive method than the X-ray techniques as the identification of gamma rays are done which reduce the matrix effects. Possibility of detection of multiple daughter nuclei of same parent elements and multiple gamma lines of different energies, as in case of Br, and Na, activation methods can give results which are reproducible with high accuracy. The

feasibility of NAA depends on various factors like the abundance of the naturally occurring isotope, energy, and intensity of the gamma rays, the efficiency of the detector to detect specific gamma lines, and the half-life of the radioisotope. For Fe, the naturally occurring isotope, Fe-56 goes to a stable state and does not produce any gamma lines by thermal neutrons and the detectable gamma lines that come from Fe-58 are less abundant (0.28 %). Hence, the determination of Fe is less preferable in NAA when the expected concentration of Fe is low. In the case of detection of Ca, NAA will not produce gamma-emitting daughter isotopes. The only isotope of Ca, which has a convenient half-life and energy for detection, Ca-47 has an abundance of 0.004% only. Hence, the determination of Ca is also prone to uncertainties. The detection of Mn-56 (846keV) in presence of Mg-27(844) results in gamma-ray interferences due to closer energies and half-lives. Detection of Sr-88 is not possible due to the much lower intensity of gamma line produced by (n, γ) reactions of Sr-88. The other isotope with a convenient half-life and gamma energy, Sr-87 results in a stable daughter nucleus after thermal neutron capture. Even though uncertainties hinder the reproduction of elemental concentration of the above-mentioned cases, NAA offers higher accuracy for elements like Rb, Zn, Cl, Br, and Au. Most of the rare earth elements like La, Sm, Pr, Sc, Sm, and Eu, have high thermal neutron cross sections and gamma lines suitable for NAA is available. Hence NAA can be very well used for the determination of these elements with high accuracy, even though these elements are present at ultra-trace levels only in herbal samples.

Photon activation Analysis is reliable for elements for which the (n, γ) produce any measurable gamma lines. PAA is very well suitable for the quantification of elements like Cr, Fe, Rb, Mn, and Ti. But the lower cross-sections for gamma-induced reactions result in lower counts and higher uncertainty. For ICPMS, the detection of elements is almost independent of the atomic number, and all the elements can be detected with equal sensitivity. Very low concentration of the order of 10^{-9} mgkg^{-1} can be determined by ICPMS. This method is thus suitable for the detection of toxic heavy metal pollutants like As, Cd,

Pb, and Hg. In the selected herbal samples and the formulations, the concentration obtained for these heavy metals is low, indicating that there is no heavy metal contamination in the prepared samples. However, ICPMS is a destructive method and the sample cannot be retrieved back after analysis. The cost of analysis act as a constraint for the detection of major and minor elements. Moreover, ICPMS involves multiple analytic procedures for sample preparation. Hence the results are prone to contamination and manual errors.

Moreover, the nature of the sample can also cause deviations in the results. For example, in case of C. zizanioides, the preparation of fine powder is a tough task in stainless steel grinders or agate mortar. The inhomogeneity in composition largely affects the results of PIXE and XRF as the beam spot probing the sample is very small. Dry digestion methods, like the ashing of the samples, can be a suitable alternative to reduce the disparity of the result. Ashing of the samples can improve the counts obtained for elements by removing the organic matrix and hence reducing the matrix effect interferences especially in PIXE and NAA. But it introduces wastage of volatile trace elements like Br, As, and Hg.

5.2 Comprehensive Analysis of Triphaladi Churna

The analysis of compound formulation together with constituent herbs helps to identify a better profile of Triphaladi Churna. The major elements obtained in the constituent herbs of Triphaladi Churna are, Ca, K, Mg, and S. Al, Cl, and P are the minor elements obtained. The concentrations of Br, Cr, Cu, Fe, Mn, Ni, Rb, Sr, Zn, La, Sm, Sc and W - the trace elements are obtained by employing different techniques. The compound formulation contains significant amounts of Ca, Rb, and Sr whereas the concentration of Br, Cu, Ni, and Zn is comparatively low. The addition of an herb G. glabra to Triphala Churna makes significant changes in the elemental concentration. Sr and Fe concentration had notable differences in the Triphala formulation compared to Triphaladi, as the

added herb G. glabra contains a significant concentration of Sr. In the similar manner, the presence or absence of elements in the prepared formulation can indicate the deficiency or excess of that herb in the formulation. Therefore, it is possible to identify elements in each herbal formulation whose concentration can be indicated by the constitution of the herb. It is also possible to identify elements characteristic of each herb, like Sr in G. glabra. Analysis of commercial formulation of Triphala Churna indicated that the commercial formulations are largely comparable to the prepared reference formulation. There observed an increase in the concentration of Al and Fe in the case of commercial samples when compared to the laboratory prepared samples. This can be due to the accidental incorporation of trace elements from the utensils and storage facilities while preparing in bulk quantities. In the commercial samples, Si and Fe showed significant enhancement in the concentration. One possible reason may be the fact that the present sample is prepared in laboratory conditions and ground using agate mortar and pestle whereas commercial samples are prepared using stainless steel equipment.

It was also observed that the elemental concentration data of the same commercial product in the three different batches were comparable with each other. It establishes that the same manufacturer, following the same method of preparation and procedure at different manufacturing periods, can produce compound formulation of a significantly uniform trace elemental profile. However, the concentration of trace elements detected depends on the washing process also. It was observed that, the concentration of many trace elements reduced considerably in P. emblica when the procedure of washing was done on dried fruit in contrast to the washing prior to drying.

5.3 Comprehensive Analysis of Nishakatakadi Decoction

The analysis of Nishkatakadi decoction has been done and the concentrations of Al, As, Ba, Br, Ca, Cd, Cl, Co, Cr, Cs, Cu, Fe, Hg, K, La, Mg, Mn, Na,

P, Pb, Rb, S, Sc, Si, Sm, Sr, Ti, V, W, and Zn are determined employing different techniques. The elemental concentration of prepared powder formulation shows that the sum of the fraction of the concentration of any particular element determined from each herb is consistent with the concentration obtained for the prepared formulation, for the corresponding elements. This ensures the homogeneity of the pellets prepared for compound formulation in powder form. But in the decoction reference, Al, Ba, Ca, Cs, Fe, La, Si, and Ti showed a significant reduction in concentration compared to powder formulation, as indicated by the ratio of the concentration of the two reference samples. This may be due to the formation of insoluble compounds which get filtered during the preparation. Br, Cl, Co, Cr, Cu, K, Mn, P, and Pb showed an increase in the extracted decoction. Hence, water-soluble compounds of elements may show higher concentration and insoluble ones may show a lesser concentration in the decoction. The estimation of filtration loss is important while determining the daily intake of elements in processed formulations like decoction and fermented liquid extracts. The method of decoction preparation is supposed to reduce the unwanted accumulation of certain non-essential elements while ensuring the availability of essential trace elements like Cu, Cr, Fe, Mn, Mg, Rb, and Zn, which are of specific interest in the drug. The presence of Cr in the reference formulation is a strong indicator of the inclusion of S. recemosa whereas the presence of Mn is an indicator of the contribution of S. recemosa. The formulation containes high concentration of Rb which may act as the signature of I. coccinea.

No major deviations in the elemental profiles of commercial samples were seen in the XRF analysis. In a closer analysis, the following observations are made. In the case of C4, there observed an unusual increase in the concentration of Br which is beyond the limit of excess or deficiency of any constituent herb, hence this may indicate the presence of adulterer herb that contains a considerably higher concentration of Br. In the case of commercial sample C8, the higher concentration of Ca and Sr indicates the excess contribution of S. reticulata, and the excess concentration of P is an indication of an excess of the

presence of C. longa in the sample. The deficiency of Mn and Rb indicates the deficiency in the proportion of S. racemosa. Deficiency of K is an indication of deficiency of A. lanata whereas deficiency of Cu is an indication of deficiency of C. zizanioides. A lower concentration of Br, Fe, S and Zn in many of the commercial samples is an indication of deficiency of sufficient quantity of I. coccinea. A lower concentration Cu is an indication of deficiency in the contribution of C. zizanioides. Similarly, excess of C. longa is seen in C2, C4, and C6 as evident from the higher concentration of Cl and K. In most of the samples, the lower concentration of Ca and Al indicates the deficiency of S. reticulata. A large disparity in the concentration of some elements in the commercial sample is an indication of adulteration. It may be noted that adulteration of herbs in herbal preparations will be more probable due to the limited availability of an herb or due to the physical similarity with another cheaper herb. In order to confirm the above fact, the samples are to be analyzed with higher statistical accuracy with a larger replica of samples.

5.4 Comprehensive Analysis of Amalakyadi Churna

The comparison of results obtained from XRF, PIXE and ICPMS shows that the presence of P. zeylanica decides the presence of the elements Fe, Cu, K and Zn in the formulation. The inhomogeneity in the sample due to difficulty to form fine powder greatly affects the concentration of elements in the herbs and the formulation. Cr concentration in P. zeylanica is overestimated by PIXE as the ICPMS results and the formulations do not contain a significant amount of Cr. Hence, the concentration of Rb alone cannot be considered as a decisive factor of the presence of T. chebula or P.longum. However, the presence of Rb, along with a higher concentration of Mn can indicate the inclusion of P. longum over T. chebula as the concentration of Mn has a significant difference in the two herbs. A higher concentration of Sr in the formulation can indicate the excess concentration of P. zeylanica, as the Sr concentration in P. zeylanica is about

3 times more than that in P. longum and T. chebula. Analyzing the results of both PIXE and ICPMS, the concentration of Sr, along with Cu, Cr, and Zn can be considered as the representative trace elements in Amalakydi Churna for the estimation of the presence P. zeylanica.

5.5 Comprehensive Analysis of Balachaturbhadrika Churna

The results of the Balachaturbhadrika Churna shows that there is a significant correlation between the XRF and ICPMS for Cu, Mn, and Rb for all herbs. P. integerrima contributes to most of the elemental concentration of Al, Ba, Cr, Fe, Mn, Rb, and Ti in the formulation. Major contribution of Zn in the formulation comes from C . rotundus and that of Sr comes from A. heterophyllum. ICPMS results also supports this observation. Zn being a strong indicator of C. rotundus, a high concentration of Zn in the formulation can indicate an excess contribution of C. rotundus in the formulation. Similarly, Ti, Mn, Rb, and Al may be the indicator of P. integerrima. Ca, Cl, and Mg may be the indicator of P. longum. P is also an indicator of C. rotundus. Ni and Sr are the indicators of A. heterophyllum in the Balachaturbhadrika Churna. It is also observed that the concentrations of heavy metals like Cd, Hg, and Pb are within the permissible limits, in Balachaturbhadrika Churna.

Even though the presence of trace elements depends upon the particular herb and the particular plant part, variations in elemental concentrations are possible due to geological and climatic factors and an exact value of concentration may not be realistic. It was also observed that variations in elemental concentration can occur during different sample processing steps like, washing, grinding, etc. These variations are to be taken in to account while generating a comprehensive elemental fingerprint data. Further, setting a permissible range of concentration for each element in each formulation is a factor t be accounted

5.6 Conclusion

XRF, PIXE, NAA, PAA, and ICPMS have been used for the preparation of an elemental profile of Ayurvedic herbal formulations, Triphaladi Churna, Nishakatakadi decoction, Amalakyadi Churna and Balachaturbhadrika Churna. The concentrations of Al, Ba, Br, Ca, Cl, Co, Cr, Cs, Cu, Fe, K, La, Mg, Mn, Na, P, Pb, Rb, S, Sc, Si, Sm, Sr, Ti, W, and Zn were determined. The ranges of elemental concentrations in different herbs have been found to vary widely with respect to one another. This facilitates the preparation of elemental fingerprint reference data for various coded formulations in systems like Ayurveda, Siddha, Unani, etc. As each method used has specific advantages towards the identification of selected elements, a fingerprint generated for compound formulation employing different techniques improves the reliability. The deviation in the elemental concentration of any formulation with respect to reference fingerprint data will be an indicator of the absence, deficiency or excess of any particular herb, in a particular formulation. It may be due to adulteration or the unavailability of the particular herb. In general, most of the commercial samples collected from authorized dealers were found to be comparable. In Nishakatakadi decoction, most of the selected commercial samples showed a significant correlation, as indicated by the correlation coefficients. Some of the samples show slight variation in the concentration of certain elements. However, this is a pioneering attempt to prepare a standard data set for fingerprinting of herbal formulations in terms of elemental profile, this data is of representative nature. In order to use it as a standard reference for fingerprint profile, samples are to be analyzed with required statistical accuracy, with a larger replica of samples. The geographical variation of elemental concentration in herbs is also to be accounted for.

5.7 Future Works

The prepared data set being a primary result, a large amount of data with higher statistical accuracy has to be generated using various techniques. Hence,

this work needs extensive follow up. In order to account for the geographical variation of trace elements, analysis of samples collected from distinct geographic regions are to be conducted. Seasonal variation of trace elements is also to be incorporated. It is also expected to generate a maximum and minimum tolerance limit for each element in any particular herb and the compound formulation.